5-1-2013

DISPLAY OF PEPTIDES AND SINGLE-CHAIN ANTIBODIES ON BACTERIOPHAGE MS2 VIRUS-LIKE PARTICLES

Christopher Andrew Lino

Christopher Andrew Lino
Candidate

BREP
Graduate Unit

This dissertation is approved, and it is acceptable in quality and form for publication:

Approved by the Dissertation Committee:

David S. Peabody , Chairperson

Bryce Chackerian

Walker Wharton

Brian Hjelle

DISPLAY OF PEPTIDES AND SINGLE-CHAIN ANTIBODIES ON BACTERIOPHAGE MS2 VIRUS-LIKE PARTICLES

BY

CHRISTOPHER ANDREW LINO

B.S., Molecular Biochemistry and Biophysics, Illinois Institute of Technology, 2007

DISSERTATION

Submitted in Partial Fulfillment of the
Requirements for the Degree of

Doctor of Philosophy
Biomedical Sciences

The University of New Mexico
Albuquerque, New Mexico

May 2013

DEDICATION

Dedicated to my parents, Barbara and Kevin Hawthorn.
Thank you both so much for all your love and support. I love you always.

ACKNOWLEDGEMENTS

I would like to thank my thesis advisor, David Peabody, for all of his contributions to my scientific education and career. I am extremely fortunate to have worked with him during my graduate career. I grew not only academically but also as a person during my time as his graduate student, and I am certain that he contributed in no small part to this. I appreciate all of the exceptional insights into my work that he provided, and I also appreciate that he never failed to push me and make me a better scientist. I have no doubt that I would not be the person I am today without having studied under him, and for that I am thankful.

I need also to express my extreme gratitude to Jerri Caldeira, a research scientist in our lab. Jerri provided nearly all of my technical training during the first few years of my graduate experience, and he was always available to help me troubleshoot problems or complete work that required late nights or weekends. Jerri is an incredibly talented scientist, and without his training and constant support there is no way that I would be as scientifically talented as I am today. I want to thank Jerri not only for being a colleague and an advisor of sorts, but also for being an amazing friend.

I would also like to thank the various members of my dissertation committee: Bryce Chackerian, would provided not only countless insights into my project and various directions in which to take it, but also performed some of the work shown here; Kip Wharton, who was a source of both knowledge and training (especially with mammalian cell culture and cell manipulation); and Brian Hjelle, whose depth of knowledge of current literature provided many useful insights.

I need to also express my gratitude to the various members of the Peabody-Chackerian lab collaboration. I enjoyed many conversations and shared many insights with everyone, both scientifically and non-scientifically. They are: Julianne Peabody, John O'Rorke, Jayne Christen, Erin Crossey, Mitch Tyler, Ebeneezer Tumban, and Kathryn Frietze.

I further want to give thanks to the other various friends and colleagues that I have met during my tenure as a graduate student at the University of New Mexico. Without all of these people, I know my graduate career would not have been the same. Also, without the support of all of my friends and family, there is no way I could have completed my degree. Though I do not have space to name them all, I would like to specifically thank Dominique Price, Jenna Lilyquist, Jason Rogers, Scarlett Swanson, and Julianne and Mitch (from above).

I must also thank my entire family, including my siblings and Barbara and Kevin, my mom and dad. Without their unshakeable love and support, I would not have even made it to graduate school, much less succeeded in obtaining my doctorate. My parents always encouraged me and pushed me to be the best that I could be, and for

that I am eternally grateful. I wish to thank them for their future support as well, as I know that they will always be there for me no matter what, and I cannot fully express my gratitude for this.

Finally, I wish to thank all of the people who helped complete work in this dissertation. They are, in no specific order: David Peabody (creation of M18-expressing MS2 VLPs and gels), Bryce Chackerian (ELISAs for M18, Dengue), Julianne Peabody (immunizations of mice for Dengue), Jerri Caldiera (immunizations of mice for *S. aureus* selectants, ELISAs for said selectants), Carlee Ashley (creation of scFv26/66 and VSV-pseudotype neutralization), John O'Rourke (selections for both *S. aureus* and *S. flexneri* antibodies), and Peter Rice (neutralization of *N. gonorrhoeae* by our VLP selectants). I would also like to thank the UNM Shared Flow Cytometry and High Throughput Screening Resource for their help with the flow cytometry equipment and interpretation of results, and the Fluorescence Microscopy Shared Resource for generation of microscopy images shown in this work.

DISPLAY OF PEPTIDES AND SINGLE-CHAIN ANTIBODIES ON BACTERIOPHAGE MS2 VIRUS-LIKE PARTICLES

BY

CHRISTOPHER ANDREW LINO

B.S., Molecular Biochemistry and Biophysics, Illinois Institute of Technology, 2007

Doctor of Philosophy
Biomedical Sciences

ABSTRACT

Phage display is a powerful technology for selection of novel binding functions from large populations of peptide or antibody fragments. From a sufficiently complex library, phage bearing peptides or antibodies with practically any desired binding activity can be physically isolated by affinity selection, and, since each particle carries in its genome the genetic information for its own replication, the selectants can be amplified in bacteria. Existing display systems are based mostly on the filamentous phage M13. It is a powerful technology, but it has limitations for certain applications. Our work has concentrated on development of a new display platform based on virus-like particles (VLPs) of bacteriophage MS2, which addresses some of these limitations. The work presented here has two main foci – the display of single-chain antibody fragments (scFvs) on the MS2 VLP surface and the affinity selection of epitopes and epitope mimic from random sequence peptide libraries using monoclonal antibodies as targets.

Here we demonstrate the display of several different scFvs via genetic fusion at the C-terminus of the MS2 coat protein single-chain dimer, including the following: M18 (scFv against anthrax protective antigen), AF-20 (scFv against AF-20 antigen, found on hepatocellular carcinoma cells), and scFv26/scFv66 (scFvs against Nipah virus G and F protein, respectively). Work with M18 demonstrates successful scFv incorporation into the MS2 VLP and intact antibody structure and function. VLPs displaying scFv AF-20 were used in both confocal microscopy and FACS experiments to demonstrate that these scFv-bearing VLPs can be specifically targeted to cells expressing the receptor. The functionality of VLPs displaying scFv26 or scFv66 was demonstrated in neutralization assays with NiV G protein-pseudotyped vesicular stomatitis virus (VSV).

We also demonstrate the affinity selection of epitopes and epitope mimics from libraries of random sequence peptide displayed within the AB-loop of the MS2 VLP. Several different antibodies recognizing both protein and carbohydrate antigens were used as the selection targets. They included the following: the 2C7 and 2-1-L8 (monoclonal antibodies directed to lipooligosaccharide of *Neisseria gonorrhoeae*), MDVP-55A and GTX29202 (antibodies against a discontinuous epitope of the

envelope protein of Dengue virus); MCA5792 (an antibody against the peptidoglycan of *Staphylococcus aureus*); and 2H1 (an antibody to the capsular glucuronoxylomannan (GXM) of the fungus *Cryptococcus neoformans*, and SYA/J6 (which recognizes the lipopolysaccharide of *Shigella flexneri*). From these selections, families of potential mimotopes were developed, and tested for activity with the selecting antibody and (in some cases) were used in mouse immunizations to attempt to promote an immune response against the original antigen. In the cases where immunizations were attempted, high-titer antibodies were generated that bound to the original antigen, suggesting the suitability of the MS2 VLP platform for identification of mimotopes for diverse epitope types.

TABLE OF CONTENTS

Chapter 1: Introduction and Background

1.1 Phage Display Concept & Technology

Phage display is a technology created in 1985 by George Smith, who showed it was possible to fuse fragments of *Eco*RI endonuclease to pIII, a protein which is present in five copies on bacteriophage M13. [1] Early on it was recognized that phage display offered a potential route to discovery of peptide epitope-based vaccines. Affinity selection on antibody targets leads to identification of epitopes and epitope mimics that could potentially serve as vaccine immunogens, perhaps while actually displayed on the phage particle itself. Here I discuss the various phage display platforms and their advantages and drawbacks for vaccine development.

Filamentous Phage Display. The most commonly used phage display systems are based on M13, a long, filamentous, single-stranded DNA phage that infects male *Escherichia coli*. It is represented schematically in Figure 1.1. M13 infects *E. coli* by the binding of pIII to TolA; this then allows for injection of the phage genome into the host cell once the F-pilus is retracted. The genome is then made into dsDNA and both expressed (to create more phage proteins) and replicated (via rolling circle amplification). When sufficient phage proteins have been created, protein synthesis is halted, new phages are assembled on pV-coated ssDNA genomes, and the new phages are assembled at the cell membrane and secreted into the environment. [2]

Smith originally fused *Eco*RI fragments to the N-terminus of pIII, the tail protein of M13. It was demonstrated that the phage both retained its infectivity and displayed the inserted peptide in a form accessible to the immune system. Peptides

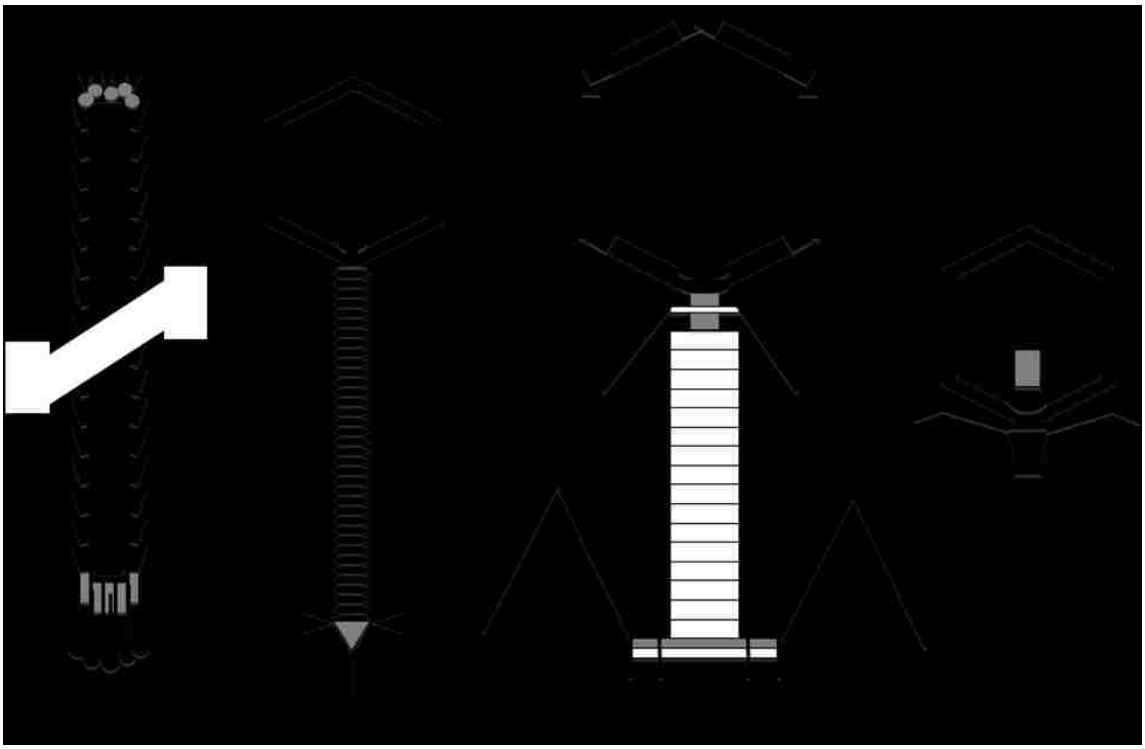

Figure 1.1 Several Common Bacteriophages Used for Phage Display. Shown are M13, lambda, T4, and T7 bacteriophages. Important features are noted here for each phage. M13: pIII (tail proteins, black ball-and-stick); pVI (gray boxes, tail of phage); pVIII (body proteins, black boxes); pVII (gray circles, top of phage); pIX (black triangles, top of phage). Lambda: gPE and gPD (icosahedral head); gPV (long tail, unshaded ovals). T4: gp23, gp24, and gp20 (head). T7: protein of gene 10 (head).

may also be fused to the N-terminus of pVIII, however, for display along the main body of the phage. There are advantages and disadvantages to each type of peptide display on M13, both for affinity selection and for immunogenic peptide display. For pIII, valency of display is clearly low, owing to the presence of only five copies of the protein in each phage. However, much larger proteins can be displayed here, including single-chain antibodies (see later in this introduction). In addition, when searching for binding partners to a specific target (e.g. an antibody), such low display density can allow for stringent affinity selection. In contrast, display on pVIII gives much higher display density, allowing for both affinity and avidity to assist in interactions with a target. That is, peptide fusion to pVIII allows for polyvalent display, which leads to avidity effects that compromise the stringency of affinity selection. Although pVIII display is polyvalent, viral assembly and morphogenesis are severely compromised when too many copies of the protein bear foreign peptide fusions. Efficient production of the recombinant particles therefore requires the co-expression of wild-type pVIII, which significantly reduces the overall density of peptide presentation. This means that valency is usually too low for pVIII-displayed peptides to serve as really effective immunogens.

As a specific example, de la Cruz et al. cloned fragments of *Plasmodium falciparum* circumsporozoite protein into pIII of bacteriophage f1, a filamentous phage closely related to M13. [3] The authors were able to show that there is utility in this display with regard to epitope mapping, as they demonstrated via electron microscopy that monoclonal antibodies to the *P. falciparum* protein only bound to the phages that displayed the appropriate fragment. They demonstrated robust anti-

f1 responses in both rabbits and different strains of mice; however, antibody titers to the inserted peptides were either low (in the case of rabbits) or non-existent (in some strains of mice).

Bacteriophage λ. Lambda phage consists of an icosahedral head atop a long, flexible tail (see Figure 1.1). The head is composed of two proteins (gpE and gpD), and the tail is composed of gpV. Of these proteins, two have been utilized for display of foreign peptides – gpD and gpV. Capsid protein gpD was a natural target for peptide display because, when the wild-type lambda genome is reduced to less than 82% of its original size, gpD transitions from essential to non-vital protein for phage infection. [4] It therefore represents an abundant (there are over 400 copies of gpD per phage), accessible, yet semi-dispensable protein on the lambda phage surface, making it an attractive target for phage display. Many proteins have been displayed using gpD, including G protein, ß-galactosidase, protein A, ß-lactamase, and p24 (an HIV protein). [5–7] In the case of gpV, naturally-occurring lambda phage mutants with truncated gpV (loss of the C-terminal domain) were discovered to still form regular phages with no loss of function. [8] Indeed, up to one-third of the C-terminal end of gpV can be deleted with no effect on shape or phage viability. This again makes it an attractive display target, and in fact, it has been utilized in this way for display of such proteins as *E. coli* ß-galactosidase and *Bauhinia purpurea* lectin. [9]

Much like M13, in most cases valency of fusion proteins must be controlled when using lambda phage as a display system for large proteins in order to avoid impacting phage fitness and infectivity. However, lambda phage has yet to be fully explored as a combination platform for display of smaller peptides and antigen

presentation system, though there is little evidence to suggest that it would be unsuited to the task.

Bacteriophage T4. T4 is composed of an icosahedral head and a contractile tail that terminates in fiber structures. The icosahedral head is composed of three main components: gp23, gp24, and gp20. In addition, there are two other proteins, known as highly immunogenic outer capsid protein (Hoc) and small outer capsid protein (Soc), that bind to the outside of the capsid. Hoc and Soc are both dispensable to infectivity and viral function, and they are both attractive sites of foreign peptide insertion. Many peptides have already been displayed at high density using either Soc or Hoc fusion constructs, including HIV gp120, poliovirus VP1, and *Neisseria meningitides* PorA protein. [10], [11] Upon immunization, the platform generated high-titer antibodies to the displayed peptides as well. Hoc and Soc fusions can either be encoded virally or can be added post-assembly to fully-formed T4 phage, where they will bind normally.

The main drawback with the use of bacteriophage T4 as a platform for phage display is that the genome is inconveniently large for high-complexity library display, owing in part to the complexity of the phage. However, it is perfectly suited to high-density display of individual peptides or proteins. These proteins can even be quite large, owing to the ability to fuse them to Hoc or Soc, fold these fusion proteins independently, and then add them to phages later. In this case, however, it is impossible to recover a sequence that encodes for the fused peptides, limiting use as a platform for display of peptide libraries.

Bacteriphage T7. Phage T7 is made up of an icosahedral head connected to a short tail with fibers. The icosahedral head is composed of gene 10 protein, which is found in two forms in the head structure: the major form, 10A, is 344 amino acids long, and the minor form, 10B (which arises from a programmed frameshift in the genome) is 397 amino acids long. Wild-type capsids are natural mosaics, but a fully functional T7 capsid can be composed entirely of either 10A or 10B. This immediately indicated a predisposition to a tolerance of different lengths of proteins (in this case, C-terminal fusions) and provided an attractive site for fusion and display of foreign peptides. Indeed, there are commercially-available kits for display of foreign peptides on the T7 surface, even going as far as to allow for the control of valency of the fused peptide. This is important in the case of large peptide fusions (i.e. larger than the normal frameshift, ~50 amino acids) and in the case of deliberate limitation of valency to increase stringency of binding (again, affinity vs. avidity).

Though T7 phage is better-suited than the filamentous phages discussed above for use as a peptide display and presentation platform, it has not been utilized much in this capacity. This is surprising because of its tolerance of fairly large fusion peptides and its ease of use/commercial availability.

1.1.1 Other Platforms for Peptide Display

Bacteriophages are not the only systems utilized for the display and affinity-selection of foreign peptides (though not necessarily as a presentation platform for vaccination). Other common systems include yeast display, bacterial display, and ribosome/mRNA display.

Yeast display. Developed by Dane Wittrup in 1997, yeast surface display is a powerful technology. [12]Yeast cell mating is modulated by two related receptors known as *a*-agglutinin and α-agglutinin. The *a*-agglutinin receptor is composed of two subunits: Aga1p, the larger of the two, which anchors the receptor to the cell wall, and Aga2p, that is linked to Aga1p by disulfide bonds. Proteins of interest can be fused to the C-terminus of Aga2p and displayed on the surface of the yeast cell. This fusion allows for the protein of interest to be displayed and projected off of the yeast. In fact, libraries of scFvs have been displayed on the cell surface of yeast, and they have been successfully screened to find scFvs that bind to specific targets. [12]

Compared to phage display, yeast display has several advantages and disadvantages. The first advantage is that, as a eukaryotic display system, post-translational processing of proteins occurs much as it does in most mammals, allowing for the display of proteins that require this specific processing to be displayed. In addition, owing to the large surface area available on which to display foreign peptides, display is more uniform (i.e. there is less variation in number of displayed peptides from cell to cell) and there is more display of the foreign peptide per cell. Also, libraries displayed on organisms as large as yeast can be screened rapidly and efficiently via FACS. However, library sizes are often limited in complexity in the yeast system, with typically no more than 10^5-10^6 members. The technology is still relatively new, though, and methods to allow the generation of more complex libraries (up to 10^9 different clones) are emerging. [13] Generation time for libraries is also vastly greater in yeast than in phages; it is not uncommon for a single round of selection to take upwards of three weeks in yeast. In addition,

carbohydrate modifications can differ between yeast and mammalian cells, such that glycoproteins made in yeast are often unsuitable as therapeutics.

Bacterial display. Bacterial display of foreign peptides is accomplished using *E. coli*. Developed by Francisco et al. in 1993, the bacterial display system relies on the fusion of the desired peptide to a chimeric polypeptide that consists of parts of the *E. coli* major outer member lipoprotein (Lpp) and outer membrane protein OmpA. [14] These two proteins both target the fused protein to the *E. coli* outer cell wall and anchor it there, allowing it to be displayed away from the surface of the bacterium. Once again, libraries of scFvs have been displayed and screened on the surface of *E. coli* using this technique. [15]

As with yeast display, there are advantages and disadvantages to bacterial display with respect to traditional phage display. *E. coli* display enjoys similar advantages to yeast display in terms of number of displayed foreign proteins and overall uniformity of display. Also as in yeast, displayed proteins can be screened on the surface of *E. coli* via FACS. In addition, the time in between rounds of selection of is decreased when compared to yeast (though still increased from traditional phage display). Library size and complexity is still an issue with bacterial display, however, owing both to the fact that *E. coli* is a prokaryote (and thus may encounter folding issues with large mammalian proteins) and potential steric hindrance from the cell membrane (despite the presence of the peptide used for projection).

Ribosome/mRNA Display. Although these two display technologies are different, they are sufficiently similar to group together for the purposes of discussion. Both of these methods represent entirely *in vitro* display and screening

systems. In ribosome display, the library to be displayed is genetically fused to a spacer sequence that contains no stop codon. When translation proceeds *in vitro*, a small fraction of the translated protein will not be released from the ribosome but will still fold, as it has exited the ribosome tunnel. The resulting protein-ribosome-mRNA complex is then cooled on ice and stabilized with addition of cations; these complexes are then used directly in selections. This method has been used to generate scFv libraries with vast complexities. [16] For mRNA display, puromycin chemistry is utilized. All members of the starting library have attached to their 3' ends a linker sequence and puromycin, which mimics an aminoacylated tRNA. When translation arrives at the 3' end of the mRNA, puromycin enters the ribosome A-site and is incorporated into the peptide chain. This causes dissociation of the ribosome, and the polypeptide remains attached to the puromycin-mRNA. This molecule is then directly used in selections. As in all previous cases, this method has also been used to generate and select against vast libraries of scFvs. [17]

The advantages of ribosome/mRNA display when compared to phage display are readily apparent. The entire system is contained *in vitro*, meaning that there is no need to account for transformation efficiency. This means that extremely vast library complexities – 10^{12} - 10^{15} – can be obtained with these systems. These systems are also not limited to only natural amino acids, nor is there any concern of limitation due to poor fitness imparted by a fused protein. In addition, mutagenesis can be performed in between rounds of selection with ease, allowing for a process similar to that of a B-cell's affinity maturation to occur. Both of these methods have drawbacks as well. These are technically challenging methods, owing to both the

amount of manipulation required and the strict necessity of maintaining an RNase-free environment at all times. Also, either the ribosome-mRNA complex or the fused mRNA has the potential of interfering with the selection because of their attachment to the protein of interest. Additionally, proteins that require anchoring to a membrane or extensive chaperone help to fold are not ideal for either ribosome or mRNA display.

1.1.2 Ideal Characteristics of a Combination Display/Presentation Platform

Yeast, bacterial, ribosome, and mRNA display all represent additional methods for foreign peptide display. However, they are unable to function as combination platforms for both the display of potential target antigens and their presentation to the immune system. For this application, the phage display systems detailed earlier are far more ideal. The use of any phage display system as a combination display and antigen presentation platform is predicated upon the ability to recover the binders and then to amplify them in preparation for additional rounds of selection. This phenotype-to-genotype link provides the very foundation for affinity selection of peptide libraries displayed on phages (see Chapter 1.6 for more information regarding affinity selection).

When attempting to use phage display as a combination epitope display and antigen presentation platform, three basic, overarching characteristics apply and make for an ideal system. First, there must exist a site on the surface of the phage that can accept foreign sequence insertions without disruption of protein folding or phage assembly. Second, the phage must encapsidate nucleic acid sequences that encode it and the foreign peptide it displays. It is also helpful if the valency of the

desired foreign peptide can be varied. This allows the user of the system to take advantage of both high valency (in the case of initial selection rounds or presentation to the immune system as a dense repetitive array) and low valency (to increase stringency of selection by limiting binding to affinity and not avidity effects). Virus-like particles (VLPs) of bacteriophage MS2 fulfill all three of these requirements.

1.2 Bacteriophage MS2

Bacteriophage MS2 is a male-specific small RNA virus that infects *Escherichia coli*. [18] The capsid of MS2 is composed of 180 copies of a single coat protein arranged in T=3 symmetry. The monomeric coat proteins interact with one another to form dimers before assembly into the viral shell (Figure 1.2). The shell also contains a single copy of maturase that is required for infectivity of the phage but is not required for assembly of the capsid. In addition to these two proteins, the phage also encodes for a replicase and a lysis protein.

The structure of the MS2 coat protein monomer has an unusual fold. Rather than maintaining an extensive β-barrel structure, as is the case for the vast majority of known virus coat proteins, the protein consists of five β-strands in a sheet facing the inside of the particle and two α-helices facing the outside. [18] The β-strands form a β-hairpin loop (known as the AB-loop) that is also presented to the outside of the capsid; in fact, it is this loop that is most distal to the center of the virus (Figure 1.2). This makes it an ideal location for insertion of a foreign peptide to both maximize accessibility and minimize the chances that the insertion inhibits coat protein folding or viral shell assembly.

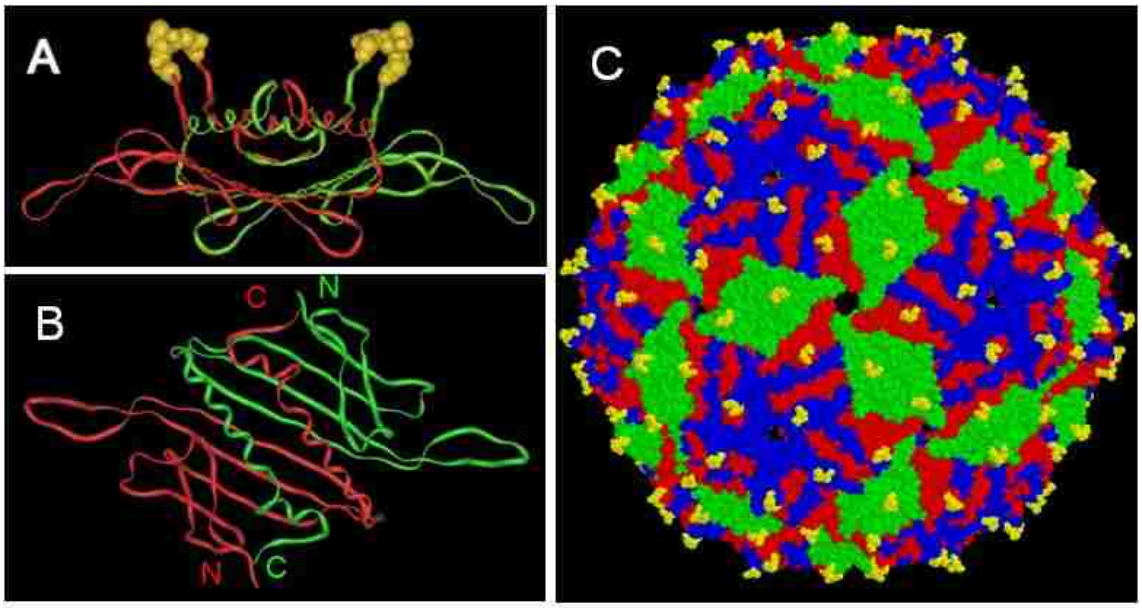

Figure 1.2 The Structure of the Bacteriophage MS2 VLP and Coat Protein Dimer. This model of MS2 was generated using iMol (http://www.pirx.com/iMol). (A) The MS2 coat protein dimer viewed side-on. One subunit is colored green and the other is colored red. Once again, the AB-loop is colored via gold balls. (B) The MS2 coat protein dimer as viewed from inside of the VLP. Note the close spatial proximity of the N-terminus of one coat protein to the C-terminus of the other; it is this proximity that allows for the creation of the genetic fusion of the two monomers to form the so-called "single-chain dimer". (C) The monomeric subunits within the particle are pseudocolored to demonstrate the five-fold and quasi-six-fold axes of symmetry. The gold balls represent the so-called AB-loop, an important site for small peptide insertion within the coat protein.

1.2.1 Creation of MS2 VLPs

Virus-like particles, or VLPs, consist of viral coat proteins that self-assemble into a non-infectious viral shell. In the case of bacteriophage MS2, the single viral coat protein can be expressed from a plasmid vector in *E. coli*. [19] The coat protein dimerizes and assembles into VLPs that can be extracted and purified from bacterial cultures. In addition, the VLP packages the RNA from which it was translated, allowing for its recovery and amplification. [20] However, because there is no viral genomic material present, these particles are completely non-infectious.

Unfortunately, insertions into the MS2 AB-loop are often poorly tolerated, leading to protein misfolding and assembly defects. [21] The solution to this problem is a genetic fusion of two coat protein monomers to form one protein, the "single-chain dimer" or SCD. As seen in Figure 1.2, the C-terminus of one monomer in a coat protein dimer is proximal to the N-terminus of the other, and this is where the fusion occurs. This fusion confers a far greater stability to the overall dimer, and it also allows for a vast array of tolerated peptide insertions into the AB-loop of the downstream copy of coat protein. [21] Thus, the particles used in this work are MS2 VLPs expressed in *E. coli* from a plasmid that encodes for a single-chain dimer form of the coat protein.

1.3 Display of Foreign Peptides on MS2 VLP Surface

As noted above, the SCD coat protein fusion allows for many diverse peptide insertions into the AB loop of MS2 VLPs. Specific examples of peptide insertions include V3 (extracellular loop of HIV envelope protein) and ECL2 (extracellular loop of macaque CCR5), done by Peabody et al. [21] Both of these insertions are 10 amino

acids in length, and both resulted in fully-formed and properly folded VLPs. Upon injection into C57Bl/6 mice, both were also shown to cause generation of antibodies against the appropriate antigen, indicating that the antigens were properly displayed to the extracellular environment (and that VLPs can be highly immunogenic – see "Uses for Peptide-Displaying VLPs").

In addition, random peptide libraries of various lengths can be displayed on MS2 VLPs. [21] To test the tolerance of the single-chain dimer of insertions in the AB-loop of its C-terminal half, 6-, 8-, and 10-amino acid peptide insertions were introduced using the basic codon framework NNY, where N is any nucleotide and Y is C or T. This allows for considerable diversity by coding for 15 of 20 amino acids while not allowing any random stop codons. It was found that 100% of 6-mer, 87% of 8-mer, and 84% of 10-mer libraries produced functional, properly-assembled VLPs. The diversity of such libraries is impressive; a 6-mer library generated in this fashion can theoretically contain $\sim 1 \times 10^7$ different peptide sequences, an 8-mer library can have $\sim 3 \times 10^9$ different peptides, and a 10-mer library can have $\sim 6 \times 10^{11}$ different peptides.

1.3.1 Locations for Peptide Insertion/Fusion

As has already been mentioned, its prominent exposure on the VLP surface makes the AB-loop of MS2 an ideal location for foreign peptide insertion and display. However, it is not the only location where insertions or fusions have been attempted on MS2 or related phages. For example, the N-terminus of the MS2 coat protein also resides near the external surface of the VLP; it therefore also presents a good target for peptide fusion and display. Peabody fused FLAG, an 8-amino acid

peptide, to the N-terminus of MS2 coat protein. [22] In the case of standard wild-type monomer, the fusion did not inhibit proper folding of the coat protein, but it did inhibit VLP assembly. However, through the use of the single-chain dimer, this limitation was overcome and FLAG was successfully displayed as an N-terminal fusion on the surface of MS2. This was presumably due to the fact that the single-chain dimer lowers valency (from 180 copies of coat protein fusion to 90), thus limiting the effects of steric hindrance. A former graduate student in the Peabody lab, Sheldon Jordan, attempted insertions of random sequences of 10 amino acids at the N-terminus of MS2 coat protein. [23] Through of use of creative genetic engineering, including the use of flanking serine residues around the peptide insertions, he was able to create functional, assembled VLPs.

Another potential peptide fusion site is the C-terminus of the coat protein. Pumpens et al. demonstrated this with bacteriophage Qβ, a close relative of bacteriophage MS2. [24] The coat protein of Qβ is similar in overall structure to that of MS2, with the principle difference of the conformation of the AB-loop. Qβ phage can produce a read-through version of its coat protein that contains 196 extra amino acids (known as A1) fused to the C-terminus of the protein, paving the way for insertions of foreign peptides here. [25] Pumpens et al. demonstrated that, if kept at low enough copy number, the A1 peptide could be truncated to various lengths and still be displayed on the surface of the Qβ particle. [24] As Qβ and MS2 are closely-related bacteriophages with nearly-identical coat protein structures, it follows that this is also a potential insertion site in MS2. The work presented here

will utilize both AB-loop insertion and C-terminal fusion for display of foreign peptides on the surface of MS2.

1.4 Uses for Peptide-Displaying VLPs

The ability of MS2 VLPs to display heterologous peptides on the surface of the particle allows for many practical applications. Among these are the following three: targeted delivery of VLPs (and cargo) to specific cells; vaccination (with the goal of targeting the immune response to the displayed peptide); and affinity selection from a random library of peptides of binding partners to any specific target (e.g. a monoclonal antibody).

MS2 VLPs have been loaded with various cargoes, including both dyes and cytotoxic drugs, and have been delivered to specifically to hepatocellular carcinoma (HCC) cells and not to hepatocytes in work done by Ashley et al. [26] In this case, targeting peptides were chemically rather than genetically attached to the surface of the VLPs, though the end result is the same. When the encapsidated cargo was the A-chain of ricin, a potent toxin that inhibits ribosomal function, concentrations of only 100 fM of ricin A-chain were required to specifically kill Hep3B cells (an HCC cell line) and not THLE-3 cells (a hepatocyte cell line). This demonstrates the usefulness of foreign peptide-bearing MS2 VLPs in targeting specific cells for binding and drug uptake.

To demonstrate the effectiveness of MS2 VLPs as platforms for vaccine development, we return to the work previously described wherein Peabody et al. displayed portions of V3 and ECL2 in the AB loop. As mentioned earlier, VLPs bearing these two peptides were injected into C57Bl/6 mice, serum was collected,

and an enzyme-linked immunosorbent assay (ELISA) was performed to determine antibody titer. In both cases, animals showed end-point dilution titers of greater than 10^4 directed to each specific antigen, showing that MS2 VLPs are highly immunogenic with no need for exogenous adjuvant. [21] The antibodies both bound to full-length V3 and ECL2, showing they were also functional. This demonstrates how effective MS2 VLPs are with respect to generation of vaccine candidates. These results have since been confirmed with dozens of different peptide epitopes, such as epitopes against HPV. [27]

Finally, MS2 VLPs can be engineered to display complex libraries of random-sequence peptides within the AB-loop; these can then be used in affinity selection to find specific binding partners for a target (see "Affinity Selection of VLP Libraries" for more information on the process of affinity selection itself). Chackerian et al. demonstrated this ability using antibodies with known epitope targets - anti-FLAG, anti-anthrax protective antigen (PA), and 2F5, an HIV-1 neutralization antibody. [28] In all three cases, affinity selection was able to generate important features of the known epitope (e.g. DYKSDD selected vs. DYKDDD wild-type FLAG epitope). In the case of both FLAG and PA, the selected VLPs were used in the immunization of mice, generating antibodies that recognized and bound to full-length FLAG and PA. This demonstrates the efficacy of using MS2 VLPs bearing random peptide library sequences for affinity selection.

1.5 Single-Chain Antibody Structure and Function

As previously mentioned, work presented here will focus on two sites of insertion or fusion into the MS2 VLP coat protein – the C-terminus and the AB-loop.

The polypeptide chosen for display at the C-terminus is the single-chain antibody, or scFv.

ScFvs are the variable heavy (V_H) and light (V_L) domains from a standard immunoglobulin molecule (such as IgG). These two regions are fused together into a single molecule via a linker peptide, typically a repeat of glycines and serines. [29] Figure 1.3 demonstrates schematically the properties of both a parent antibody molecule and an scFv. Because these variable heavy and light domains contain the complementarity-determining regions, or CDRs, of the parent antibody, the scFv retains all of the high affinity and specificity for the target molecule of the original parent antibody. The scFv is also monovalent rather than bivalent, making it an extremely compact form of the original antibody at the expense of potential positive effects of avidity on overall binding strength.

ScFvs have many uses in research and medicine. [29] These are often based upon the convenience of the scFv structure; it is smaller than the parent antibody, allowing for better entry into target tissues and eventual clearance when compared to full-sized antibodies. Also, owing to the lack of an Fc region, scFvs are often non-immunogenic. This is because the Fc region is responsible for effector functions of the antibody, such as binding to cellular receptors and activating immune cells. ScFvs have been conjugated to dyes and used for cell imaging, administered as immunotherapy agents in place of full antibodies, and even have been used as antibodies against intracellular targets (known as intrabodies). The work completed in this studying concerning scFv display on MS2 demonstrates how, even attached to a VLP, scFvs are capable of targeting to specific antigens displayed on a cellular or

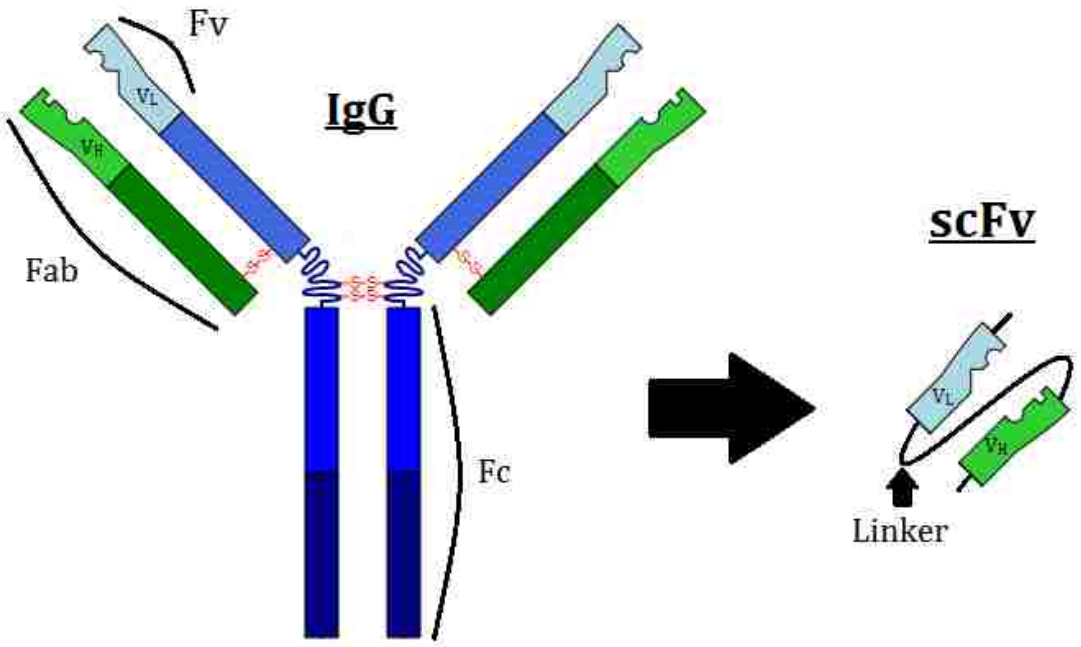

Figure 1.3 The Structure of the scFv. On the left is a full-size parent IgG molecule. Note the various features, including the Fc region (completely eliminated in the scFv), Fab region, and Fv region (which will comprise the final scFv structure). The Fv region is the variable region for both the heavy (V_H) and light (V_L) chains of the IgG molecule. This is here that the complementarity-determining regions, or CDRs, are located; they are preserved in the transition to scFv. On the right is the scFv molecule. Note the V_H and V_L domains are joined together by a flexible linker, often a repeated set of glycines and serines. Though the scFv is much smaller and mono- rather than bi-valent, it retains the high affinity of the parent IgG owing to the preservation of the CDRs.

viral surface. This work will focus primarily on the display of the scFvs against anthrax protective antigen (M18), AF-20 antigen (AF-20 scFv), and proteins F and G of Nipah virus (NiVG/F scFvs, also known as scFv26 and scFv66). A more thorough introduction of the scFvs used in this work is present in the Introduction to Chapter 2.

How would the world benefit from a new platform for display of scFvs? As demonstrated earlier, scFvs have been displayed on numerous platforms, including phages, yeast, bacteria, ribosomes, and mRNA. However, each platform had drawbacks as well as advantages. We feel that the MS2 VLP platform has a unique combination of advantages while also minimizing the disadvantages found in other systems.

First, display of scFvs would allow VLPs to be targeted to bind arbitrary targets. This could have a number of applications (e.g. in production of new diagnostic reagents), but one obvious possibility is their use to target VLPs to specific cell types as vehicles of drug or imaging agent delivery.

Second, it opens the possibility of construction of complex libraries and affinity selection of scFvs with specific ligand binding activities. Several systems for scFv display and affinity selection already exist. Systems utilizing filamentous phage allow the construction of very complex libraries and affinity selection from such libraries has yielded many new antibodies. However, different scFvs can exhibit significant differential effects on phage fitness, meaning the frequency of occurrence of specific antibodies in a selectant population is frequently a poor reflection of their relative affinities for the selection target. Such fitness effects are generally related to

scFv protein folding effects that to one degree or another compromise phage morphogenesis. We think that MS2 VLPs should be less subject to some of these effects because they are less complex than filamentous phage. Furthermore, because of its simplicity, both the libraries and the MS2 VLP itself can be expressed and assembled entirely *in vitro*. Much like ribosome/mRNA display, this should allow for increased ease in construction of high complexity libraries by avoiding the necessity of transformation of bacteria.

1.6 Affinity Selection of VLP Libraries

Affinity selection is the process of taking a random library of peptides and screening it against a specific target to find high-affinity interactions; it is also known as "biopanning". The work described here will use affinity selection to attempt to generate vaccine candidates that promote a specific antibody response against viruses and bacteria. This is usually accomplished by discovering mimotopes – that is, typically small peptides that mimic an epitope (in structure or conformation).

The process of affinity selection is diagrammed in Figure 1.4. The monoclonal antibody against the target antigen is immobilized on a solid matrix - for example on the plastic surface of the well of an ELISA plate. Then, the random peptide-displaying VLP library is incubated with the mAb, and unbound VLPs are washed away. The bound VLPs are then eluted, RNA is extracted from the capsids, and reverse-transcription (RT)-PCR is performed to make cDNA clones of the selected VLPs. This cDNA is then amplified by PCR and re-cloned in an expression plasmid to

make VLPs for the next round of selection. This process is performed iteratively until high-affinity binders for the mAb have been found.

As mentioned at the beginning of this introduction, George Smith is the pioneer of phage display and affinity selection. In addition to the work done displaying *Eco*RI fragments on pIII of M13, Smith and colleagues were also the first to construct and display a library of random peptides (roughly 10^7 different peptides) fused to the same pIII protein and performing rounds of affinity selection against antibodies to show enrichment of binding sequences. [30] Since this first library and selection, many aspects of the affinity selection process have changed. For example, higher-complexity libraries (up to 10^{11} different clones) allow for the screening of more potential binding partners. [31] In addition, it is not simply short peptides that can be displayed as a library anymore. As mentioned earlier, libraries of scFvs have been presented on a range of different peptide display systems. As in the case of short peptides, these scFv libraries have been successfully screened against specific targets to enrich for scFvs that bind to them.

As will be demonstrated in this work, affinity selection is a powerful tool for library screening. The ability to discover novel binding partners (e.g. a peptide to a monoclonal antibody, or an scFv to a known epitope) from complex starting libraries has many potential applications which have been outlined in this introduction. We will now focus on the types of epitopes that affinity selection of a library of random peptides can help identify.

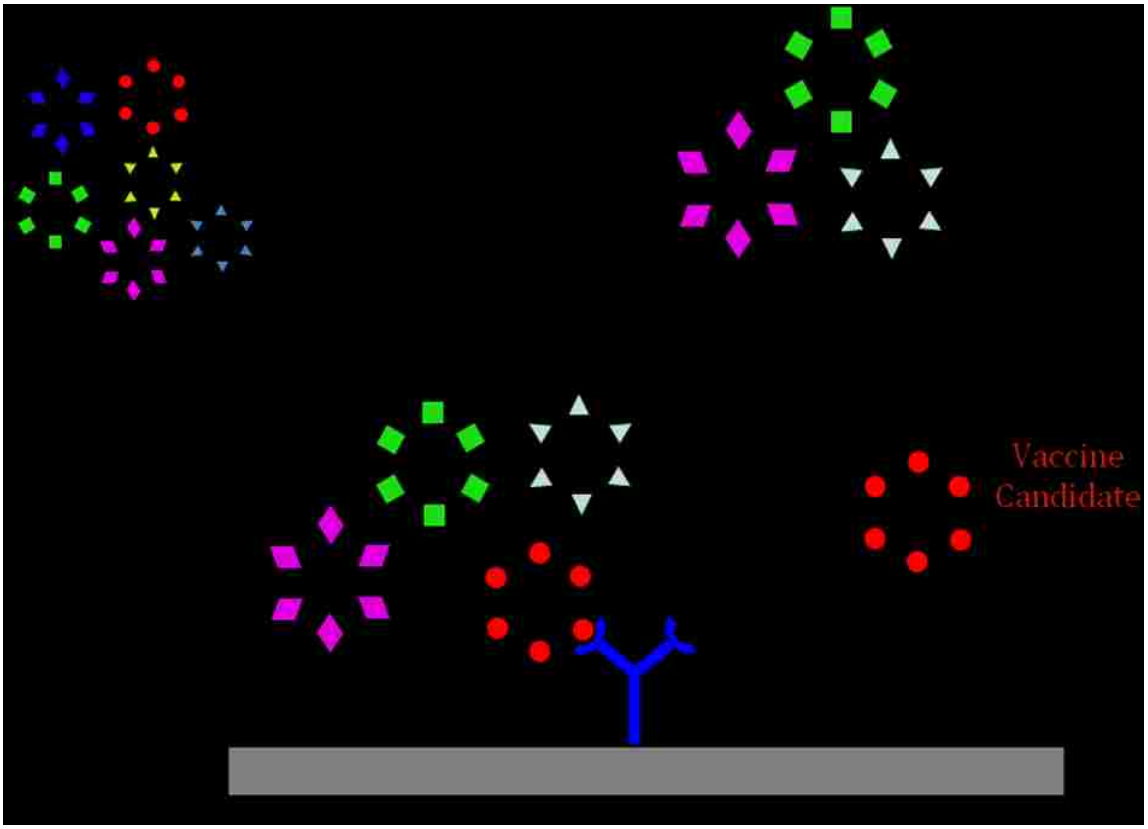

Figure 1.4 Affinity Selection Overview. The monoclonal antibody (mAb) against the target antigen is immobilized on a surface. Then, the random peptide-displaying VLP library is incubated with the mAb, allowing time for VLPs whose random peptide binds to the antibody binding pocket to do so, and unbound VLPs are washed away. The bound VLPs are then eluted, RNA is extracted from the capsids, and reverse-transcription (RT)-PCR is performed to make cDNA clones of the selected VLPs. This cDNA is then amplified by traditional PCR and reinserted into vectors for new library production. After enough iterations, the end result is a VLP displaying a peptide specific to the binding pocket of the selecting mAb. This VLP is now a vaccine candidate.

1.6.1 Types of B-Cell Epitopes

There are two main classes of epitope targets that the affinity selection process can help identify – linear epitopes and conformational epitopes. Linear epitopes are short contiguous stretches of amino acids found within a protein's primary structure that by themselves contain the information needed for antibody recognition. These are relatively easy to identify via affinity selection protocols because the random peptide libraries are themselves composed of short contiguous peptides. However, many antibodies do not recognize simple amino acid sequences, but rather recognize structures formed when the protein folds. Sometimes the antibody-contacting amino acids are near each other in a contiguous stretch of amino acids that in the context of the folded protein folds an element of secondary structure (e.g. an alpha helix), but others are discontinuous epitopes, assembled by the conjunction in space of amino acids that are distant from one another in the protein's amino acid sequence, but are brought together by the its tertiary fold. In such cases affinity selection does not find a peptide with straight-forward homology to the antigen sequence, but rather somehow structurally mimics the epitope. Such peptides are called mimotopes.

Many attempts to find mimotopes via affinity selection from libraries of random peptides displayed on phages have been made. For example, Tungtrakanpoung et al. took both monoclonal antibodies and patient sera against *Leptospira* bacterium and performed affinity selection against them using libraries displayed on M13, discovering quite a few mimotopes, some even represented in as much as 27.3% of

the final selected population. [32] Three of their mimotopes reacted with both mAbs and patient sera, indicating that they might be potential targets for immunization (though the group did not perform this work). In similar work, Na-ngam et al. used monoclonal antibodies against *Burkholderia pseudomallei* and random peptide libraries displayed on M13 and T7 to discover mimotopes that tested positive for binding to selecting antibodies via ELISA. [33] More recently, Tewawong et al. used random peptide libraries (again, displayed on T7 and M13) and selected against antibodies to the house dust mite. [34] Though the most predominant mimotopes in this case were linear, they also discovered a mimotope that corresponded to an epitope that mapped to the folded structure of protein Der f 2. Finally, Shanmugam et al. performed exciting studies using random peptide libraries displayed on filamentous phage fd and selecting against a monoclonal antibody specific to prostate secreted antigen, or PSA. They found four distinct mimotopes and, upon immunization with Balb/c mice, found that one of those mimotopes produced antibodies that recognized and bound to original PSA. [35] This demonstrates the discovery of an immunological mimotope; that is, not only does the mimotope bind to and react with the selecting antibody, it is capable of raising antibodies that can interact with the original protein. The examples provided each contain a unique look at different types of mimotopes, but they are hardly the only examples. Also, it is not just antibodies to specific proteins (whether those antibodies be directed against linear or conformational epitopes) that can be used as selecting antibodies to find mimotopes. Indeed, one of the other classes of molecule to which antibodies can be raised is carbohydrates.

Carbohydrate antigens are attractive vaccine targets, due in part to their accessibility on the surfaces of many bacteria and viruses. Famous examples, such as PneumoVax and Prevnar, are already available and have been shown to be efficacious in humans. [36], [37] However, many challenges exist to creating an effective carbohydrate vaccine. Primarily among these is that carbohydrate vaccines promote T-cell independent responses, which lead to less B-cell help and less antibody response. [38], [39]. The antibodies that are created often have affinities several orders of magnitude lower than those created against peptide targets. Also, the vaccines seem to be more effective in healthy, non-immune-compromised adults than in the elderly and children, two groups that have a more immediate need for protection against dangerous pathogens. Consequently, carbohydrate vaccines usually require conjugation to a protein carrier capable of mediating T-help. An approach that used a VLP carrying a peptide mimic of a carbohydrate epitope would solve this problem by utilizing an immunogen consisting only of protein.

1.6.2 Difficulties in Finding Immunological Mimotopes

The process of affinity selection allows for the discovery of small peptides that can act as mimotopes to the original antigen recognized by an antibody. However, there are a variety of reasons that a given antibody will not yield mimotopes when subjected to affinity selection.

Antibody poly-specificity. An example of this is seen with 2F5 and 4E10, antibodies found in some patients infected with HIV-1. [40] These antibodies are specific to gp41, an HIV-1 envelope protein, but they are also capable of binding to anionic phospholipids found in the body. In this way, they are considered poly-

specific; though they have a specific target against which they were selected in the body, they are capable of binding to other epitopes as well. In the same way, affinity selection can yield peptides that bind antibody and inhibit antigen binding, but do not structurally or immunogenically mimic the antigen. This means that, upon immunization with these types of peptides, a high-titer anti-peptide antibody response will be generated that has little to no interaction with the original antigen; the result of this is no protective response generation. Clearly, this can still be of some practical use (for example, depending on the affinity of binding, perhaps the peptide found can be used as an inhibitor of the original selecting antibody), this outcome is not useful in discovering new potential vaccine candidates.

Structure context effects. This means that peptide affinity optimized on one platform often decreases when moved to another platform due to the peptide no long being under the same pressures with regard to secondary structure and folding; this was briefly touched upon earlier, when discussing drawbacks of traditional filamentous phage display platforms. A peptide selected in a highly constrained environment may be forced to adopt a conformation that is not the most favored when such constraints are removed. Because of this, it is possible to find a peptide that would in fact be an excellent vaccine candidate in one environment and is completely ineffective when removed from that environment. Monette et al. demonstrated an example of this with the NANP repeat sequence of *Plasmodium falciparum* circumsporozoite protein displayed on the surface of filamentous phage fd. [41] This group used NMR to show that every displayed copy of this peptide on the surface of fd adopted a single, uniform conformation imposed

by the nature of display on the phage and that this is what grants it immunogenicity when presented in this context. In addition, peptides such as the G-H loop region of VPI protein in foot-and-mouth disease cannot be crystallized and analyzed in soluble form but adopt a single conformation (that actually gives the region its known antigenicity) when placed in a constrained environment. [42]

Epitope size and shape. Some antibodies recognize epitopes that are the result of secondary or even tertiary protein structure, and these discontinuous epitopes are seen as large bumps on the protein surface. These can be difficult or even impossible to mimic via small contiguous peptides. As there is an upper limit on peptide size as displayed in the MS2 AB-loop, it is feasible that there exist antibodies to which this method of affinity selection is ill-suited. In addition, it is possible that the necessary mimotope has unfavorable characteristics for display on the surface of MS2. Peabody et al. demonstrated that insertions into the AB-loop that were extremely hydrophobic in nature caused misfolding of coat protein and prevented assembly of VLPs, even when the single-chain dimer was used. [21] Because the AB-loop is so exposed to solvent, this is not an unexpected outcome; however, it also means that if a mimotope of this type was required, it would not be discoverable by our system.

The MS2 platform is capable of at least partially ameliorating these problems, however. Though it is impossible to completely eliminate the effects of antibody poly-specificity and hard-to-mimic epitopes, a mitigating factor is large library size. The more diverse and complex the original library, the better the chance of finding a desirable peptide mimotope. To this extent, the libraries used here are extremely

diverse combinations of 6-, 8-, and 10-amino acid random peptides. In the case of structure context effects, the MS2 platform essentially eliminates the problem. Because MS2 is suitable as both the affinity selection and immunization platform, the peptide is presented to the immune system under the same constraints as were present when it was selected. Again, there are some aspects that the platform cannot solve (such as mapping epitopes with characteristics that make them unable to be displayed in the AB-loop); however, we still expect it to be a more elegant solution in nearly all cases than traditional phage display platforms.

1.7 Thesis Overview

This work has two different foci, though both are based upon the genetic insertion or fusion and display of peptides on the surface of bacteriophage MS2 VLPs.

Chapter 2 demonstrates the display of several different scFvs via genetic fusion at the C-terminus of the MS2 coat protein single-chain dimer, including the following: M18 (scFv against anthrax protective antigen), AF-20 (scFv against AF-20 antigen), and scFv26/scFv66 (scFvs against Nipah virus G and F protein, respectively, also known in this work as NiVG/NiVF). Work done with M18 is proof-of-concept for scFv display, and it includes tests to demonstrate successful incorporation into the MS2 VLP and intact antibody structure and function. VLPs displaying scFv AF-20 were used in both confocal microscopy and FACS experiments to demonstrate that these scFv-bearing VLPs can be specifically targeted to cells. VLPs displaying scFv26 or scFv66 were used in neutralization assays with pseudotyped vesicular stomatitis virus (VSV) to demonstrate another

use of scFv-displaying VLPs. In all cases, scFvs were successfully fused to the MS2 coat protein and shown to be functional in a variety of assays.

Chapter 3 focuses on the display of random peptide libraries within the AB-loop and the use of these libraries in affinity selection. Several different antibodies to different epitope types (including traditional protein antigens and carbohydrate antigens) were used as the targets of the affinity selection procedure. The selecting antibodies include the following: 2C7/2-1-L8 (antibodies directed to lipooligosaccharides of *Neisseria gonorrhoeae*; these are examples of attempting to find peptide mimotopes), MDVP-55A/GTX29202 (antibodies against the envelope protein of Dengue virus; these are examples of traditional protein antigens); MCA5792 (an antibody against the peptidoglycan of *Staphylococcus aureus*; another attempt to generate a mimotope); and 2H1/SYA/J6 (antibodies against capsular glucuronoxylomannan (GXM) of the fungus *Cryptococcus neoformans* and the lipopolysaccharide of *Shigella flexneri*, respectively). From these selections, families of potential mimotopes were developed, and these peptides were then tested for activity with the selecting antibody and (in some cases) were used in mouse immunizations to attempt to promote an immune response against the original antigen.

Chapter 2: scFv Display and Function

2.1 Introduction

As previously discussed, scFvs have many important applications in research and medicine. Already, monoclonal antibodies are used as treatments and therapies for a wide variety of cancers, including nasopharyngeal carcinoma [43], colorectal cancer [44], and others [45]. These antibodies often bind to receptors on the cellular surface and inhibit signaling, eventually leading to cell death. We sought to develop a system for scFv display on MS2 VLPs with two applications in mind:

(1) Targeted Drug Delivery. We previously described the use of VLPs as a vehicle for targeted drug delivery. In those studies, particles were loaded with a cytotoxin (e.g. ricin A-chain) and their surfaces were decorated with a peptide that binds a receptor present specifically on the surface of hepatocellular carcinoma cells (HCC). Although peptides can serve as effective targeting agents, the ability to display scFvs on VLPs would allow us to take advantage of the high affinity and high specificity of antibodies already in existence that recognize a variety of cellular receptors.

(2) MS2 VLPs for scFv Library Construction and Affinity Selection. Existing systems for display of scFv libraries provide a means to find scFvs with desired specificities by affinity selection. However, those systems suffer from limitations, some of which we think can be overcome through the use of MS2 VLPs. Displaying individual scFvs on the surface of MS2 has potential applications in a wide variety of fields. However, the true power of this technology lies in the potential to, via affinity selection, discover novel scFvs to targets from complex scFv libraries. ScFv libraries

already exist, as do a variety of methods for their synthesis; for example, Pansri et al. created a library with 1.5 x 10^8 members using human B-cells [46] and Ge et al. created a library with roughly ten-fold more complexity using *in vitro* mutagenesis [47]. Even larger scFv libraries exist; Glanville et al. reported the creation of a library with roughly 3 x 10^{10} different members, though construction of this library required the use of 654 different human donors and over 300 transformations of display vectors to achieve. [48] Such libraries have been displayed on a variety of different platforms, including filamentous phage, yeast, bacteria, ribosomes, and mRNA (see Chapter 1). As mentioned previously, the MS2 VLP naturally encapsidates the nucleic acid that directs its synthesis. If this remains the case for the scFv fusion constructs, the possibility exists that novel scFvs can be discovered via affinity selection and utilized in the context in which they were discovered, eliminating the need to change platforms or remove any spatial constraints acting on the scFv during selection. Also, due to the simplicity of the MS2 VLP, libraries can be constructed and selected entirely *in vitro*, allowing for the automation and simplification of the process, and possibly the use of even more complex libraries. Therefore, ensuring that the scFv fusion VLPs encapsidate the nucleic acid that directs their synthesis becomes an important concept for the use of the platform in this manner.

As proof of concept we set out to display several specific scFvs. They included the following: (1) M18 recognizes anthrax protective antigen, (2) anti-AF-20 recognizes a receptor on HCC, (3) scFv26 binds the envelope glycoprotein of Nipah Virus (NiV), while (4) scFv66 recognizes the NiV fusion protein. The idea was to

express each of these scFvs as a fusion to the MS2 coat protein C-terminus in a manner that they would be displayed in active form on the surface of the VLP. Anticipating a possible need to manipulate the average number of scFvs displayed per particle, fusions were constructed with a suppressible stop codon at the fusion boundary. In this manner the efficiency of fusion can be manipulated by controlling nonsense suppression efficiency.

We will now provide background on the specific scfVs used in this study.

ScFv M18. *Bacillus anthracis* (anthrax) is widely studied due to both the ease with which it can be produced and its potential applications as a bioweapon. [49] One of the toxins produced by the bacterium is protective antigen, or PA. PA is important in the shuttling of anthrax lethal factor and edema factor into cells, leading to cellular death. [50] M18 is an scFv specific for PA. It was chosen as a model scFv for our system for several reasons. One, PA is available commercially, allowing for testing of the correct folding and function of the scFv displayed on the VLP surface. Two, both the nucleotide sequence and the three-dimensional structure in complex with PA have been determined [51]; this allowed for the synthesis of the gene via assembly PCR and fusion of the scFv to the C-terminus of coat protein.

ScFv AF-20. In the United States, primary liver cancers represent the fifth and ninth leading causes of cancer deaths of men and women, respectively. Incidence of this cancer has been rising for the past twenty years despite general advancements in cancer therapy and treatment. [52] There is a clear need for additional, targeted therapies for this cancer type, and the work described earlier by Ashley et al. shows promise in this field. [26] AF-20 is monoclonal antibody that recognizes and binds to

AF-20 antigen, an unidentified 180-kD homodimeric glycoprotein found on the surface of all characterized hepatocellular carcinoma (HCC) cell lines and primary patient samples. [53] While present in high quantity on the cell surface of HCC and some other cancers, expression of AF-20 antigen on other cells (even tumor-adjacent normal hepatocytes) is minimal. Upon binding, the antibody/antigen complex is rapidly internalized, making this an ideal target for both identification of HCC and potential therapy. In 2006, Yik Yeung created an scFv against AF-20 antigen from the published sequence of a monoclonal antibody as part of his thesis work at MIT. [54] Characterization of the scFv showed that it retained all important characteristics of the parent monoclonal antibody, including high specificity, affinity, and even kinetics of endocytosis upon binding. Because work had already been completed in our group by Ashley et al. using hepatocellular carcinoma cell lines, this scFv derived from AF-20 was an ideal target for display and testing against live cells.

ScFv26/ScFv66. Nipah virus is a virus of the family *Paramyxoviridae*. It was discovered in 1998 when it was shown to be the causative agent in an outbreak of fatal encephalitis in Singapore and Malaysia. [55] It is most closely related to Hendra virus; in fact, Nipah fusion (F) and attachment (G) proteins share 74% and 70% sequence homology with similar proteins in Hendra. These surface glycoproteins are essential to successful viral entry into cells; G is responsible for binding to ephrin-B2 or ephrin-B3 on the cellular surface and F mediates fusion between virus and host cell. [56] They are therefore natural targets to target to inhibit cellular infection; indeed, Guillaume et al. expressed G and F glycoproteins as vaccinia virus

recombinants and demonstrated effective neutralization via antibodies *in vivo*. [57] Hector Aguilar recently synthesized and characterized monoclonal antibodies against G and F protein [58], [59], and Benhur Lee at UCLA developed scFvs from these mAbs. Displaying these two scFvs on the MS2 surface has two potential applications. First, it should be possible to neutralize Nipah virus using scFv-displaying VLPs; second, because G and F proteins are displayed on the surface of infected cells, one could load the VLPs with cytotoxic drugs and target them directly to infected cells for selective killing.

2.2 Materials and Methods

2.2.1 C-terminal Fusion

The plasmids and phages described here were constructed using standard molecular biology methods and have the characteristics described in the text and illustrated in various figures throughout this text. Briefly, pDSP1, pDSP62 and their derivatives contain the phage T7 promoter and terminator regions of pET3d, and the kanamycin resistance gene and replication origin of pET9a (from Novagen). In a precursor common both to pDSP1 and pDSP62, an unwanted *Sal*I site and other nearby extraneous plasmid sequences were removed by *Bal* 31 deletion. Compared to pDSP1, pDSP62 contains three additional features. The first is the M13 origin of replication taken from pUC119, the second is the replacement of the upstream half of the single-chain dimer sequences with a synthetic "codon-juggled" version of coat protein, and the third is the elimination of the double stop codon at the end of the coat protein sequence. This double stop was replaced by a single amber stop codon to be used for nonsense suppression. The codon-juggled sequence was designed

using the web-based program GeneDesign available at http://genedesign.thruhere.net/gdo/index.html, and synthesized by assembly PCR from synthetic oligonucleotides.

The plasmids known as pDSP1(am) and pDSP62(am) were constructed by site-directed mutagenesis of pDSP1 and pDSP62 to introduce an amber stop codon at the junction between the two halves of the single-chain dimer. To allow for low-level suppression of the stop codon, we constructed pNMsupA, which uses the replication origin and chloramphenicol resistance of pACYC18422, and the lac promoter of pUC19 to express an alanine-inserting amber suppressing tRNA. In addition to pNMsupA, an additional suppressor was created, termed here pNMsupS2. The construct is identical to pNMsupA in all respects except for the suppressing tRNA that it expresses. SupS2 is a serine-inserting amber suppressing tRNA that is similar to previously-published *sup*D [60]. SupS2 differs from *sup*D in a single A -> G mutation in the anticodon loop that drastically lowers the efficiency of stop codon suppression.

All scFv fusion constructs utilize pDSP62 as a backbone. Downstream of the single amber stop codon exists a *Bam*HI site, and further downstream of that, a *Pst*I site. In the case of M18 and AF20, the scFvs were assembled via an assembly PCR method. Briefly, the sequences of the scFvs were optimized via the GeneDesign program for expression in *E. coli* and then submitted to GeneDesign for creation of oligonucleotides. A series of overlapping oligonucleotides was created for each scFv, with the first primer containing a *Bam*HI site and small flexible linker of three glycines and the final primer containing an opal stop codon and a *Pst*I site. The

method of assembly used is Gibson assembly PCR. [61] In our case, these oligonucleotides were then combined in equimolar amounts and subject to a PCR reaction with no amplification primers. The assembly reaction contained on Vent polymerase and consisted of an initial denaturation step at 94^{0}C, then eight cycles of 94^{0}C for 30 seconds, 45^{0}C for 30 seconds, and 72^{0}C for 30 seconds, then a final extension of 72^{0}C for seven minutes. This reaction produced trace amounts of the fully-assembled scFv. A second, traditional PCR was performed using this initial reaction as the template and the first and last assembly primers as the amplification primers. The end result of these reactions is a fully-assembled scFv with a *Bam*HI site and polyglycine linker on the 5' end and an opal stop codon and *Pst*I site on the 3' end. This was then digested with *Bam*HI and *Pst*I and inserted into pDSP62 digested with the same enzymes. The final result is pDSP62-M18 and pDSP62-AF20.

For NiVG and NiVF, the scFv genes were synthesized by IDT [62] for expression as soluble scFvs. These synthesized genes were utilized as template in PCR reactions with primers that conferred the same *Bam*HI site, flexible glycine linker, opal stop codon, and *Pst*I site as above. These were then also inserted into pDSP62 to create pDSP62-NiVG and pDSP62-NiVF.

2.2.2 Protein Expression and Purification

For scFv-VLP fusion protein expression, each scFv fusion plasmid was introduced into *E. coli* strain C41(DE3) along with a suppressor tRNA plasmid (either pNMsupA or pNMsupS2) and plated on growth media that contained both kanamycin and chloramphenicol to select for the presence of both plasmids. Individual colonies were picked to 1 mL cultures of LB media and grown to A_{600} of

0.4 (mid-log phase), where they were induced for protein expression with 1mM isopropyl β-D-1-thiogalactopyranoside (IPTG) and allowed to grow for an additional three hours. These cultures were then lysed and the separated into soluble and insoluble fractions and subjected to 17.5% SDS-PAGE analysis and 1% agarose gel (containing 50mM potassium phosphate, pH 7.4) analysis. The SDS gels were stained with 0.1% Coomassie Brilliant Blue to visualize protein bands. To verify the identity of the proteins, the contents of the SDS gel were transferred to a nitrocellulose membrane and probed with rabbit anti-MS2 serum and alkaline phosphatase-conjugated goat anti-rabbit IgG antibodies. The agarose gels were stained with ethidium bromide to reveal the presence of VLPs, which contain the RNA that directed the synthesis of the VLPs. The identity of the VLPs was then confirmed by transferring the contents of the gel to nitrocellulose and probing with rabbit anti-MS2 serum and an alkaline phosphatase-labeled second antibody.

Upon verifying that scFv-VLP fusions were properly expressed and assembled, large-scale 100 mL cultures were grown in LB media to mid-log, induced with 1mM IPTG, and grown for an additional three hours. These cultures were then pelleted and frozen. After thawing, the cells were resuspended in 10 mM Tris, pH 8.0, and disrupted by lysozyme treatment (2 mg/ml for one hour on ice), 0.25M deoxycholate treatment, and sonication (5 bursts, 1 min each, on ice). Cellular debris was removed by centrifugation at 10,000 rpm for 30 minutes. Proteins were precipitated from the supernatant with ammonium sulfate at 50% of saturation and collected by centrifugation. The ammonium sulfate pellet was then resuspended in 0.1 M NaCl, 0.01 M Tris-HCl (pH 7.5), 0.1 mM MgS04, 0.01 mM EDTA, applied to a 2.5

X 50-cm column of Sepharose CL-4B, and eluted in the same buffer. Sepharose CL-4B is a gel filtration matrix with an exclusion limit of 2 x 10^7 Daltons. VLPs elute at a position half-way between void volume and a lysozyme standard. Proteins present in each column fraction were separated by electrophoresis in a 17.5% SDS gel and 1% agarose phosphate gel. Coat protein was visualized by Coomassie Blue staining and ethidium bromide staining, respectively. Fractions from the Sepharose column that contained coat protein were concentrated by ammonium sulfate precipitation (50% saturation), and the protein pellets were redissolved and dialyzed against the Sepharose column buffer. VLP concentration was determined via Bradford assay.

2.2.3 Northern Blot

To determine whether scFv-VLP fusions encapsidated the fusion RNA that directs their synthesis, Northern blot analysis was performed. 2 mg of each VLP sample (wild-type, M18, and AF20) suspended in 500 ul of Sepharose column buffer were added to 500 ul phenol:chloroform and thoroughly mixed. This solution was then centrifuged at 14,000 rpm for 15 minutes to separate the aqueous and organic phases. The aqueous phase, now containing RNA from within the VLPs, was removed and 1/10 volume of 3M sodium acetate was added. After addition of 2.5 volumes of ethanol, the new solution was incubated on ice for 30 minutes. This was then centrifuged at 14,000 rpm for 10 minutes and the supernatant discarded. The pellet containing the RNA from within the VLP was then suspended in DEPC-treated water and the concentration of RNA within the pellet was measured by NanoDrop (Thermo Scientific).

RNA concentration across all samples was normalized and loaded at a concentration of 1 mg/ml in Sample Denaturation Buffer (65% formamide, 8% formaldehyde, 1.2x MOPS) into a 1% agarose gel containing 3.7% formaldehyde and 1x MOPS buffer (0.2M MOPS, 50mM NaOAc, 10mM EDTA). This gel was run in duplicate to both stained with ethidium bromide to visualize RNA and subject to Northern blot to verify the identity of the nucleic acid as MS2-specific. The contents of the gel were transferred to nitrocellulose using 20x SSC overnight. The membrane was then baked at 80^{0}C under vacuum for 2 hours and incubated in pre-hybridization solution (25mM KPO_4, 5x SSC, 5x Denardt's solution, 50 ug/ml herring testis DNA as carrier, 50% formamide) for 2 hours. Next, the membrane was incubated overnight with hybridization solution, which is identical to pre-hybridization solution except that it also contains 0.1 nmol of biotin-labeled negative-sense MS2 RNA. The next day, the membrane was developed with the BrightStar Kit and protocol (Ambion) and exposed to chemiluminescent film (Kodak) to visualize results.

2.2.4 Enzyme-linked immunosorbent assay (ELISA)

To determine whether M18 was displayed in a functional manner on the VLP surface, 500 ng of anthrax protective antigen (Invitrogen) was used to coat Immulon 2 ELISA plates (Thermo Scientific) at 4°C overnight. Wells were blocked for 2 hours at room temperature with 0.5% non-fat dry milk in PBS buffer. Serial dilutions of either wild-type or M18-expressing VLPs were added to each well and incubated for 2 hours at room temperature. Mouse anti-MS2 was added at a 1:2000 dilution to each well and incubated for 2 hours at room temperature, followed by horseradish

peroxidase (HRP)-conjugated goat anti-mouse IgG at a 1:5000 dilution for 1 hour at room temperature. The plates were developed with 2,2′-azino-bis(3-ethylbenzthiazoline-6-sulfonic acid) (ABTS) and reactivity was determined by measuring the mean optical density (OD) values at 405 nm.

2.2.5 Mammalian Cell Culture

Hep3B and hepatocytes were obtained from Carlee Ashley (originally obtained from ATCC) and grown per manufacturer's instructions. Hep3B were maintained in culture plates in EMEM with 10% FBS. Hepatocytes were grown in culture plates coated with BSA, fibronectin, and bovine collagen type I. The culture medium used was BEGM (gentamicin, amphotericin, and epinephrine were discarded from the BEGM Bullet kit) with 5 ng/mL epidermal growth factor, 70 ng/mL phosphatidylethanolamine, and 10% FBS. All cells were maintained at 37°C in a humidified atmosphere (air supplemented with 6% CO_2). Cells were passaged with 0.05% trypsin at a sub-cultivation ratio of 1:7. Vero cells (CCL-81), Dulbecco's Modified Eagle's Medium (DMEM), fetal bovine serum (FBS), and 1X trypsin-EDTA solution (0.25% trypsin with 0.53 mM EDTA) were purchased from American Type Culture Collection (ATCC). Vero was maintained in DMEM with 10% FBS. Cells were passaged with 0.25% trypsin at a sub-cultivation ratio of 1:10.

2.2.6 Fluorescence Activated Cell Sorting (FACS)

VLPs (wild-type and AF-20) were labeled per manufacturer's instructions with Alexa Fluor 488 (Invitrogen) and an aminated 12mer of polyethylene glycol (PEG, Pierce) in conjunction with EDC (Pierce) to reduce background binding. 1 x 10^6 cells of either Hep3B or hepatocytes were exposed to increasing amounts of VLPs (4 x

10^{12} – 4 x 10^{15}) for 1 hour at 37^{0}C. Cells were then pelleted and washed in FACS buffer (1x PBS, 1% BSA, pH 7.4) before being fixed with 3.7% formaldehyde and resuspended in FACS buffer. Cell samples were immediately analyzed with a FACSCalibur flow cytometer (Becton Dickinson; Franklin Lakes, NJ) equipped with BD CellQuest software at the UNM Shared Flow Cytometry and High Throughput Screening Resource. Data were acquired with the FSC channel in linear mode and all other channels in log mode. Events were triggered based upon forward light scatter, and a gate was placed on the forward scatter-side scatter plot that excluded cellular debris. Samples were excited using the 488-nm laser source, and emission intensity was collected in the FL-1 channel. Fluorescence intensity was determined using the BD CellQuest software and data were plotted using Microsoft Excel.

2.2.7 Confocal Microscopy

1 × 10^{6} cells/mL of either Hep3B or hepatocytes were seeded on sterile coverslips (25-mm, No. 1.5) coated with 0.01% poly-L-lysine and allowed to adhere for 4–24 hours at 37^{0}C. 10 ug of either wild-type or AF-20 VLPs were incubated with the cells for 2 hours at 37^{0}C, washed three times with 1X PBS, fixed with 3.7% formaldehyde (10 minutes at room temperature), and mounted with an anti-fade reagent (SlowFade Gold). Prior to fixation, cells were stained with CellTracker Red CMFDA (Invitrogen) to visualize cytoplasm and Hoechst 33342 (Invitrogen) to visualize the nucleus. Three- and four-color images were acquired using a Zeiss LSM510 META (Carl Zeiss MicroImaging, Inc.; Thornwood, NY) operated in Channel mode of the LSM510 software; a 63X, 1.4-NA oil immersion objective was employed in all imaging. Typical laser power settings were: 30% transmission for the 405-nm

diode laser, 5% transmission (60% output) for the 488-nm Argon laser, 100% transmission for the 543-nm HeNe laser, and 85% transmission for the 633-nm HeNe laser. Gain and offset were adjusted for each channel to avoid saturation and were typically maintained at 500–700 and −0.1, respectively. 8-bit z-stacks with 1024 × 1024 resolutions were acquired with a 0.7 to 0.9-µm optical slice. LSM510 software was used to overlay channels and to create 3D projections of z-stack images, which are depicted here.

2.2.8 Neutralization Assay

Renilla Luciferase Assay System (E2810) was purchased from Promega. 1X Dulbecco's phosphate-buffered saline (D-PBS) was purchased from Invitrogen Life Sciences. G418 disulfate salt and gelatin were purchased from Sigma-Aldrich. This assay was first developed by Tamin et al. [63] and is also described here. Vero cells were grown in culture flasks to approximately 80% confluence and harvested using 0.25% trypsin. Cells were seeded in Dulbecco's Modified Eagle's Medium (DMEM) with 10% fetal bovine serum (FBS) onto pre-treated 96-well plates at a concentration of 8000 cells/well, and allowed to adhere for approximately 18 hours at 37°C. The tested samples were diluted 4-fold serially, and each of the diluted samples was incubated with the diluted pseudotype virus for 30 minutes at room temperature. The pseudotype-serum mixture was then added to the adhered Vero cells in the 96 well plate, and the cells were incubated with the mixture for 90 minutes at 37°C. After incubation, the cells were washed three times with 1X D-PBS; 150 uL of DMEM with 10% FBS was then added to the wells. The plates were incubated for 18 hours at 37°C. Following this incubation, the cells were washed

three times with 1X D-PBS. Cells were lysed and Renilla luciferase was detected per manufacturer's instructions (Promega). Briefly, after washing the cells, 20 uL of the diluted Renilla Luciferase Assay Lysis Buffer was added to each well. The plates were incubated for 1 hour at room temperature with agitation. Using a luminometer, 100 uL of luciferase substrate was added to each well and the luminosity was read integrated over 10 seconds with a 2 second delay.

2.3 Results

2.3.1 Expression and Functional Testing of M18-MS2 VLPs

The first scFv we chose to display of the surface of MS2 is M18, an scFv against anthrax protective antigen. This was a convenient proof-of-concept scFv for the reasons detailed in the introduction of this chapter. Importantly, testing of expression and functionality of M18 on MS2 was accomplished entirely using well-known and documented assays, allowing for rapid testing and determination of success of display.

2.3.1.1 Construction and Expression of M18-MS2 VLPs

The nucleotide sequence of M18 is known, aiding in the creation of M18-MS2 coat fusion proteins. [51] This sequence was entered into the GeneDesign program for optimization of expression in *E. coli* and for design of a series of overlapping primers to cover the entire sequence. To the 5' end of the sequence, we added a *Pst*I site and a small linker consisting of three glycines; to the 3' end, we added a *Bam*HI site to facilitate the cloning of the gene downstream of the MS2 single-chain dimer (SCD) construct in plasmid pDSP62. The sequence of M18 with these elements is presented in Figure 2.1. The overlapping primers were used in equimolar

Figure 2.1 Sequence of M18 with Protein Translation. Noted features are bolded and colorized for emphasis. Blue, *Pst*I (5' end) and *Bam*HI (3' end) restriction sites; orange, flexible linker between variable light and heavy domains consisting of four repeats of GGGS (note the "juggled" nature of the codons in the linker to ensure correct assembly via PCR); red, opal stop codon. Opal was used due to the presence of an amber suppressor in the system.

concentrations and assembled via the Gibson assembly PCR protocol [61], then amplified in a traditional PCR using the two end primers for amplification. The resulting PCR fragment was digested with *Bam*HI and *Pst*I and inserted into pDSP62-PstAm that had been digested with the same enzymes. The resulting construct, named pDSP62-M18, is depicted in the top panel of Figure 2.2. Of note is the amber stop codon that separates the MS2 SCD from the M18 scFv.

The presence of the stop codon separating the SCD from the scFv is vital to successful incorporation of the fusion protein into VLPs. When the stop codon between the SCD and the scFv is removed or is nearly fully suppressed, an abundance of M18-MS2 fusion protein is created but no VLPs are formed. This is most likely due to steric hindrance of the proper folding of coat protein; the scFv is roughly the size of the SCD coat protein, making it quite large with respect to the VLP. Therefore, we placed the stop codon where it is seen in Figure 2.2, and pDSP62-M18 is co-expressed in *E. coli* with a plasmid called pNMsupA. This plasmid expresses a suppressor tRNA that recognizes amber stop codons (UAG) and inserts an alanine; thus, rather than translation terminating, it continues until it encounters another stop codon.

Both pDSP62-M18 and pNMsupA were introduced by transformation into C41(DE3) cells for expression. Upon induction with IPTG, this strain expresses T7 RNA polymerase, allowing for transcription and translation of genes with T7 RNA polymerase promoters. pDSP62-M18 requires this polymerase, and pNMsupA contains the *lac* promoter and is directly induced by IPTG (see Chapter 3 for a schematic depiction of pNMsupA). Cells were cultured, lysed, and VLPs were

A

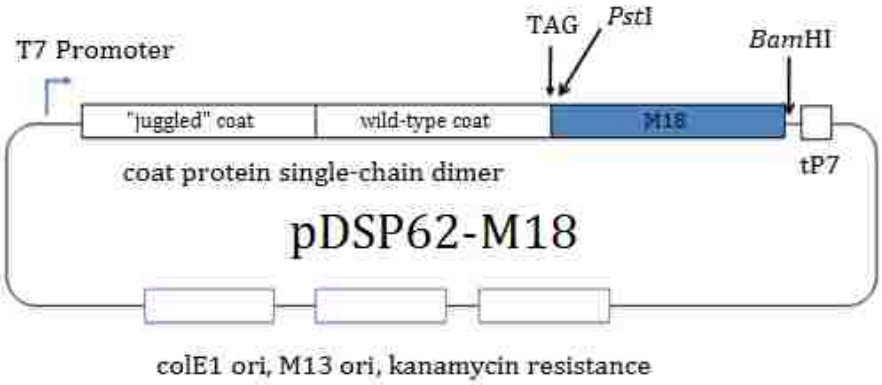

B

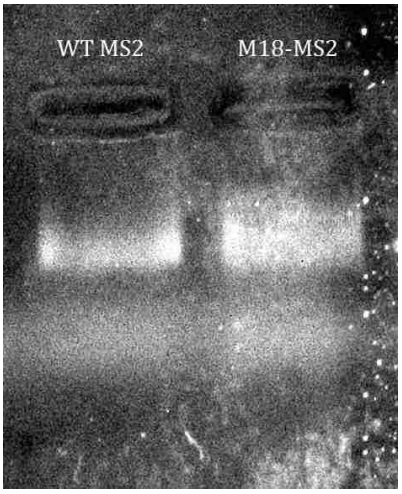

C

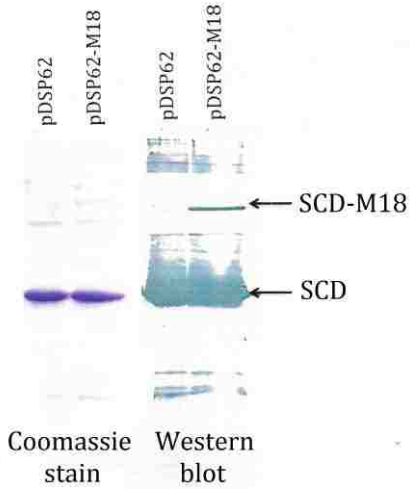

Figure 2.2 Details of M18 scFv Expression on MS2 VLPs. (A) Schematic representation of pDSP62-M18. Note the presence of the amber stop codon that must be read through for successful M18 expression. (B) Agarose gel stained with ethidium bromide indicating the presence of VLPs in both wild-type (WT) and M18 fusion samples. (C) SDS-PAGE results for wild-type and M18 fusion samples. Note the presence of the higher-molecular weight band corresponding to SCD-M18 fusion protein.

purified from the resulting lysate using Sepharose CL-4B column chromatography. The purified VLP was analyzed by phosphate agarose gel electrophoresis, SDS-PAGE, and Western blot to assess both fusion protein production and successful incorporation into MS2 VLPs. Panels B and C of Figure 2.2 show the results. On the left, the agarose gel indicates that VLPs are being properly formed via ethidium bromide staining of the nucleic acid within the capsid. On the right, the SDS gel indicates that wild-type protein is being expressed, though it is difficult to determine if fusion protein is also expressed. To ascertain this, Western blot analysis was performed on the SDS gel. The blot is probed with a primary mouse anti-MS2 antibody and a secondary goat anti-mouse IgG conjugated to horseradish peroxidase (HRP), and it is developed with 3,3',5,5'-tetramethylbenzidine (TMB). The blot reveals both the primary band corresponding to wild-type MS2 coat protein single-chain dimer and a secondary, higher molecular weight band that reacts with anti-MS2 antibodies. It is this band that corresponds to the MS2-M18 read-through fusion protein. These experiments demonstrate several important features of the MS2-M18 fusion VLPs: both wild-type single-chain dimer and SCD-M18 fusion proteins are expressed from the combination of pDSP62-M18 and pNMsupA; VLPs are properly formed; and these VLPs do incorporate the MS2-M18 fusion protein.

2.3.1.2 Functional Testing of M18-MS2 VLPs

To this point, we have demonstrated that we can produce MS2-M18 fusion proteins, that these proteins are available to be incorporated into VLPs, and that VLPs are indeed properly formed in the presence of the read-through protein, at

least suggesting that the MS2 coat portion of the protein is properly folded. It is now necessary to ensure that the M18 scFv is folded properly; that is, that it is functional on the surface of the VLP. Owing to the convenience and availability of anthrax protective antigen, we chose an enzyme-linked immunosorbent assay (ELISA) to show functionality of M18 on MS2.

The ELISA was performed with protective antigen bound to the well plate. Varying amounts of VLPs – either wild-type or M18-bearing – were incubated in the wells, and detection was through a primary mouse anti-MS2 antibody and a goat anti-mouse IgG conjugated to HRP. 2,2′-azino-bis(3-ethylbenzthiazoline-6-sulfonic acid) (ABTS) was used as the detection reagent, providing a colorimetric signal detected by a plate reader. Figure 2.3 shows the results of the assay. At the highest amount of VLP used – 50 ug – there is an approximate six-fold increase in signal from WT to M18-bearing VLPs. At 25 ug VLP, the other amount tested common to both WT and M18-bearing VLPs, there is an approximate three-fold increase in signal. Even at only 5 ug of M18-bearing VLPs, there is still a slight increase in signal from even the 25 ug of WT VLP reading. These data indicate that M18 is in fact expressed in a functional manner on the surface of MS2 VLPs via genetic insertion.

2.3.2 Expression and Functional Testing of AF20-MS2 VLPs

With preliminary studies demonstrating the viability of genetic display of scFvs complete, we turned our attention to the display of a second scFv. This was for several reasons, including that we wanted to ensure that scFv display on MS2 was not limited to one particular scFv. We chose an antibody specific for the AF-20 antigen, which is found expressed on a wide variety of human hepatomas. Prior

Volume M18 VLP (ul @ 5 mg/ml)	OD
10	1.265
5	0.767
2.5	0.555
1	0.304
Volume SCD VLP (ul @ 5 mg/ml)	**OD**
10	0.267
5	0.232

Figure 2.3 ELISA Results for WT (SCD) and M18-Bearing VLPs against APA. Varying amounts of wild-type VLPs (from 50 ug – 25 ug) and M18 VLPs (from 50 ug – 5 ug) were incubated on wells with 500 ng anthrax protective antigen (APA). Signal was detected via optical density at 405 nm on a digital plate reader. There is an approximate six-fold increase in M18 VLP signal over wild-type at 50 ug VLP and an approximate three-fold increase in signal at 25 ug VLP.

work in our laboratory had already demonstrated that a peptide specific for a receptor present on hepatocellular carcinoma cells (HCC) could mediate specific binding and endocytosis of VLPs, so it seemed natural to utilize the same methods to detect scFv-mediated binding of VLPs to HCC.

2.3.2.1 Construction and Expression of AF20-MS2 VLPs

Construction of the AF-20 scFv proceeded much in the same way as M18. The nucleotide sequence of AF-20 was procured from the thesis of Yik Yeung, a graduate student at MIT [54] who constructed an scFv from a known monoclonal antibody to AF-20. Once again, the sequence was modified as in the M18 construct, with a *Pst*I site and a three-glycine linker at the 5'-end, and an opal stop codon with a *Bam*HI site at the 3' end. This sequence was then codon-optimized for expression in *E. coli* via GeneDesign, and GeneDesign was subsequently used to break the sequence into overlapping oligonucleotides for Gibson assembly PCR. The complete sequence is displayed in Figure 2.4. Again, the resulting PCR fragment was digested with *Bam*HI and *Pst*I and ligated into an identically-digested pDSP62 backbone, with the resulting plasmid (pDSP62-AF20) displayed schematically as the top panel of Figure 2.5. Though AF-20 is slightly smaller than M18 (738 vs. 759 nucleotides, 7 amino acids), there is no functional difference in the methods used in its creation and insertion into pDSP62.

As in M18 fusion VLPs, pDSP62-AF20 was introduced into C41 (DE3) cells. However, rather than using pNMsupA, a different suppressor plasmid called pNMsupS2 was co-transformed. This plasmid encodes a suppressor we call supS2, which is an amber-suppressing serine-inserting tRNA. Its design is based on *sup*D,

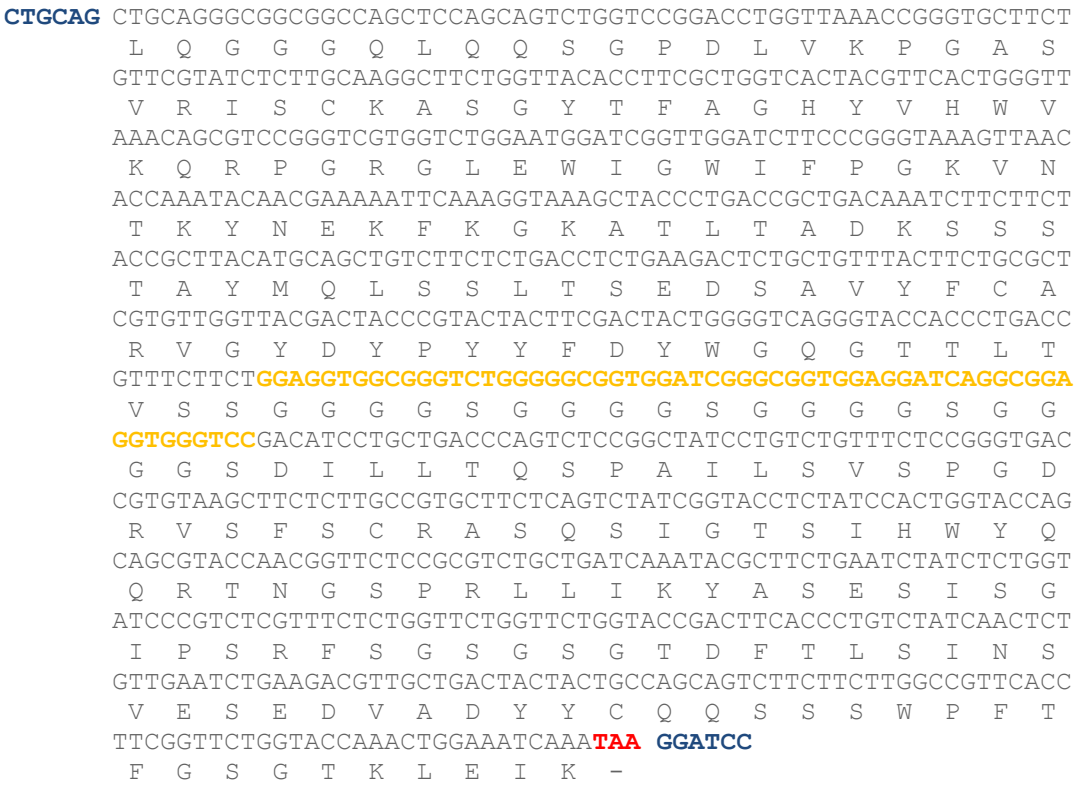

Figure 2.4 Sequence of AF-20 with Protein Translation. Noted features are bolded and colorized for emphasis. Blue, *Pst*I (5' end) and *Bam*HI (3' end) restriction sites; orange, flexible linker between variable light and heavy domains consisting of four repeats of GGGS (note the "juggled" nature of the codons in the linker to ensure correct assembly via PCR); red, opal stop codon. Opal was once again used due to the presence of an amber suppressor in the system.

A

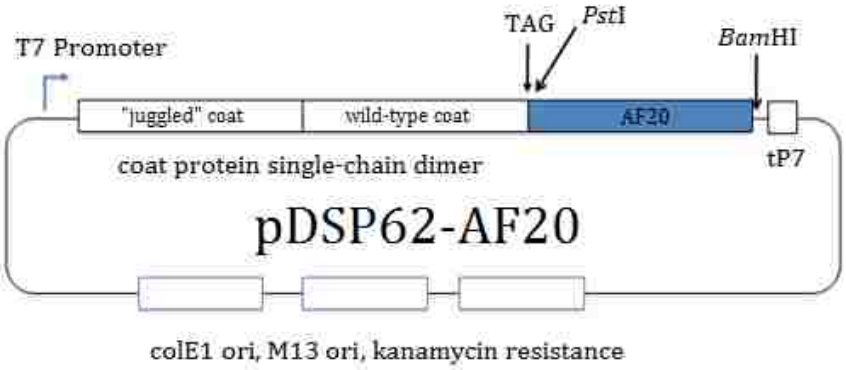

B

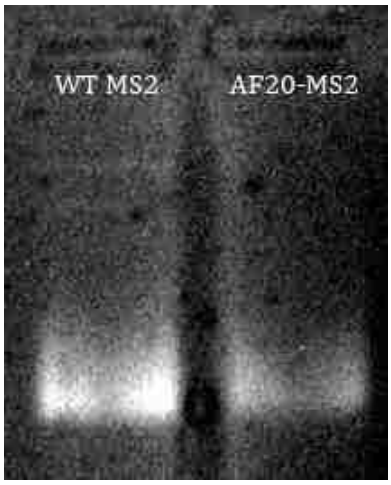

C

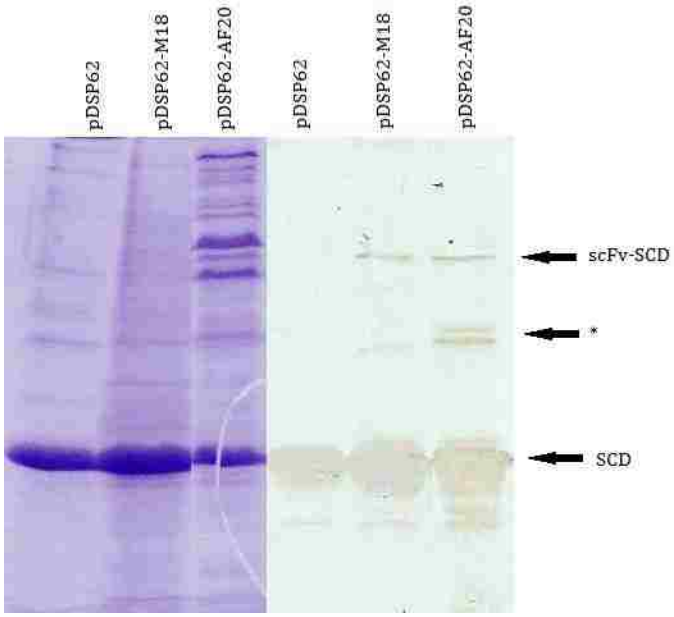

Figure 2.5 Details of AF-20 scFv Expression on MS2 VLPs. (A) Schematic representation of pDSP62-AF20. (B) Agarose gel stained with ethidium bromide indicating the presence of VLPs in both wild-type (WT) and AF-20 fusion samples. (C) SDS-PAGE and Western blot results for wild-type and AF-20 fusion samples. * = non-specific binding.

which is an extremely efficient nonsense suppressor first characterized in 1965. [60] Bacterial strain *Su-1* contains this nonsense suppressor and translates nonsense codons into serine; this was shown through the use of a class of nonsense mutants of bacteriophage f2 known as su-3. These mutants have an amber stop codon in the major coat protein species, resulting in defective particle formation unless this stop codon is suppressed. SupS2 is a modification of supS, which is a direct clone of the sequence of *sup*D. SupS2 was created with a modification to the anticodon loop of the parent suppressor in an attempt to make it less efficient. This goal was accomplished, as supS2 shows slightly more efficient suppression than supA, but nowhere near the ~100% efficiency shown by supS. This has the effect of maximizing the number of scFvs present on the surface of any given MS2 VLP (for a characterization of the valency of displayed scFvs, see below). As before, cells were transformed, grown, induced, then lysed, and the lysates were purified on Sepharose CL-4B columns. Panels B and C of Figure 2.5 show both the agarose gel (to demonstrate proper formation of VLPs) and the SDS-PAGE/Western blot (to demonstrate expression and incorporation of read-through protein) as before in the case of M18.

Again, evidence is provided that VLPs are created that incorporate the MS2-AF20 fusion protein, even when using a different, more efficient suppressor tRNA.

2.3.2.2 Characterization of ScFv Valency on MS2

Suppressor supS2 seems to provide maximum nonsense suppression efficiency for this system. When small-scale 1 mL cultures containing C41(DE3) cells that express pDSP62-AF20 and pNMsupS2 are grown, lysed, separated out into soluble

and insoluble fractions, and analyzed using SDS-PAGE, there is an intense band corresponding to MS2-scFv fusion protein that is visible via both Coomassie staining and Western blot (data not shown). This band is far more intense than the band that appears in the soluble fraction, which is the population of fusion protein that has been incorporated into VLPs. This indicates that a suppressor that is more efficient than supS2 will not actually increase valency of the scFv on the MS2 surface; rather, it will simply function to decrease the amount of wild-type SCD and thus decrease the total yield of particles. Because we have a maximum-efficiency suppressor for this scFv system, we now chose to characterize the valency of expression of scFvs on MS2 by using pDSP62-AF20 and pNMsupS2.

Because precise quantification was unnecessary, we chose to use an approximation system whereby we started with a known concentration of AF-20 VLPs (in this case, 1 mg/ml) and performed serial two-fold dilutions of the VLPs. Each of these dilutions was then subjected to SDS-PAGE followed by Western blot with mouse anti-MS2 primary and goat anti-mouse IgG conjugated to HRP secondary. The resulting blot, developed with TMB, is seen in Figure 2.6. The idea for quantification is that we look for the dilution where the coat protein band matches in intensity to the original, undiluted sample's read-through band. In this case, the sample at 32-fold dilution matched the original read-through band in intensity. Because the starting concentration was 1 mg/ml, this corresponds to 0.03125 mg/ml. Thus, in the original 1 mg/ml dilution, 0.96875 mg was single-chain dimer protein and 0.03125 mg was scFv read-through protein. 0.03125/0.96875 = 0.032, or 3.2% of all coat protein single-chain dimers contain the scFv read-through.

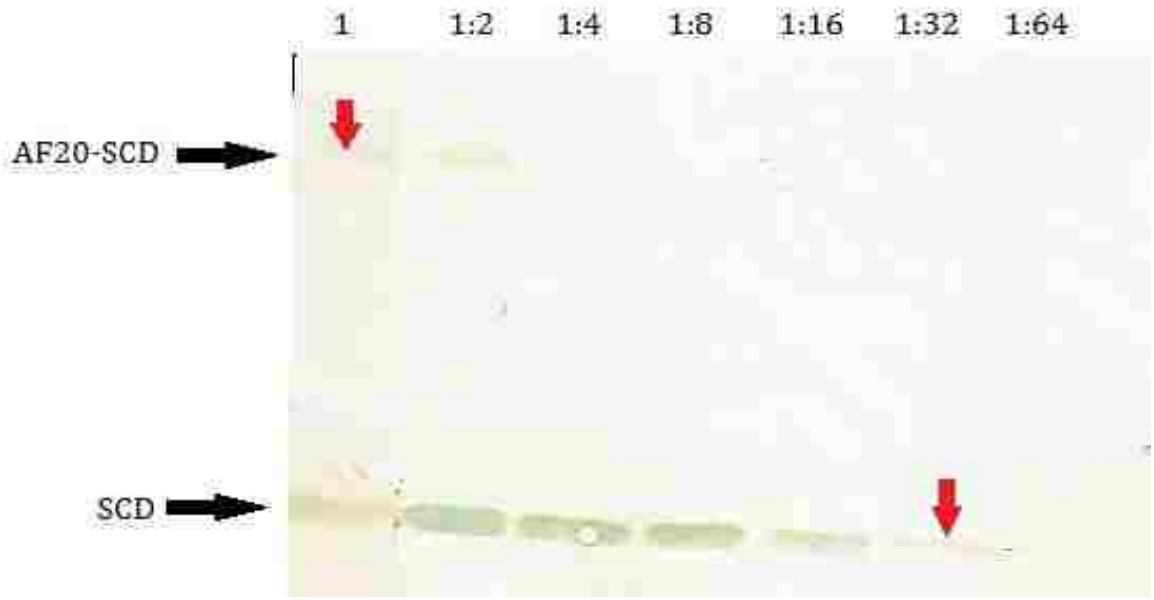

Figure 2.6 scFv Quantification on the MS2 VLP surface. Starting with undiluted VLPs ("1"), serial two-fold dilutions were performed on a sample of AF-20 VLPs. These samples were then subjected to SDS-PAGE and Western blot; the blot is shown here. The point where the diluted single-chain dimer protein most closely matches the original SCD-AF20 fusion band in intensity is where calculations of scFv display density are made; this is marked here at the 1:32 dilution. From this analysis, we determine there are roughly three copies of any given scFv per MS2 VLP.

There are 90 dimers per VLP, so 90*0.032 = 2.9. We can then say that there are roughly three copies of the scFv per VLP. This would appear to be the maximum number of scFvs that can be displayed on the MS2 surface via the genetic insertion strategy we describe here.

2.3.2.3 Functional Testing of AF20-MS2 VLPs

Unfortunately, no soluble form of AF-20 antigen exists; indeed, this has made its characterization difficult to date. [53] This means that a traditional ELISA, as was performed to test the functionality of M18, is not possible in this case. Therefore, we instead took the approach of studying the way wild-type and AF-20-fusion VLPs bind to and interact with live cells. We chose to accomplish this in two separate ways – via confocal microscopy and via flow cytometry.

First we tested whether VLPs displaying the anti-AF20 scFv interacted specifically with hepatoma cells. We used THLE-3, a standard hepatocyte cell line, and Hep3B, a standard hepatocellular carcinoma cell line (both cell lines from ATCC). 10 ug of AF-20-bearing VLPs labeled with AlexaFluor 488 (Invitrogen) were incubated with either cell line for two hours at 37^{0}C in serum-free EMEM; the cells were at 70% confluency for the incubation. Cells were then fixed with 3.7% formaldehyde and stained with CellTracker Red CMFDA to visualize the cytoplasm and Hoechst 33342 to visualize the genetic material in the nucleus. Cells were then imaged with a Zeiss LSM510 META confocal microscope. Figure 2.7 shows the results of this experiment. The images in the panels on the left show only the green channel, where we would expect AlexaFluor 488-labeled VLPs to fluoresce, and the images in the panels on the right are composite images showing the cytoplasm and

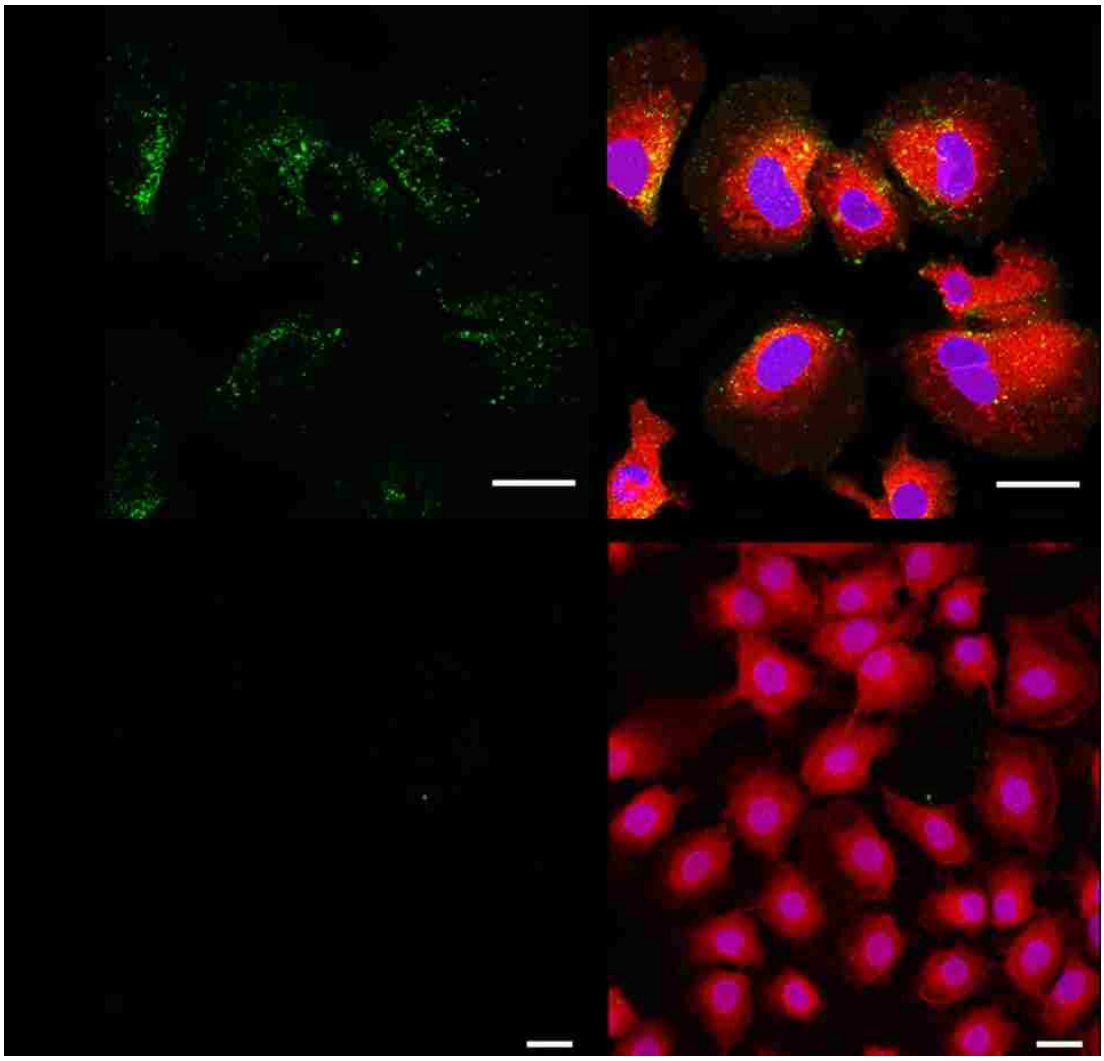

Figure 2.7 Confocal Microscopy of AF-20-bearing VLPs to Hep3B and THLE-3 cells. Cells at 70% confluency were incubated with 10 ug of AlexaFluor 488-labeled AF-20-bearing VLPs for two hours at 37^{0}C in serum-free EMEM. Cells were then fixed with 3.7% formaldehyde and stained with CellTracker Red CMFDA to visualize the cytoplasm and Hoechst 33342 to visualize the genetic material in the nucleus. Cells were then imaged with a Zeiss LSM510 META confocal microscope. Scale bars = 10 um.

nuclei of the cells. It is clear from the images that AF-20-bearing VLPs bind quite strongly to Hep3B cells but not at all to THLE-3 cells. Because Hep3B cells express AF-20 antigen at very high levels and THLE-3 cells do not express any AF-20 antigen, this is strong evidence that our AF-20-bearing VLPs are able to recognize and bind to the AF-20 antigen present on Hep3B cells. Interestingly, though the images seen in all four panels are composites of flattened z-stack images, the individual z-stacks reveal that there are VLPs both on the cellular surface and internalized within cells (images not shown), providing further evidence that the AF-20-bearing VLPs are binding to AF-20 antigen because it is known that this antigen is rapidly endocytosed upon binding. The confocal microscopy provides evidence that AF-20-bearing VLPs are capable of binding to cells differentially depending on the presence or absence of AF-20 antigen. We next wanted to use a more quantitative approach by using flow cytometry. We also wanted to utilize both wild-type and AF-20-bearing VLPs for the flow cytometry experiments. Because the confocal microscopy experiments indicated promising evidence to support the idea that it was the AF-20 scFv on the VLP surface that was allowing targeting of Hep3B but not THLE-3 cells, we wanted to ensure that there was not something inherent in the VLP itself that allowed it to non-specifically interact with only Hep3B cells. Cancer cells are generally known to either display new proteins (as in the case of AF-20) or upregulate expression of normal surface markers [64], [65], so there are more targets to interact with on the surface of a typical cancer cell. Also, because the two cell lines are not absolutely identical (in that the positive cell line is not simply the negative cell line transfected to display AF-20 antigen), it is important to further

ensure that the binding of AF-20-bearing VLPs is due to the AF-20 scFv interacting with AF-20 antigen.

We took 1 x 10^6 of either THLE-3 or Hep3B cells and exposed them to increasing amounts of either wild-type or AF-20-bearing VLPs (4 x 10^{12} – 4 x 10^{15} total particles) labeled with Alexa Fluor 488 for one hour at 37^0C. Cells were then pelleted and washed before being fixed with 3.7% formaldehyde and resuspended in FACS buffer. Cell samples were immediately analyzed with a FACSCalibur flow cytometer. The mean fluorescent intensity of each sample was then taken and plotted for each of the four combinations of VLPs and cell types. The results of this experiment are seen in Figure 2.8. A few things are immediately evident from the graph. First, neither wild-type nor AF-20-bearing VLPs bind particularly well to THLE-3 cells; it is only when there are at least 10^9 more VLPs than cells that any binding at all is detected. This is expected due to the sheer number of particles in the solution at that point; nonspecific interactions between proteins increase as the overall concentration of protein in a solution increases. This changes in Hep3B, as even wild-type VLPs bind better to these than either wild-type or AF-20-bearing VLPs did to THLE-3 cells. However, this occurs once again at extremely high amounts of VLPs. In the range of 4-5 x 10^{14} particles, wild-type VLPs are still binding to Hep3B cells at the same background levels seen with THLE-3 cells. The AF-20-bearing VLPs, though, demonstrate ten-fold higher binding to Hep3B cells than wild-type VLPs do at this point, increasing to about twelve-fold higher binding. This increase is maintained even at very high amounts of VLPs, but it does seem to plateau.

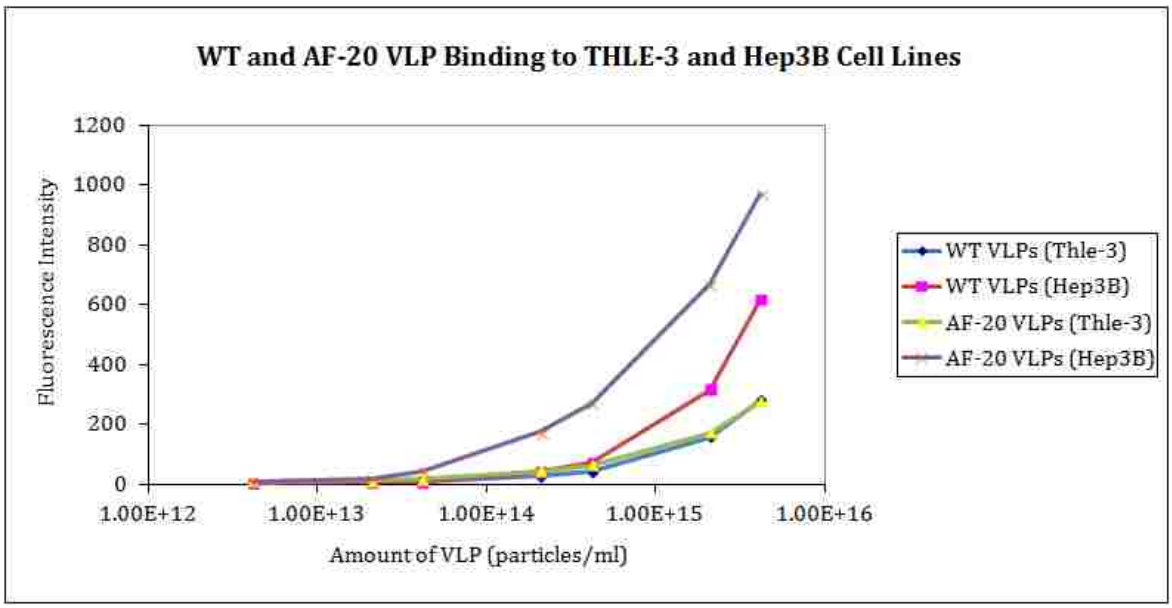

Figure 2.8 Binding of WT and AF-20-Bearing VLPs to THLE-3 and Hep3B cells. The key of the figure indicates which VLP and cell type is being anaylized per color. 1 x 10^6 of either THLE-3 or Hep3B cells were incubated with increasing quantities of either wild-type or AF-20-bearing AlexaFluor 488-labeled VLPs for one hour at 37^{0}C. Cells were then fixed and washed, and mean fluorescent intensity was measure via FACSCalibur. Note that neither WT nor AF-20-bearing VLPs bind particularly well to THLE-3 cells (negative for AF-20 antigen), wherease only AF-20-bearing VLPs bind at lower amounts to Hep3B cells (positive for AF-20 antigen).

Curious about this, we then decided to treat the binding of the wild-type VLPs to each cell line as "background" and subtract that mean fluorescent intensity value from the value measured for the AF-20-bearing VLPs to each cell line, calling this the "signal". The resulting graph is display in Figure 2.9. There is little or no binding of AF-20-bearing VLPs to THLE-3 cells above non-specific background binding in this case. However, for Hep3B cells, AF-20-bearing VLPs bind above background in an exponentially-increasing fashion to the cells, eventually plateauing at extremely high particle numbers. Again, this plateau is not unexpected due to the high number of particles present in the solution at that time. As non-specific interactions increase, it becomes more difficult to separate out specific interactions.

Between the confocal microscopy and flow cytometry experiments, we believe that we have shown sufficient evidence that AF-20 is both present and active when displayed via genetic insertion on the MS2 surface. In the case of the microscopy, both the composite image and the individual z-stack images demonstrate that AF-20-bearing VLPs are capable of binding to and being endocytosed by cells that display AF-20 antigen but not by cells that do not display this antigen. Through flow cytometry, we demonstrate again that AF-20-bearing VLPs bind specifically to Hep3B and not THLE-3 cells. However, we also demonstrate that this binding is quite a bit above standard wild-type particles in the case of Hep3B cells, providing evidence that it is not something inherent in the MS2 VLP that causes binding to Hep3B cells.

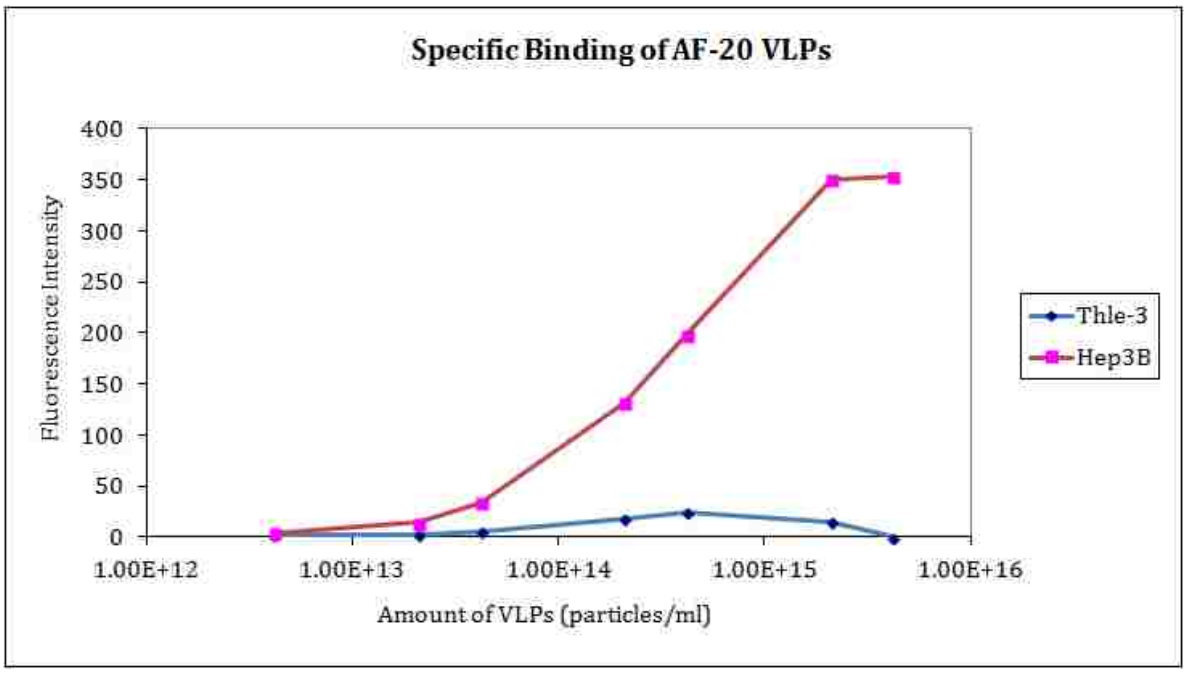

Figure 2.9 Background Subtraction of WT VLP Binding from AF-20-Bearing VLP Binding to THLE-3 and Hep3B Cells. For each cell type from Figure 2.8, the value obtained for WT VLPs was treated as "background" binding and was subtracted from the value obtained for AF-20-bearing VLPs, which were considered "signal". The result is minimal/no binding to THLE-3 cells and an exponential increase in binding to Hep3B cells to a plateau that occurs at extremely high numbers of particles.

2.3.3 Expression and Functional Testing of NiVG- and NiVF-MS2 VLPs

As an additional demonstration of the VLP as an scFv display platform, we utilized scFvs that recognize Nipah virus G and F proteins. The method of their construction differed from that described above for M18 and AF-20. The sequences of the scFvs were developed by Benhur Lee at UCLA from two monoclonal antibodies, mAb26 [59], which recognizes G protein, and mAb66 [58], which recognizes F protein. Dr. Carlee Ashley (Sandia National Laboratories) provided two plasmids that had been synthesized by IDT to contain the sequences of the scFvs. All that was required was the design of two flanking primers for PCR that primed the scFv sequence and contained overhangs that inserted the correct elements (*Pst*I site and small glycine linker, opal stop codon and *Bam*HI site) into the finished PCR product. Figure 2.10 shows the sequences and amino acid translations for both NiVG and NiVF. The top panel of Figure 2.11 schematically shows the plasmids created in both cases; they are identical in both cases to pDSP62-M18 and pDSP62-AF20 except for the single-chain antibody.

As was the case for AF-20, the plasmids to create NiVG- and NiVF-fusion VLPs were introduced (one at a time) into C41 (DE3) *E. coli* competent cells along with pNMsupS2 to provide the amber nonsense suppressor. However, rather than performing a large-scale purification, only a small-scale (1 mL vs. 100 mL) culture was grown, induced, and harvested for VLPs. Instead of a Sepharose CL-4B column, VLPs were purified with a more basic Amicon Ultra-4 Spin Column with a 100 kDa cut-off. The protocol used by Dr. Ashley did not require a more rigorous purification

NiVG

```
CTGCAG    ATGGGCGACATGACCCAGACCCCGGCTTCTGTTGAAGCTGCTGTTGGTGGTACCGTTACC
           M  G  D  M  T  Q  T  P  A  S  V  E  A  A  V  G  G  T  V  T
          ATCAAATGCCAGGCTTCTCAGTCTATCTCTATCTACCTGTCTTGGTACCAGCAGAAACCG
           I  K  C  Q  A  S  Q  S  I  S  I  Y  L  S  W  Y  Q  Q  K  P
          GGTCAGCCGCCGAAACTGCTGATCTACAAAGCTTCTGACCTGGCTTCTGGTGTTCCGTCT
           G  Q  P  P  K  L  L  I  Y  K  A  S  D  L  A  S  G  V  P  S
          CGTTTCTCTGGTTCTGGTTACGGTACCGAATTCACCCTGACCATCTCTGACCTGGAATGC
           R  F  S  G  S  G  Y  G  T  E  F  T  L  T  I  S  D  L  E  C
          GCTGACGCTGCTACCTACTACTGCCAGTCTACCGCTTACTCTACCTCTGGTAACGCTTTC
           A  D  A  A  T  Y  Y  C  Q  S  T  A  Y  S  T  S  G  N  A  F
          GGTGGTGGTACCGAAGTTGTTCTGAAAGGTGAAGAAGGTGGTGGTGGTTCTGGTGGTGGT
           G  G  G  T  E  V  V  L  K  G  E  E  G  G  G  S  G  G  G  G
          GGTTCTGGTGGTGGTGGTTCTGGTGGTGGTGGTTCTTCTGGTGGTGACCTGGTTAAACCG
           G  S  G  G  G  G  S  G  G  G  G  S  S  G  G  D  L  V  K  P
          GGTACCTCTCTGACCCTGACCTGCACCGCTTCTGGTTTCTCTTTCTCTCCGTCTCACTAC
           G  T  S  L  T  L  T  C  T  A  S  G  F  S  F  S  P  S  H  Y
          ATGTGCTGGGTTCGTCAGGCTCCGGGTAAAGGTCTGGAATGGATCGGTTGCATCAACTCT
           M  C  W  V  R  Q  A  P  G  K  G  L  E  W  I  G  C  I  N  S
          GGTTCTAACACCTACATCTACTACGCTTCTTGGGCTGAAGGTCGTTTCATCATCTCTAAA
           G  S  N  T  Y  I  Y  Y  A  S  W  A  E  G  R  F  I  I  S  K
          ACCTCTTCTACCACCGTTACCCTGCAGATGTCTTCTCTGACCGTTGCTGACACCGCTACC
           T  S  S  T  T  V  T  L  Q  M  S  S  L  T  V  A  D  T  A  T
          TACTTCTGCGCTCGTGGTGACTCTATCATCTACTACGGTTCTGACCTGTGGGGTCCGGGT
           Y  F  C  A  R  G  D  S  I  I  Y  Y  G  S  D  L  W  G  P  G
          ACCCTGGTTACCGTTTCTTCTGGTCAGTAA GGATCC
           T  L  V  T  V  S  S  G  Q  -
```

NiVF

```
CTGCAG    ATGGTTATGACCCAGACCCCGGCTTCTGTTGAAGCTGCTGTTGGTGGTACCGTTACCATC
           M  V  M  T  Q  T  P  A  S  V  E  A  A  V  G  G  T  V  T  I
          AAATGCCAGGCTTCTCAGAACATCATCTCTTCTCTGGCTTGGTACCAGCAGAAACCGGGT
           K  C  Q  A  S  Q  N  I  I  S  S  L  A  W  Y  Q  Q  K  P  G
          CAGCGTCCGAAACTGCTGATCTACTACGCTTCTACCCTGGCTTCTGGTGTTCCGTCTCGT
           Q  R  P  K  L  L  I  Y  Y  A  S  T  L  A  S  G  V  P  S  R
          TTCAAAGGTTCTGGTTCTGGTACCCAGTTCACCCTGACCATCTCTGACCTGGAATGCGCT
           F  K  G  S  G  S  G  T  Q  F  T  L  T  I  S  D  L  E  C  A
          GACGCTGCTACCTACTACTGCCAGTCTTACTACTACTCTGGTATCACCTACGGTAACGCT
           D  A  A  T  Y  Y  C  Q  S  Y  Y  Y  S  G  I  T  Y  G  N  A
          TTCGGTGGTGGTACCGAAGTTGTTGTTAAAGGTGAAGAAGGTGGTGGTGGTTCTGGTGGT
           F  G  G  G  T  E  V  V  V  K  G  E  E  G  G  G  G  S  G  G
          GGTGGTTCTGGTGGTGGTGGTTCTGGTGGTGGTGGTTCTTCTGGTGGTGGTCTGGTTAAA
           G  G  S  G  G  G  G  S  G  G  G  G  S  S  G  G  G  L  V  K
          CCGGGTGGTACCCTGACCCTGACCTGCAAAGCTTCTGGTTTCACCCTGTCTTCTTACTGG
           P  G  G  T  L  T  L  T  C  K  A  S  G  F  T  L  S  S  Y  W
          ATGTGCTGGGTTCGTCAGGCTCCGGGTAAAGGTCTGGAACTGATCGCTTGCCTGTACACC
           M  C  W  V  R  Q  A  P  G  K  G  L  E  L  I  A  C  L  Y  T
          AACGGTGCTACCACCTGGTACGCTTCTTGGGTTAACGGTCGTTTCGCTATCTCTCGTTCT
           N  G  A  T  T  W  Y  A  S  W  V  N  G  R  F  A  I  S  R  S
          ACCTCTCGTAACACCGTTGACCTGAACATGACCTCTCTGACCGCTGCTGACACCGCTACC
           T  S  R  N  T  V  D  L  N  M  T  S  L  T  A  A  D  T  A  T
          TACTTCTGCGCTCGTGGTTCTGGTTCTGGTTGGTCTTGGTTCAACATCTGGGGTCCGGGT
           Y  F  C  A  R  G  S  G  S  G  W  S  W  F  N  I  W  G  P  G
          ACCCTGGTTACCGTTTCTTCTGGTCAGTAA GGATCC
           T  L  V  T  V  S  S  G  Q  -
```

Figure 2.10 Sequences of NiVG and NiVF with Protein Translation. Noted features are bolded and colorized for emphasis. Blue, *Pst*I (5' end) and *Bam*HI (3' end) restriction sites; orange, flexible linker between variable light and heavy domains consisting of four repeats of GGGS; red, opal stop codon; green, the pieces of the sequences used to prime against the provided plasmid and add required elements via PCR. Opal was once again used due to the presence of an amber suppressor in the system. Note that in this case the linker is not juggled; though this is feature is necessary for assembly PCR to avoid improper alignment of overlapping oligonucleotides, these sequences were professionally prepared and thus assembly was not performed.

A

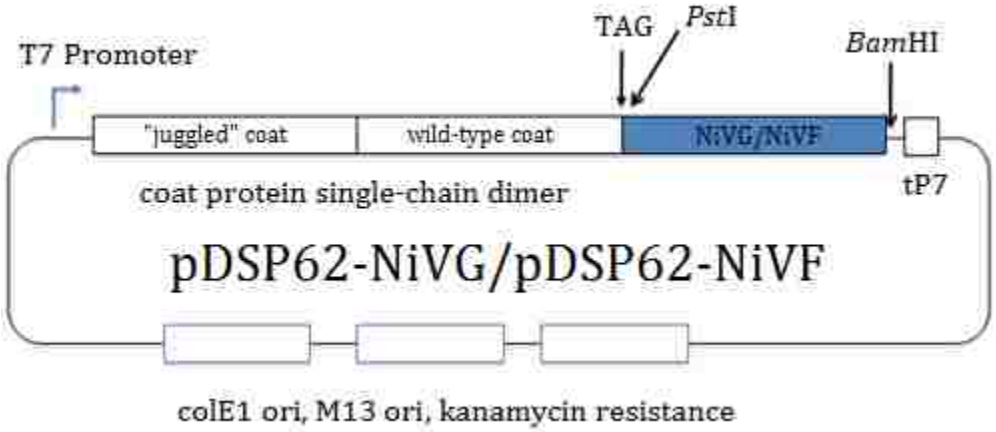

B

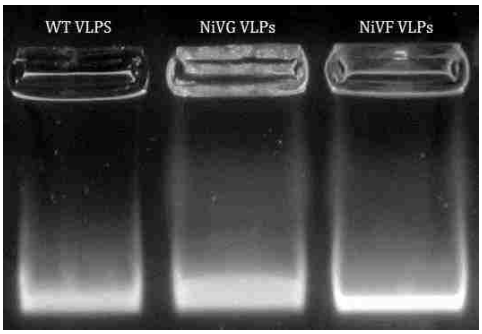

C

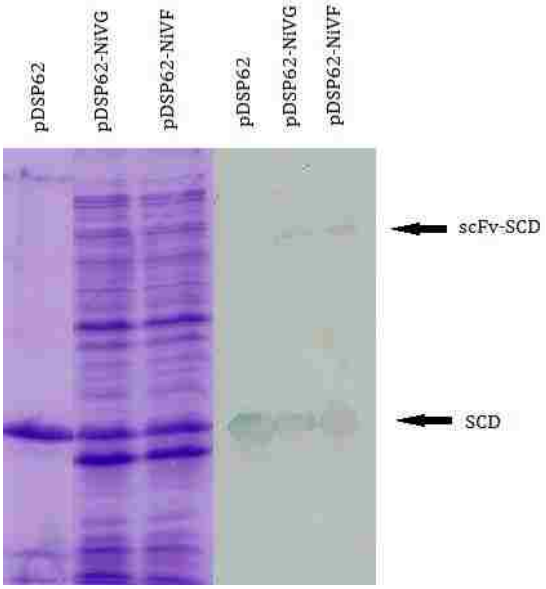

Figure 2.11 Details of NiVG/NiVF scFv Expression on MS2 VLPs. (A) Schematic representation of pDSP62-NiVG/NiVF. (B) Agarose gel stained with ethidium bromide indicating the presence of VLPs in both wild-type (WT) and NiVG/NiVF fusion samples. (C) SDS-PAGE and Western blot results for wild-type and NiVG/NiVF fusion samples.

protocol to initially test the scFv-displaying VLPs for the ability to neutralize Nipah virus, so it was not performed.

2.3.3.1 Functional Testing of NiVG- & NiVF-MS2 VLPs

Because Nipah virus is a BSL-4 agent, the neutralization assays (performed in Dr. Ashley's laboratory) were not conducted with NiV itself, but with vesicular stomatitis virus pseudotyped with Nipah G and F proteins. The recombinant virus expresses luciferase when it infects cells, making it possible to measure neutralization as simple inhibition of luciferase expression. Varying amounts of NiVG- or NiVF-bearing VLPs were incubated with a constant amount of virus, and then these viruses were used in a round of infection of cells. Cells that become infected with the pseudotyped VSV fluoresce due to luciferase expression, allowing the measurement of neutralization of infection by measuring relative light units (RLU). The results of the first neutralization experiment are shown in Figure 2.12. In the figure, VLP-scFv26 is NiVG-bearing VLPs and VLP-scFv66 is NiVF-bearing VLPs. As the concentration of either particle increases, neutralization (as measured by a decrease in RLU) also increases. Though anti-NiVG-bearing VLPs seem to be slightly better at neutralizing pseudotyped VSV than anti-NiVF-bearing VLPs, both types of particles are capable of neutralizing the virus.

As mentioned earlier, the scFvs to G and F protein are derived from monoclonal antibodies. The scFvs themselves also exist in soluble form. Therefore, another question we wanted to explore was how well the NiVG- and NiVF-bearing VLPs neutralize the pseudotyped VSV compared to these other known neutralizers. Figure 2.13 shows the results of this experiment. Here, the concentration of the

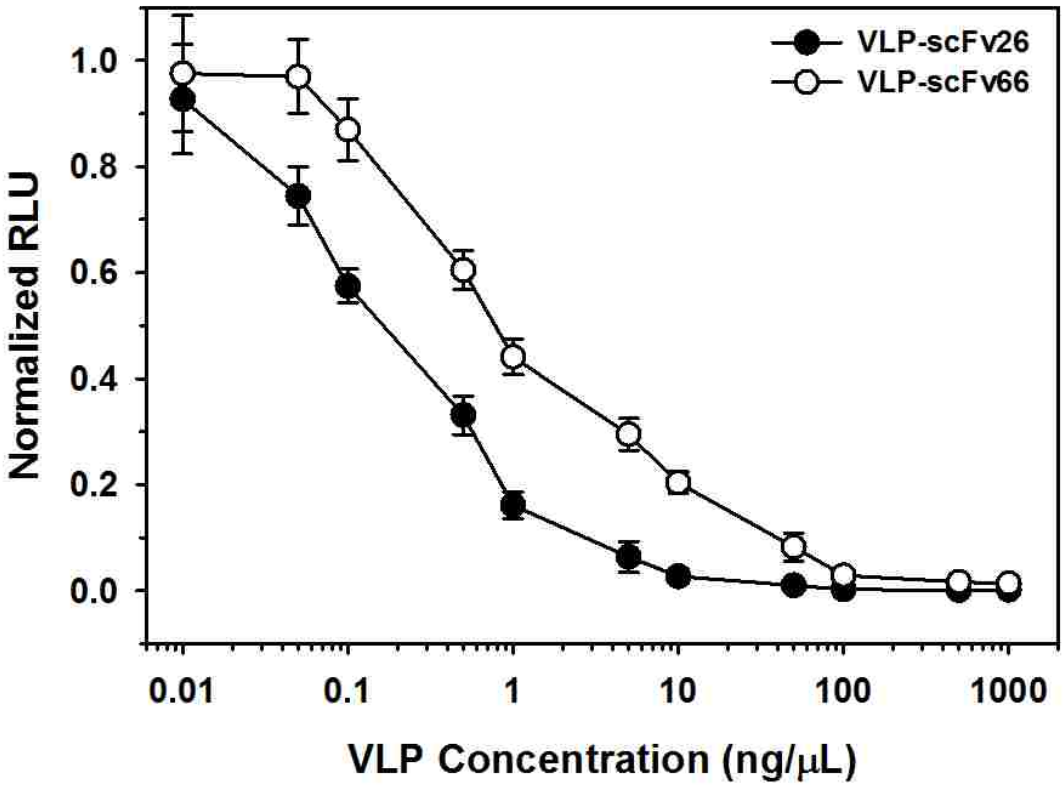

Figure 2.12 Neutralization of Pseudotyped VSV by NiVG- or NiVF-bearing VLPs. Varying concentrations of VLPs were incubated with a single concentration of pseudotyped VSV (designed to express Nipah G and F proteins and express luciferase), and then these pseudotyped viruses were used in an infection. Relative light units (RLU) due to infection of cells by non-neutralized VSV are measured in each case. There is neutralization in both cases, though neutralization by NiVG-bearing VLPs is slightly better than neutralization by NiVF-bearing VLPs. VLP-scFv26 = NiVG-MS2 VLP; VLP-scFv66 = NiVF-MS2 VLP.

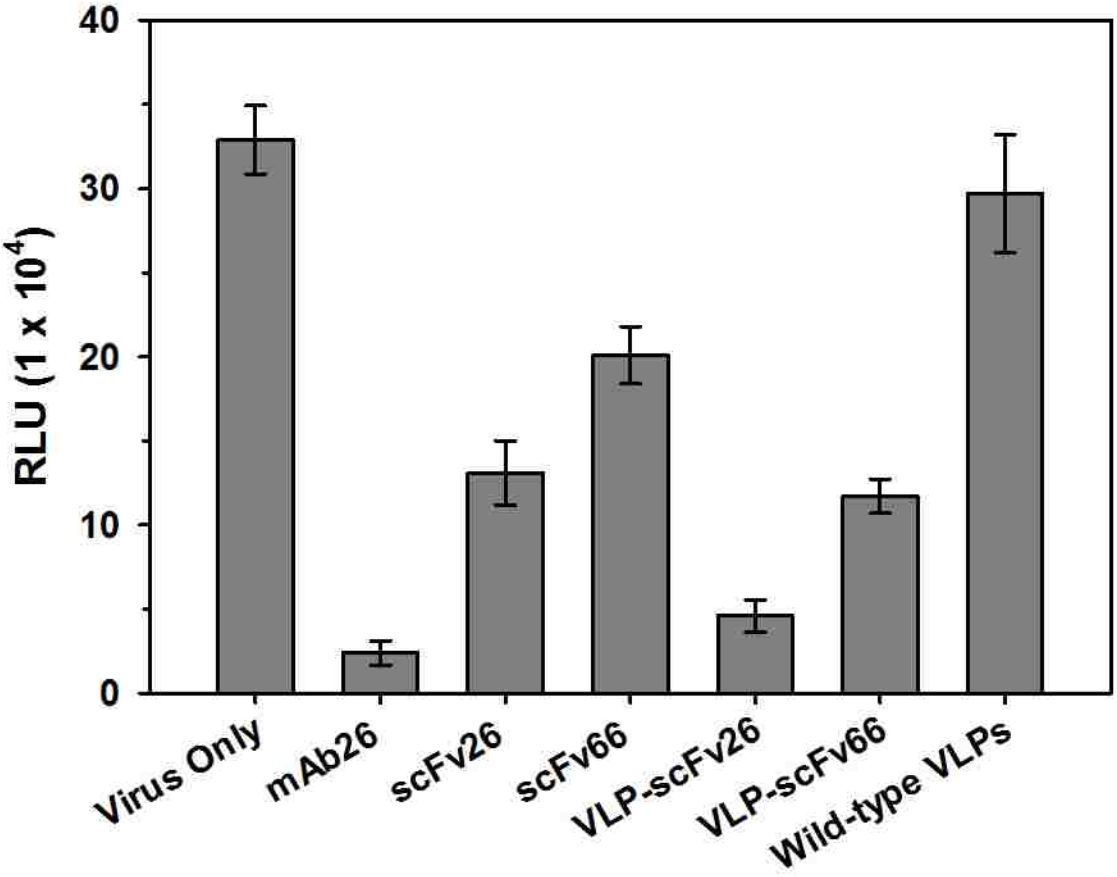

Figure 2.13 Neutralization of Pseudotyped VSV by Various Neutralizers. A constant 1.5 ng/ul concentration of each potential neutralizer of pseudotyped VSV (shown on the horizontal axis) was used with a constant concentration of VSV, followed by a round of infection. Relative Light Units (RLU) was measured from luciferase expression to determine neutralization. mAb26 = G-specific monoclonal antibody (scFv parent); scFv26 = NiVG-specific scFv; scFv66 = NiVG-specific scFv; VLP-scFv26/scFv66 = NiVG/NiVF-bearing MS2 VLPs.

potential neutralizer was held constant at 1.5 ng/ul and the same neutralization assay as in Figure 2.12 was performed. "Virus only" provides a baseline measurement of RLU. Using wild-type VLPs in an attempt to neutralize the virus is almost as ineffective as using nothing at all. Once again, "26" refers to G protein-specific antibodies and "66" refers to F protein-specific antibodies. The best neutralizer is the monoclonal antibody to G protein; this is not surprising because the scFv to G protein was previously shown in Figure 2.12 was more effective than the one to F protein, and the monoclonal antibody is divalent instead of monovalent like the scFv. Both soluble scFvs – scFv26 and scFv66 – are effective in neutralizing the virus, but not as effective as mAb26. However, when displayed on the MS2 surface, scFv26 is nearly as effective a neutralizer of pseudotyped VSV as mAb26, and is far better than soluble scFv26. Even scFv66, which in soluble form is a weaker neutralizer, is effective when displayed on the VLP surface, showing a roughly three-fold decrease in RLU compared to virus alone. It is clear that both NiVG- and NiVF-bearing VLPs are capable of binding to and neutralizing pesudotyped VSV from these data.

2.3.4 Proof-of-Concept of Potential to Affinity-Select scFv-VLPs

So far, we have shown four cases of display of specific, functional scFvs on the surface of MS2. This suggests that the MS2 VLP may be able to serve as a platform for display of scFvs generally and opens the possibility of display of scFv libraries. Much like the display of random peptide libraries to find specific binders (for example, to an antibody of interest, see Chapter 3), display of random libraries of scFvs could allow for the discovery of novel scFvs to specific targets. These scFvs

could then have a variety of uses, including detection and treatment of disease. The simplicity of the synthesis and assembly of the MS2 VLP also allows for the possibility of performing all of the above work *in vitro* and automating the process.

As mentioned in the Introduction, the foundation of the ability to affinity-select any heterologous-peptide-bearing VLP (from random six-amino acid peptides to scFvs) is that the MS2 VLP encapsidates the RNA that directs its synthesis. This allows direct recovery of this sequence by reverse transcription and PCR amplification, followed by reinsertion into an expression vector for further rounds of selection. We have shown in previous work that both wild-type MS2 VLPs and MS2 VLPs that contain heterologous peptides in their AB-loops encapsidate the RNA that encodes their synthesis. [27], [28] Though we anticipate that this is the case for all peptide insertions or fusions into the MS2 VLP coat protein, this must be confirmed for the case of scFvs to even allow for the possibility of the display and affinity selection of random scFv libraries.

2.3.4.1 Northern Blot Analysis of scFv-Bearing VLPs

To determine whether scFv-bearing VLPs are able to encapsidate the RNA that directs their synthesis, we first decided to simply extract the RNA from within the VLP and subject it to formaldehyde gel electrophoresis and Northern blot using a biotinylated negative-sense anti-MS2 RNA probe and detecting with Ambion's BrightStar development kit. The results of this experiment are seen in Figure 2.14. All samples experienced some form of degradation of RNA (even the smallest contamination with RNase will cause this), but the overall trend is clear. The wild-type single-chain dimer control runs at the indicated arrow, and the scFv fusion

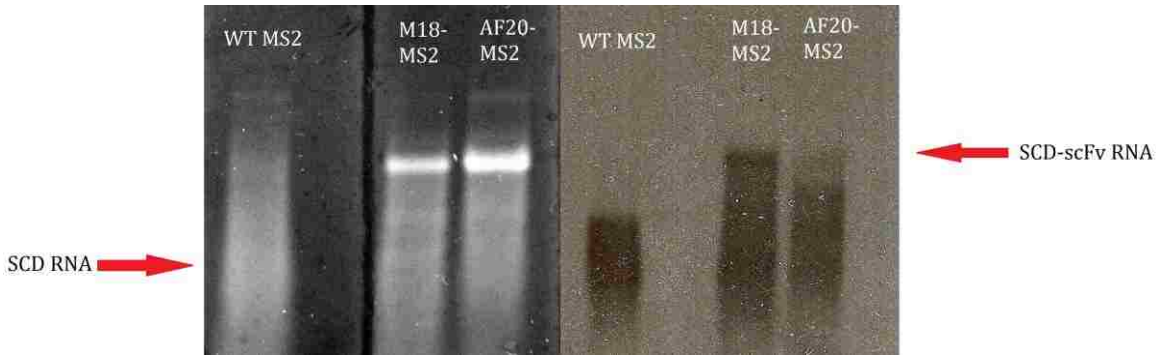

Figure 2.14 Ethidium Bromide-Stained Agarose Gel and Northern Blot of scFv-MS2 Fusion RNA. On the left is the ethidium stained gel, and on the right is a Northern blot of the same gel. The Northern was probed with anti-MS2 biotinylated RNA and developed using Ambion's BrightStar kit. Though there is some degradation in all samples, it is clear that the scFv-MS2 fusion constructs exhibit a prominent, large band that is positive for MS2 RNA, indicating that the fusion VLPs do in fact package the RNA that directs their synthesis.

constructs (shown here are M18 and AF-20) run substantially slower, consistent with their higher molecular weight. This is the expected case, as an scFv is roughly the size of the single-chain dimer; thus, in this fusion, the RNA should roughly double in size.

2.3.4.2 RT-PCR of Mock Affinity-Selected M18

Next we subjected the scFv-VLP to a mock affinity selection protocol to determine whether its packaged RNA could be recovered and amplified. To do this, we utilized the M18-bearing VLP due to the fact that protective antigen was available and made performing the experiment convenient. For a detailed treatment of the affinity selection protocol used, see Chapter 3. Briefly, 500 ng of protective antigen was placed in a well of an ELISA plate and incubated at 37^{O}C overnight. The next day, varying amounts of M18-bearing VLPs were incubated in the wells for 2 hours following blocking. After washing, the bound VLPs were eluted using acid elution, neutralized, and then used directly in a reverse transcription (RT) reaction. This RT reaction was then used in a PCR reaction in an attempt to amplify the coat protein-scFv fusion RNA. The results of this experiment are shown in Figure 2.15. The coat protein-scFv fusion RNA should run at approximately 1500-1600 base pairs on an agarose gel, and at 100 ug and 1 ug of M18-bearing VLPs, we note a band after PCR amplification. This band was not sub-cloned and put back into a vector for expression, but that it is the right size (and there were no such bands in negative controls, not shown) is promising. A more thorough characterization is required, but it would appear as though full-scale random scFv library display via genetic insertion on MS2 should be possible.

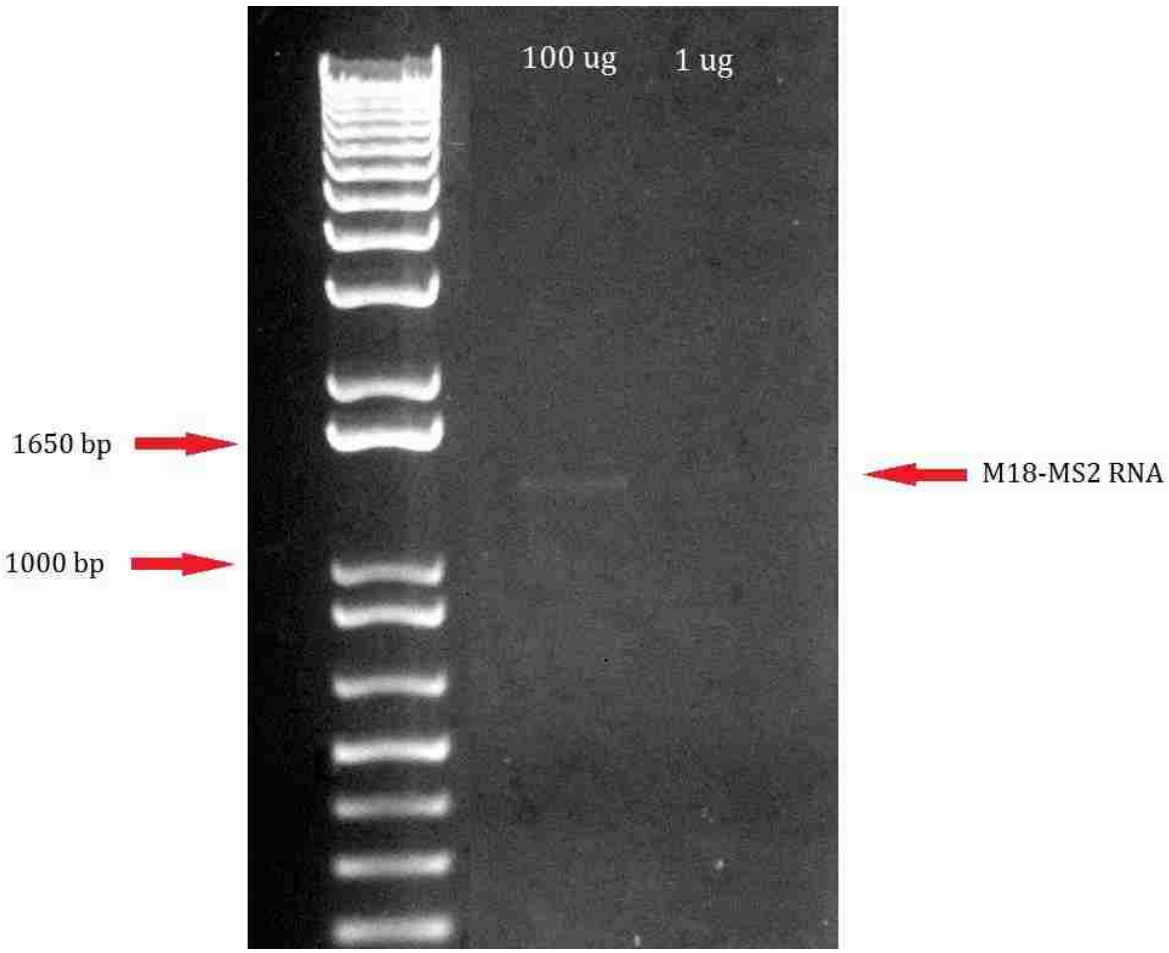

Figure 2.15 RT-PCR of Mock Affinity Selected M18-Fusion VLP RNA. 500 ng of protective antigen was placed in a well of an ELISA plate and incubated at 37^{O}C overnight. The next day, either 100 ug or 1 ug of M18-bearing VLPs were incubated in the wells for 2 hours following blocking. After washing, the bound VLPs were eluted using acid elution, neutralized, and then used directly in a reverse transcription (RT) reaction. This RT reaction was then used in a PCR reaction for amplification. The M18-MS2 RNA fusion molecule is marked on the gel.

2.4 Discussion

In this study, we constructed four scFvs: two we constructed ourselves by assembly PCR of overlapping synthetic oligonucleotides (M18 and AF-20). Two others were synthesized commercially and then cloned by us into pDSP62-PstAm. In all four cases, the scFv was fused to the coat protein of MS2 via genetic insertion and displayed on the surface of the fully-formed MS2 VLP. In each case, we showed that the scFv was both present and functional (folded properly) on the surface of the VLP. This was accomplished using methods ranging from simple ELISA (M18) to binding to cells (AF-20) to neutralization of pseudotyped VSV (NiVG/F). This was important because we were unsure whether the folding of coat protein and its assembly into a VLP would be significantly impaired by the presence of a 250 amino acid protein at the C-terminus.

We limited the number of scFvs on the VLP surface via a system of nonsense suppression. By separating the coat protein and the C-terminally-fused scFv with an amber stop codon, we can control the number of coat-scFv fusion proteins that are created. The efficiency of nonsense suppression is influenced by a variety of factors, including the concentration of the suppressor, the sequence of the suppressor's anti-codon loop, and the context under which the stop codon appears within the mRNA. [66] We took the approach of changing the suppressor's anti-codon loop because it was the most straightforward for us. The relevant suppressors, including the amino acid that they insert into the polypeptide chain, the structures of their anticodon loops, and their general suppression efficiencies with regard to amount of scFv fusion protein incorporated into VLPs, are documented in Table 1.1. It has been

	Inserted Amino Acid	Anticodon Loop Structure	Suppression Efficiency
supA	alanine	5' – AU**AUC**AU – 3'	~1-2%
supS	serine	5' – CU**AUC***A*A – 3'	~100%
supS2	serine	5' – CU**AUC***G*A – 3'	~3%
supS3	serine	5' – CU**AUC***C*A – 3'	~1-2%

Table 1.1 Nonsense Suppressors Created. supA represents the wild-type *E. coli* alanine tRNA with a mutation in the anticodon loop (GGC -> AUC) to allow for it to recognize amber stop codons. Its suppression efficiency is low, roughly 1-2%. SupS, supS2, and supS3 are all related suppressors. SupS, also known as *sup*D in the literature, is a naturally-occuring amber nonsense suppressor that inserts serine. In our system, its suppression efficiency is near 100%, allowing little to no expression of wild-type coat protein. This results in no VLP formation and, as such, supS is not used in this work to create functional VLPs. SupS2 and supS3 are both modifications of supS at a single base in the anticodon loop, shown in blue in the table. SupS2 represents a change from A->G at this position, which is a purine->purine transition and is expected to have less impact on suppression efficiency than supS3, which is A->C and represents a purine->pyrimidine shift. Indeed, the while severely impacted, the efficiency of supS2 (roughly 3%) is greater than that of supS3, whose efficiency is similar to supA at 1-2%.

demonstrated that changes to the anti-codon loop of a tRNA (not even changes to the anti-codon itself) can have very drastic effects depending on where the mutation is made. Simple pyrimidine-to-purine transversions can completely ablate suppression efficiency. Suppression efficiency can be exquisitely controlled in most cases. In our specific case, this finely-tuned control is not possible because of the limited number of scFvs that are tolerated on the VLP surface when using our genetic insertion strategy. We find via SDS-PAGE analysis that, even at lower levels of suppression, a large amount of fusion protein ends up in the insoluble fraction of a cell lysate. This indicates that as many fusion molecules as are able are already being utilized, and our system would not benefit from raising the suppression efficiency (though lowering it to allow for less copies of scFv would be technically possible). We determined that roughly three copies of any given scFv are present on the surface of the VLP using this display method.

We also showed that the MS2 VLP is capable of encapsidating the RNA that directs its synthesis in the case of scFv fusion constructs, and we demonstrated that this sequence can be recovered and amplified, thus suggesting the possibility of displaying scFv libraries on the surface of MS2 via genetic insertion. Because the RNA that directs the synthesis of the coat-scFv fusion protein is encapsidated, libraries of scFvs displayed on MS2 VLPs can be subjected to affinity selection against specific targets. This is important for a number of reasons. First and perhaps most importantly, the simplicity of MS2 VLPs would allow for the creation of and affinity selection from these libraries entirely *in vitro*. This is accomplished via a technology known as emulsion transcription/translation, developed by Tawfik et al.

[67] In this system, a population of DNA molecules is separated into individual bacterium-sized aqueous compartments within an oil emulsion. These compartments contain the necessary machinery for both transcription and translation; also, because the process ensures that there is only one DNA molecule per compartment, the genotype-to-phenotype link essential to affinity selection is preserved. Once the transcription and translation are complete, the emulsion can be broken and the resulting VLPs can be used in affinity selections just as VLPs generated *in vivo*. ScFv libraries have been displayed on other systems, including bacteriophage fd and M13 [46], [68], but these systems require expression in bacteria for proper assembly of the phages. The possibility that MS2 VLPs could be produced entirely in vitro makes it easier to produce high complexity libraries and introduces the possibility of automation. Furthermore, the phages incur differential fitness costs as a function of the individual scFvs each expresses, so that the frequency of specific scFvs in a population of affinity selectants does not necessarily directly reflect their affinity for the target. The simplicity of the MS2 VLP raises the possibility that such fitness costs, if they exist, will be lower.

Additionally, using random libraries of scFvs allows for the possibility of the discovery of novel scFvs against specific targets. Libraries of scFvs can be created in many different ways, including amplification of B-cell variable heavy and light domains via primers [46] and randomization of CDRs on an scFv scaffold [47]. This means that the potential complexity of an scFv library is quite large ($>10^{12}$), and the odds of discovering novel scFvs via affinity selection increase as library complexity increases. Of course, overall library complexity of an *in vitro*-generated scFv library

is limited by the number of aqueous compartments that can be produced in a convenient volume, and overall complexity of an *in vivo*-generated library is limited by transformation efficiency. However, especially through the use of several *in vitro* emulsions in parallel, libraries of sufficient complexity to discover novel scFv binders to a target can be generated.

Using our MS2 VLP system to display scFvs – especially scFvs that have been discovered via affinity selection from potentially libraries – has a number of advantages. Chief among these is the potential use of the VLP as a targeted drug delivery vehicle. The MS2 VLP is essentially hollow, and it can be loaded with a variety of cargoes. Indeed, Ashley et al. loaded MS2 VLPs with cargoes ranging from imaging agents (Q-dots) to cytotoxins like doxorubicin, cyclin-inactivating siRNAs, and ricin A-chain. [26] This means that an scFv can be displayed on the MS2 surface, the MS2 VLP can be loaded with some cargo, and the particles can be targeted directly to cells.

We also showed that MS2 VLPs bearing scFvs against Nipah virus G and F proteins are capable of neutralizing pseudotyped VSV. This is important because it grants yet another application to our scFv-displaying VLPs. The fusion VLPs were capable of neutralizing VSV Nipah pseudotypes at a level near monoclonal antibodies; in both cases, they were more effective neutralizers than soluble scFvs, presumably because of the avidity effects associated with simultaneous display of several copies of the scFv on each VLP.

Overall, we have shown in this study that scFvs presented on the MS2 VLP surface are functional and impart a variety of potential uses to the VLP. Practically,

we have shown evidence for our scFv-bearing MS2 VLPs having application in imaging cells, separating cells that express an antigen from those that do not, and neutralizing pseudotyped virus. We have also given evidence that suggests that creation and affinity selection of random scFv libraries on MS2 is possible and has many exciting applications.

.

Chapter 3: Random Peptide Library Display and Affinity Selection

3.1 Introduction

The process of affinity selection, or biopanning, is an extremely powerful technique that enables us to start with vast random libraries of peptides of various sizes and pull from those libraries peptides that interact with high affinity to a specific target molecule, e.g. an antibody. Figure 1.4 (Chapter 1) graphically depicts the process of affinity selection, and the details of the methodology are presented in the Materials and Methods and Results sections of this chapter. The rest of this introduction will focus on specific pathogens and the neutralizing monoclonal antibodies we used as targets in affinity selection experiments.

Neisseria gonorrhoeae. 2C7 and 2-1-L8 are two antibodies that recognize lipooligosaccharides found on the surface of *N. gonorrhoeae*, the causative agent of gonorrhea. [69], [70] Gonorrhea is a sexually transmitted disease that the CDC estimates is contracted by roughly 700,000 people per year in the United States. [71] In women, untreated gonorrhea can cause pelvic inflammatory disease (PID), which can cause the loss of the ability to bear children; in men, untreated gonorrhea can cause epididymitis, which can cause the loss of the ability to father children. In both men and women, severe cases of gonorrhea infection can spread to the blood and become systemic and life-threatening. There is also evidence that infection with *N. gonorrhoeae* can actually leave an individual more susceptible to HIV-1 infection.

As a bacterial infection, gonorrhea is often cured through the prescription of antibiotics. However, since the early 2000s, drug-resistant strains of *N. gonorrhoeae* have begun presenting in clinical infections. [71] To date, *N. gonorrhoeae* has been

found to be resistant to sulfonamides, penicillin, tetracycline, and ciprofloxacin. Current therapy involves an extremely potent dual antibiotic regiment of cephalosporin ceftriaxone and either azithromycin or doxycycline. Because the United States relies on treatment rather than prevention of infection to control the bacterium, this is particularly worrisome. Therefore, there has been a move to develop vaccines to *N. gonorrhoeae* to encourage prevention rather than treatment. However, there are specific challenges to developing vaccines to *N. gonorrhoeae* that make it less than straightforward. For a variety of reasons, reviewed by Zhu et. al [72], gonorrhea infection does not seem to providing lasting immunity after clearance of infection: antibodies are not long-lived or often stored in memory [73], [74] and *N. gonorrhoeae* is capable of varying displayed antigens. [75] Though the lipooligosaccharides (LOS) can also be varied on the surface of the bacterium, variations often make the bacterium less pathogenic, making these prime vaccine targets.

It was found through a series of experiments by Gulati et al. that 2C7 probably interacts with the lactosyl substitution of heptose 2 on the oligosaccharide portion of the LOS. [69] This epitope is found in over 95% of all known strains of gonorrhea. In that same study, it was demonstrated that the binding of 2C7 to *N. gonorrhoeae* neutralizes the bacterium in two separate ways – first, via opsonization and complement-mediated killing, and second, via promotion of phagocytosis by human polymorphonuclear leukocytes (PMNLs). As little as 4.5 ug of 2C7 was capable of 100% killing *in vitro* of strains of gonorrhea expressing the 2C7 epitope, and those

same strains showed near-complete (~93%) ingestion by PMNLs when first opsonized with 2C7.

O'Connor et al. demonstrated that 2-1-L8 also binds to the heptose 2 lactosyl substitution on the OS of *N. gonorrhoeae*. [76] However, this group also determined that optimal binding of 2-1-L8 did not occur without a cyclic phosphoethanolamine substitution as well. This epitope is present in 3% of gonorrhea strains, and interestingly, 2-1-L8 typically only binds to strains of *N. gonorrhoeae* that are resistant to killing via normal human serum. [77] Though the mechanism of killing (via opsonization and both complement activation and promotion of phagocytosis) is the same as 2C7, it is clear that the specific 2-1-L8 epitope is not exposed in all infections, and that when it is exposed, the bacterium typically no longer exposes the 2C7 epitope (though this is not true in all cases).

If we create peptide mimics of the epitopes that 2C7 and 2-1-L8 bind to on the lipooligosaccharide, we may be able to stimulate an immune response that will create long-lasting, neutralizing antibodies to *N. gonorrhoeae*.

Dengue virus. MVDP-55A and GTX29202 are antibodies against a Dengue virus surface protein known as envelope, or E protein. Dengue virus is transmitted to humans from mosquitoes (most often *Aedes aegypti*) via bite. [71] There are four serotypes of Dengue virus, known by number (DENV 1, DENV 2, DENV 3, and DENV 4). Infection with Dengue can be sub-clinical, produce symptoms similar to the common cold or influenza infection, or in severe cases, result in Dengue hemorrhagic fever (DHF). DHF is extremely dangerous and can lead to Dengue shock syndrome (DSS), which is the leading cause of mortality in Dengue infection.

[78] Risk for development of DHF and DSS actually increases with a second Dengue infection of a different serotype in the same person, a condition known as antibody-mediated enhancement (ADE). [79] It has been shown that, after clearance of the initial Dengue infection, a second infection with a different serotype will cause stimulation of the memory response to the first serological infection. However, in addition to neutralizing antibodies, non-neutralizing antibodies actually facilitate the second Dengue serotype's ability to infect macrophages through FcGR, leading to a more widespread infection. [79] There is also no effective treatment for Dengue infection, even in the case of more severe disease. [71] This means that, while a vaccine against Dengue virus is of high importance, it also comes with an inherent risk – if the vaccine fails to protect against all four Dengue serotypes, it may actually do more harm than good as it exposes patients to a more severe form of infection with an unprotected serotype. MVDP-55A and GTX29202 were chosen as antibodies against which to perform selections in part because these two antibodies are capable of reacting with all four Dengue serotypes via ELISA, making them ideal targets for identification of a peptide that, upon immunization, can lead to a protective antibody response against all four Dengue serotypes.

Both MVDP-55A and GTX29202 have been extensively characterized with regard to the specific epitopes to which they bind, and both antibodies show very similar binding affinity and epitope mapping for all four Dengue serotypes. [80], [81]Both antibodies are roughly ten-fold better binders to DENV-1 and DENV-3 than to DENV-2 by measured K_D value; in the literature, neither antibody binds especially well to DENV-4, with K_D values over 3000. Both antibodies even map to overlapping

epitopes, with the same five residues on the E3 protein (L306, K308, G381,I387, and W389) critical to binding for each mAb for DENV-3. For DENV-2, the epitopes still overlap, but they consist of different vital residues (K310, I312, and W391). The epitope size is smaller for DENV-2 than DENV-3 in both cases, indicating a possible reason for the lower K_D values. Gromowski et al. have also shown that, while both antibodies are capable of neutralizing DENV-3, this does not occur until the virus is near-100% opsonized with antibody. [81] This corresponds to a needed concentration of roughly 10 nM antibody to completely neutralize ~50 pfu of Dengue.

***Staphylococcus aureus*.** MCA5792 is a monoclonal antibody against *Staphylococcus aureus* peptidoglycan, the primary component that makes up the cell wall of the bacterium. *S. aureus* is a common bacterium that is found in many places, including on the skin and mucus membranes of humans. Most strains of *S. aureus* are not dangerous, but some are capable of causing infection, including sepsis, pneumonia, endocarditis, and osteomyelitis. These are all serious infections that can lead to death. [71] In addition, strains of *S. aureus* exist that are resistant to antibiotics such as methicillin (MRSA) and vancomycin (VRSA). This makes the development of a vaccine against *S. aureus* an important priority. As the bacterial cell wall is what is presented to the outside environment, *S. aureus* peptidoglycan is an attractive target against which to attempt vaccination.

S. aureus peptidoglycan (PG) is composed of linear chains of two different amino sugars (*N*-acetylglucosamine and *N*-acetylmuramic acid) linked together by a β-(1,4)-glycosidic bond. [82] The *N*-acetylmuramic acid is attached to a four amino-

acid chain consisting of L-alanine, D-glutamine, L-lysine, and D-alanine; these four-amino acid peptides are linked together by bridges that consists solely of five glycine residues between the lysines. It is the chirality of the amino acids that grant *S. aureus* resistance to peptidases, as D-amino acids do not occur in mammalian proteins as frequently as L-amino acids. There have already been several attempts to utilize PG as a single component vaccine against *S. aureus* [83], [84]; however, these vaccines have proven to be efficacious in mice, but not in humans in Phase 2 FDA clinical trials. These vaccines utilize PG as it is found, meaning that it is primarily a carbohydrate vaccine.

Carbohydrate antigens have been targeted in the past for vaccine development. Carbohydrate antigens are typically poorly immunogenic, provide no long-last immune response, and are T-cell independent. For this reason, they are often attached to proteins to form so-called conjugate vaccines; however, these vaccines are not often uniformly efficacious in the groups that require them the most, such as the elderly and immunocompromised individuals. Finding a peptide that immunologically mimics the structure of a carbohydrate bypasses the need for a conjugate vaccine while still provoking a T-cell dependent response. Of course, it is not as straightforward as simply finding a peptide that interacts with the binding pocket of an antibody (see Chapter 1 of this work). However, performing affinity selections against MCA5792 allows for the first step of potentially finding a peptide mimotope of a carbohydrate epitope that promotes a protective immune response against *S. aureus*.

Peptide mimics of the carbohydrate epitope to which MCA5792 binds have already been discovered. Chen et al. used a PhD-12 phage display library and screened against MCA5792 for potential binding partners. [85] They discovered a linear 12-mer called Sp-31 (amino acid sequence A T W x H x L x S A G L, where 'x' are residues that were not conserved between 31 and several other similar clones), and from that created a four-branch multiple antigen peptide called MAP-P31. They found that immunization of mice with MAP-P31 not only promoted a strong anti-MAP-P31 response, but also caused a strong TNF-α and IL-6 response from mouse macrophages. In addition, serum from these mice showed bactericidal activity against *S. aureus*, and immunization with MAP-P31 showed protection from infection with *S. aureus*, leading to a statistically significant increase in mouse survival compared to non-immunized controls. We believe that, using our affinity selection protocol, we will also be able to discover peptide mimics to the epitope that binds to MCA5792.

Mimics of Carbohydrate Epitopes Using MAbs against *Cryptococcus neoformans* and *Shigella flexneri*. 2H1, a monoclonal antibody that binds to the capsular glucuronoxylomannan (GXM) of the fungus *Cryptococcus neoformans* [86], and SYA/J6, a monoclonal antibody that binds to the trisaccharide epitope of the *O*-polysaccharide of the *Shigella flexneri* variant Y lipopolysaccharide[87], are the final antibodies against which affinity selections were performed for this work. *C. neoformans* is the leading cause of death in people with HIV/AIDS in sub-Saharan Africa, and can infect people with non-compromised immune systems as well. [71] *S. flexneri* is the causative agent of shigellosis in roughly 1/3 of all cases of the disease

in the United States; symptoms include stomach cramps, diarrhea, and fever, and occasionally more severe disease. [71] The antibodies used for selections here are against carbohydrate epitopes, and selections were performed with a desire of discovering peptide mimics of the carbohydrate epitope as in each other antibody in this work outside of MDVP-55A/GTX29202. Work beyond the basic affinity selection protocol and sequencing of individual clones has not yet been performed on these two populations of selectants.

3.2 Materials and Methods

3.2.1 Plasmid Construction (AB-loop Insertion)

The plasmids and phages described here were constructed using standard molecular biology methods and have the characteristics described in the text and illustrated in Figure 3.1. As in Chapter 2, pDSP62 and their derivatives contain the phage T7 promoter and terminator regions of pET3d, and the kanamycin resistance gene and replication origin of pET9a (from Novagen). An unwanted Sal I site and other nearby extraneous plasmid sequences were removed by Bal 31 deletion. pDSP62 also contains the M13 origin of replication taken from pUC119 and a replacement of the upstream half of the single-chain dimer sequences with a synthetic "codon-juggled" version of coat protein. This sequence was designed using the web-based program GeneDesign available at http://genedesign.thruhere.net/gdo/index.html, and synthesized by assembly PCR from synthetic oligonucleotides. The plasmid known as pDSP62(am) was constructed by site-directed mutagenesis of pDSP1 and pDSP62 to introduce an amber codon at the junction between the two halves of the single-chain dimer. To

allow for low level suppression of the stop codon, we constructed pNMsupA, which uses the replication origin and chloramphenicol resistance of pACYC18422, and the lac promoter of pUC19 to express an alanine-inserting amber suppressing tRNA.

The helper phage called M13CM1 was constructed from M13K07 by replacement of the kanamycin resistance gene with the chloramphenicol resistance determinant of pACYC184, taking advantage of conveniently situated Xho I and Sac I sites in the M13K07 sequence.

Single-stranded, dUTP-substituted phagemid templates were created from a dut^-, ung^- host *E. coli* strain after transformation with pDSP62 and super-infection with M13CM1. Random sequence insertions were produced by annealing a mutagenic primer to the single-stranded circular template, which is then converted to a covalently closed double-stranded circle by the action of *in vitro* DNA polymerase and DNA ligase. The reaction was then introduced by electroporation into ung^+ *E. coli*, where the dUTP-containing parental strand is preferentially destroyed. In this way, high rates of insertion (as much as 90%) were obtained in libraries containing as many as 10^{11} individual members. The mutagenic primers used here inserted foreign peptides into the AB loop of the downstream copy of the MS2 single-chain dimer of length six, eight, and ten amino acids. Individual libraries of each of these populations were mixed and used at equal concentrations for all affinity selections performed here.

3.2.2 Protein Expression and Purification

Plasmid libraries with various insertion sizes in the downstream coat AB loop were introduced into *E. coli* 10G cells for plasmid amplification. For selections

Rounds 1 and 4, the plasmid libraries were based in pDSP62 for high-valency display of foreign peptides. For Rounds 2 and 3, conducted at low valency, the plasmid libraries were based in pDSP62(am). In either case, 10G cells were transformed and immediately grown in a 100 mL liquid culture to maximize the complexity of the plasmid library. After overnight growth, cultures were lysed and plasmids were extracted via Qiagen Midiprep kit. These amplified libraries were then transformed into *E. coli* strain C41(DE3) for VLP expression and purification. In the case of Rounds 1 and 4 of selection (high display valency), libraries were transformed into cells alone. In Rounds 2 and 3 of selection (low valency display), libraries were co-transformed with pNMsupA to allow for low-level nonsense suppression. Cells were again transformed and then grown immediately in a 100 mL liquid culture to A_{600} of 0.4 (mid-log phase), where they were induced for protein expression with 1mM isopropyl β-D-1-thiogalactopyranoside (IPTG) and allowed to grow for an additional three hours. These cultures were then lysed and VLPs were extracted. To extract VLPs, the cells were pelleted and resuspended in 10 mM Tris, pH 8.0, then disrupted by lysozyme treatment (2 mg/ml for one hour on ice), 0.25M deoxycholate treatment, and sonication (5 bursts, 1 min each, on ice). Cellular debris was removed by centrifugation at 10,000 rpm for 30 minutes. Rather than purifying on Sepharose CL-4B columns, here the solution was frozen for at least two hours (usually overnight). Upon thawing, the solution was then centrifuged again at 10,000 rpm for 30 minutes to remove any additional insoluble material. The solution was then passed through an Amicon Ultra-4 Spin Column with a 100 kDa cutoff for crude purification. These partially purified lysates were then used in

subsequent rounds of selection until the final round. After the final round of selection, the selected population was transformed into C41(DE3) cells and then plated on media containing kanamycin. Resulting colonies were individually picked and grown in 1 mL of culture to isolate plasmids for sequencing and to test for VLP production.

3.2.3 Affinity Selection

Selections were conducted against monoclonal antibodies adsorbed to the surface of plastic wells (96-well Immulon 2, Thermo Scientific). 500 ng of an antibody in PBS were adsorbed to a well overnight at 4°C. The wells were subsequently blocked by incubation for two hours at room temperature with 0.5% non-fat dry milk in PBS, and a VLP library prepared as described above was added and incubated at room temperature for two hours. The binding reactions were conducted in 50ul, with an estimated 2-5ug of VLP. Wells were washed ten times with PBS, and bound particles were eluted for 5 minutes in 50ul of 0.1M glycine, pH 2.7. The eluted VLPs were neutralized by addition of 5ul 1M Tris, pH 9.0, and 10 ul of eluate were subjected to reverse transcription for one hour in a 20ul reaction with MMLV reverse transcriptase (Promega) and 2 pmol of a primer that anneals 3′ of the coat protein coding sequence. The product of reverse transcription was amplified by PCR using Taq DNA polymerase and primer E3, which anneals just upstream of E2, and 62up, which anneals specifically directly upstream of the junction sequence between the two halves of the single-chain dimer. The resulting PCR product was digested with *Sal*I and *Bam*HI and cloned in pDSP62 for production of VLPs for use in a second round of selection, conducted identically to

the first. Round 2 and 3 selectants were cloned in pDSP62(am) for production of VLPs displaying their peptides at low valency. Apart from this reduction in the level of display valency, the conditions of selection in Rounds 2 and 3 were identical to those of the previous rounds.

3.2.4 Antibodies Used – 2C7, 2-1-L8, MDVP-55A, GTX29202, MCA5792, SYA/J6, 2H1

Antibodies 2C7 and 2-1-L8 are monoclonal antibodies that bind to lipooligosaccharides on the surface of *Neisseria gonorrhoeae* [69], [70]. MDVP-55A and GTX29202 are from ICL and GeneTex, respectively, and are monoclonal antibodies created by immunizing mice with a mixture of Dengue virus 1, 2, 3 and 4. Hybridomas were then prepared from spleen cells from these mice and clones were selected based on the ability of the antibody they produced to react with all four Dengue serotypes. MCA5792 is a mouse monoclonal antibody created by AbDSerotec that recognizes the peptidoglycan of *Staphylococcus aureus*, specifically from immunization with strain ATCC 29740. SYA/J6 is a monoclonal antibody that binds to the trisaccharide epitope of the *O*-polysaccharide of the *Shigella flexneri* variant Y lipopolysaccharide. [87] 2H1 is a monoclonal antibody that binds to the capsular glucuronoxylomannan (GXM) of the fungus *Cryptococcus neoformans* [86].

3.2.5 ELISA

To determine both whether affinity-selected sequences bound to the selecting antibody and for a relative idea of how well they did so, 500 ng of VLPs (either libraries, in the case of earlier rounds of selection, or individual clones, in the case of the final round of selection) were used to coat Immulon-2 ELISA plates (Thermo

Scientific) at 4°C overnight. Wells were blocked for 2 hours at room temperature with 0.5% BSA in PBS buffer. Serial dilutions of primary antibody (in every case, this was the antibody against which the selection was performed) were then incubated in the wells for 2 hours. Horseradish peroxidase (HRP)-conjugated goat anti-mouse IgG at a 1:5000 dilution for 1 hour at room temperature was used as secondary antibody. The plates were developed with 2,2′-azino-bis(3-ethylbenzthiazoline-6-sulfonic acid) (ABTS) and reactivity was determined by measuring the mean optical density (OD) values at 405 nm.

3.2.6 Immunizations of Balb/c Mice

For experiments involving MDVP-55A and GTX29202 selectants, Balb/c mice were administered 5 ug of either wild-type VLPS or VLPs bearing the selected peptide from the final round of selection (R Q E K I D V T Y R). Mice were subsequently boosted before serum was harvested and purified. To perform the ELISA to detect anti-Dengue antibodies, 250 ng of recombinant Dengue E protein was used to coat plates. For experiments involving MCA5792 selectants, the same protocol was followed, except that rather than Dengue E protein, *S. aureus* peptidoglycan was used to coat plates for ELISA.

3.3 Results

3.3.1 Affinity Selections – 2C7 and 2-1-L8

Neisseria gonorrhoeae is the causative bacterial agent of gonorrhea. Because it is experiencing something of a resurgence in incidence in the United States, including strains that are resistant to current treatments, there is interest in developing new vaccines. As mentioned in the introduction, vaccines against *N. gonorrhoeae* have

traditionally been difficult to develop. Not only is the bacterium adept at masking and varying important antigens from the immune system, but memory response to the bacterium is also lacking in most cases. We believe that, were we able to discover an immunological mimotope of the epitope to which 2C7 and 2-1-L8 bind, we would be able to create an efficacious vaccine to *N. gonorrhoeae* that also provided long-term protection. We obtained two mouse monoclonal antibodies from Peter Rice (University of Massachusetts) that recognize lipooligosaccharide epitopes found on the surface of *N. gonorrhoeae*, known as 2C7 and 2-1-L8. In many gonorrhea infections, circulating antibodies such as these two are detected. [69] Our affinity selection system might enable us to discover peptide mimics of more complex structures, such as carbohydrates; it is possible that, upon immunization with a VLP bearing a selected peptide, an antibody response can be raised that mimics natural-forming antibodies against carbohydrate structures with regard to binding specificity and affinity.

3.3.1.1 Affinity Selections, VLP Selectants, and Sequencing

We constructed random peptide libraries of 6-, 8-, and 10-amino acids displayed on our MS2 VLPs. The peptides are displayed in the downstream copy of the coat protein single-chain dimer AB-loop, allowing for maximum display density (at high valency, this is 90 copies of the inserted peptide per VLP) while not interfering with coat protein folding or VLP assembly. Equimolar amounts of each size library were combined and utilized in the first round of selection. The selection was carried out by placing 500 ng of either antibody (2C7 or 2-1-L8) on an Immulon-2 plate and incubating overnight at 4^{0}C. The next day, 40 ug of the combined 6-, 8-, and 10-

amino acid random peptide VLP library was incubated with the antibodies bound to the plate. Following thorough washing to remove all unbound VLPs, the bound VLPs were eluted using acid elution followed by neutralization. The eluted VLPs were then used directly in a reverse transcription (RT) reaction, and this reaction was then directly used in a PCR amplification to recover the downstream copy of the single-chain dimer (that contained the peptide insert in the AB-loop). This cDNA was then re-inserted into an expression vector for the growth of a new plasmid and VLP library.

After Round 1, this vector was switched from pDSP62 to pDSP62(am) to allow a move from low to high valency. Figure 3.1 details these two constructs, along with pNMsupA, the plasmid encoding the tRNA also used in Chapter 1 to allow for amber nonsense suppression. Selection occurred at low valency in Round 2, and then again at low valency in Round 3, before one final round at high valency (Round 4). After Round 4, the plasmid library was transformed into C41(DE3) cells and, rather than being grown in liquid culture, was plated on media containing kanamycin. This was to allow for the selection of individual colonies for sequencing and testing. For both 2C7 and 2-1-L8 selectants, following Round 4, between 12-24 colonies were selected for individual testing and sequencing. Figure 3.2 is a phosphate agarose gel stained with ethidium bromide that shows the VLPs obtained from single colonies. It is clear that, compared to wild-type controls, most samples demonstrate changes in mobility on the gel. This is explainable mostly due to charge differences – depending on the composition of the peptide insertion in the AB-loop, the overall effect on the VLP can be to make it more positive or negative, thus affecting mobility on gels that

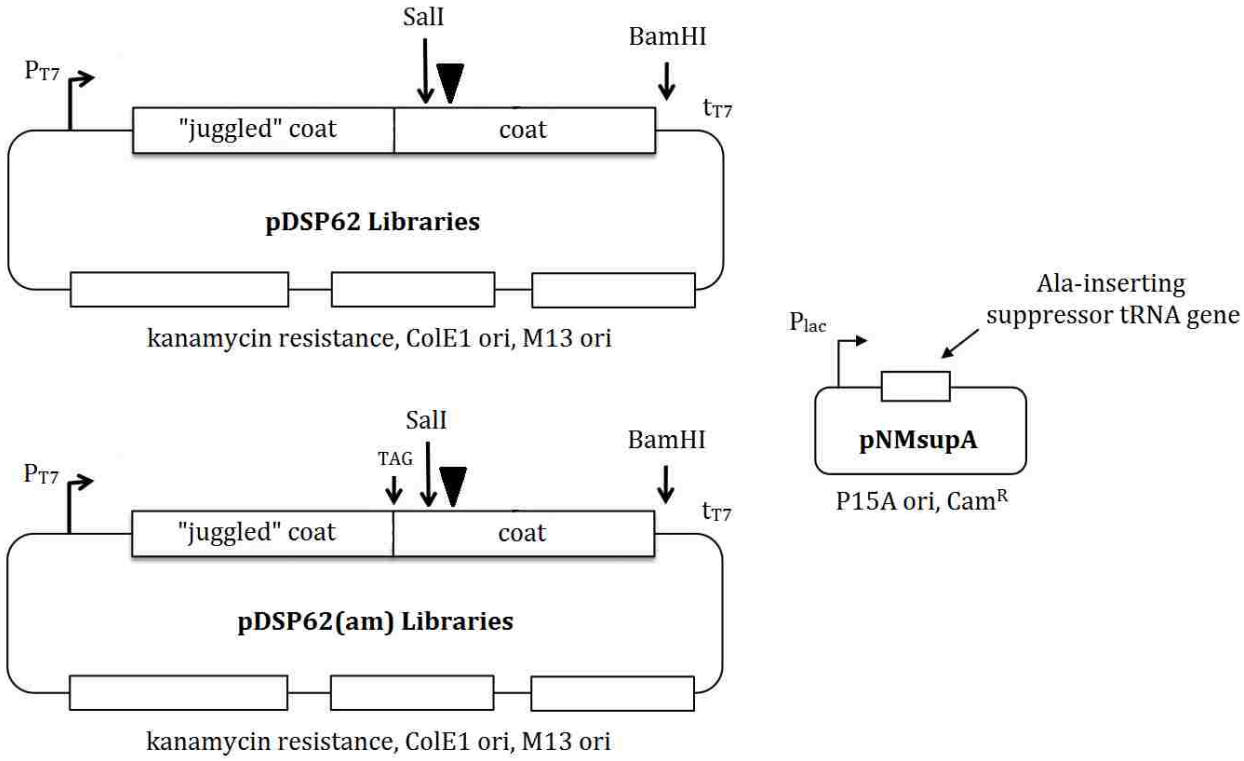

Figure 3.1 Schematic Details of Random Peptide Libraries on pDSP62 and pDSP62(am). The plasmid pDSP(62) has the same structural details as in Chapter one, except that instead of a C-terminal fusion, the peptide is an insertion into the AB-loop (depicted in both plasmids as a black triangle). pDSP62(am) differs in that it contains an amber stop codon between the two halves of the single-chain dimer, allowing for low-level expression of single-chain dimmers (compared to wild-type monomers) that contain peptide insertions in the AB-loop. This is accomplished via use of pNMsupA, also shown here.

A

B

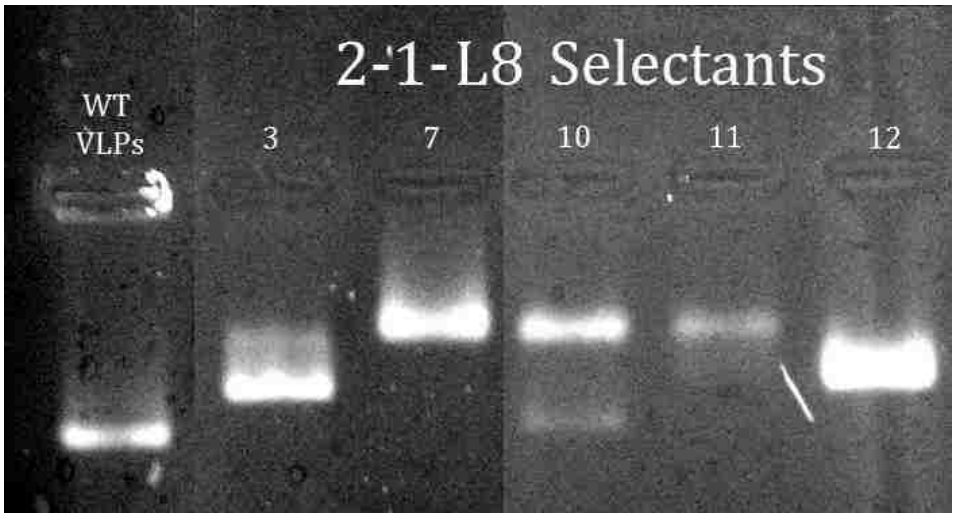

Figure 3.2 Individual VLP Clones for Final-Round Selectants from 2C7 and 2-1-L8. Gels are phosphate agarose (1%) stained with ethidium bromide to visualize RNA within capsids. (A) shows VLP selectants from 2C7 and (B) shows VLP selectants from 2-1-L8. Note that there are more selectants from 2C7 than from 2-1-L8; this is because several picked colonies for 2-1-L8 did not yield functional VLPs. Also note the mobility differences in VLPs between selectants and when compared to the wild-type control.

separate based upon both size and charge. This also means that, because each VLP does not have the same mobility on the gel, there must be different inserts in at least some VLPs. However, there are also a number of VLPs in both cases that, while differing from wild-type, show similar mobilities to one another; these VLPs may contain similar or identical insertions.

We then sequenced the VLP cDNAs to see determine the sequence of the peptide insert in the AB-loop. Figure 3.3 shows the results of the sequencing of the population of VLPs. The sequencing results for these selections have a few notable features. First, both populations consist of only 6-amino acid selectants, even though the original library of VLPs was composed of 6-, 8-, and 10-amino acid random peptides. Second, the population of 2C7 selectants is quite a bit more diverse than the population of selectants from 2-1-L8; though most sequences display some level of similarity, only a few are exactly identical. The third is that both of the sequences selected when 2-1-L8 was the selecting antibody also appear as selectants in the 2C7 population. As both antibodies target lipooligosaccharides on the surface of *N. gonorrhoeae*, this may not be an entirely surprising result, but it does suggest that, at least in the specific structural context under which peptides are displayed in the MS2 VLP AB-loop, there is enough similarity in the binding pocket of both mAbs that the peptide sequences selected are identical, and therefore that the carbohydrate epitopes they recognize are probably structurally similar.

3.3.1.2 Functional Testing of VLP Selectants

To confirm that these affinity-selected peptides bind the antibody, we purified four of them for use in ELISA. The four we chose are labeled in Figure 3.3; the

A

C1	CTG GAC TAC GAG CGG ATC	L D Y E R I	***
C2	CTG GAC TAC GAG CGG ATC	L D Y E R I	
C3	CTG GAC TAC GAG GGC AAC	L D Y E G N	
C4	TTG GAC TAC ATG CGC ACC	L D Y M R T	
C5	CCG CTC TGG AGG GGC ACC	P L W R G T	***
C7	CTG GAC TAC CAG AGG GTG	L D Y Q R V	
C9	TTG GAC TAC ATG CGC ACC	L D Y M R T	
C10	CCG CTC TGG AAG GGC AAC	P L W K G N	
C11	GTG GAC TAC GAG AGG ATC	V D Y E R I	
C14	GTG GAC TAC GAG AGG ATC	V D Y E R I	
C15	GAG CTG TGG AGG GGG ACG	E L W R G T	
C18	CCC CAG GGC TAC CCG GAG	P Q G Y P E	***
C19	GAG CTG TGG AGG GGG ACG	E L W R G T	
C21	CTG GAC TAC ATG CGC ACC	L D Y M R T	
C22	TTG GAC TAC ATG CGC ACC	L D Y M R T	***
C23	CTG GAC TAC CAG AGG GTG	L D Y Q R V	

B

L3	CCG CTC TGG AGG GGC ACC	P L W R G T
L7	CCG CTC TGG AGG GGC ACC	P L W R G T
L10	CCG CTC TGG AGG GGG ACC	P L W R G T
L11	CCG CTC TGG AGG GGC ACC	P L W R G T
L12	TTG GAC TAC ATG CGG ACT	L D Y M R T

Figure 3.3 Sequences from Final Round Selections against 2C7 and 2-1-L8. Shown here are all relevant sequences obtained from both selections. The selection against 2C7 (A) showed a fair bit of sequence diversity, even after four rounds of selection; the selection against 2-1-L8 (B) showed a more restricted population. The color codes on the sequences show various points of interest. Red and blue, sequences common to both 2C7 and 2-1-L8 selections; green, sequence found only in 2C7 selections but demonstrating close homology to other sequences; orange, sequence found only in 2C7 selections but demonstrating no real homology to other sequences. *** = chosen for testing for reaction with selecting antibodies via ELISA.

samples are known hereafter as #1 (L D Y E R I), #5 (P L W R G T), #18 (P Q G Y P E), and #22 (L D Y M R T). #5 and #22 were chosen because they are represented in both selecting populations. #1 was chosen because, though it is only found in 2C7 selectants, it bears close homology to other sequences (including #5). #18 was chosen because it does not resemble any other selecting sequence in the population, making its inclusion one of curiosity; we wanted to determine if it actually did bind to the selecting antibody or if it was a case of possible contamination in the selection. We also decided to test all four of these selectants against both 2C7 and 2-1-L8, even though two of the sequences did not appear within the L8 selectants. The reasoning was that if the two antibodies do in fact recognize the same epitope, we might see some cross-reactivity.

We performed the ELISA by placing 500 ng of each VLP population (#1, #5, #18, and #22) onto Immulon-2 plates and incubating overnight at 4^{o}C. After washing, we then used serial dilutions of both selecting antibodies (2C7 and 2-1-L8) as primary antibodies and HRP-conjugated goat anti-mouse IgG as secondary for detection of signal from cleavage of ABTS. The results of the ELISA are shown in Figure 3.4. The trends are generally clear at all primary antibody dilutions, but are especially visible at the 1:100 dilution. We see generally good reaction of both antibodies with #1, #5, and #22; however, #18 does not interact with either antibody above background (even 2C7, the antibody under which it was presumably selected). This could indicate that it was some form of contamination, or possibly that it is specific to the material from which the wells used for selections are constructed (i.e. it is a "plate binder"). Of the three that do react well, #1 and #22 seem to be the strongest for

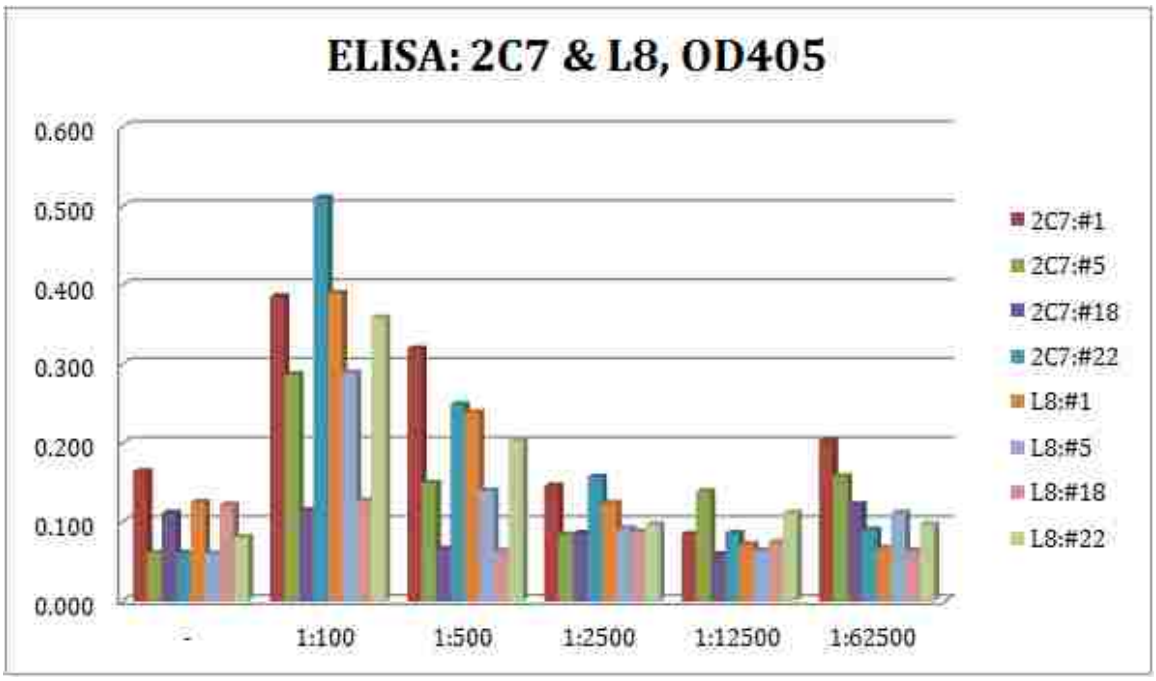

Figure 3.4 ELISA Results from 2C7 or 2-1-L8 Interaction with Four VLP Selectants. Optical density at 405nm (OD405) is shown on the vertical axis and dilution of primary antibody is shown on the horizontal. The antibody being diluted is designated by the color of the bars. The first four bars at any given dilution represent various VLP selectants using 2C7 as primary, and the second four bars are the same VLP selectants using 2-1-L8 as primary. (-), ELISA performed with no primary antibody. Primary antibodies were used in serial five-fold dilutions.

both antibodies, with #5 still reacting above background but falling off more quickly than the other two as the dilution of primary antibody increases. This is interesting because it was #5 and #22 that appear specifically in both selecting populations; sample #1 only appeared in 2C7 selectants. This shows strong evidence that there is in fact cross-reactivity between the two antibodies. It is important to note that the sequence could have appeared in 2-1-L8 selectants but it was simply not discovered by the testing done here; however, in either case, the two antibodies are able to recognize and bind to the same sequences.

In an attempt to provide more evidence that 2C7 and 2-1-L8 do in fact recognize the same epitope, we sent wild-type VLPs, #1, #5, #18, and #22 to Peter A. Rice at the University of Massachusetts Medical School. Dr. Rice works very closely with *N. gonorrhoeae*, and specifically with developing vaccines against the bacterium. Dr. Rice and his group took the VLPs we sent and performed an inhibition assay with them. The assay consisted of incubating our VLPs with either 2C7 or 2-1-L8 and then testing the resulting mixture for its ability to bind to FA1090, a strain of *N. gonorrhoeae*. The results of this assay are seen in Figure 3.5. Panels A and B represent inhibition of the binding of antibody 2C7 to FA1090, and Panels C and D represent inhibition of the binding of antibody 2-1-L8 to FA1090. Panel A shows our five VLP samples; VLPs #1, #5, and #22 show 15-45% inhibition of the binding of 2C7 in a dose-dependent manner, while #18 shows no inhibition over the wild-type control. The lower panel of A demonstrates inhibition of 2C7 binding by various peptides discovered by Dr. Rice via affinity selection against 2C7 on *E. coli* flagellin. It is clear that these peptides are better suited to inhibit 2C7 than our VLPs, but

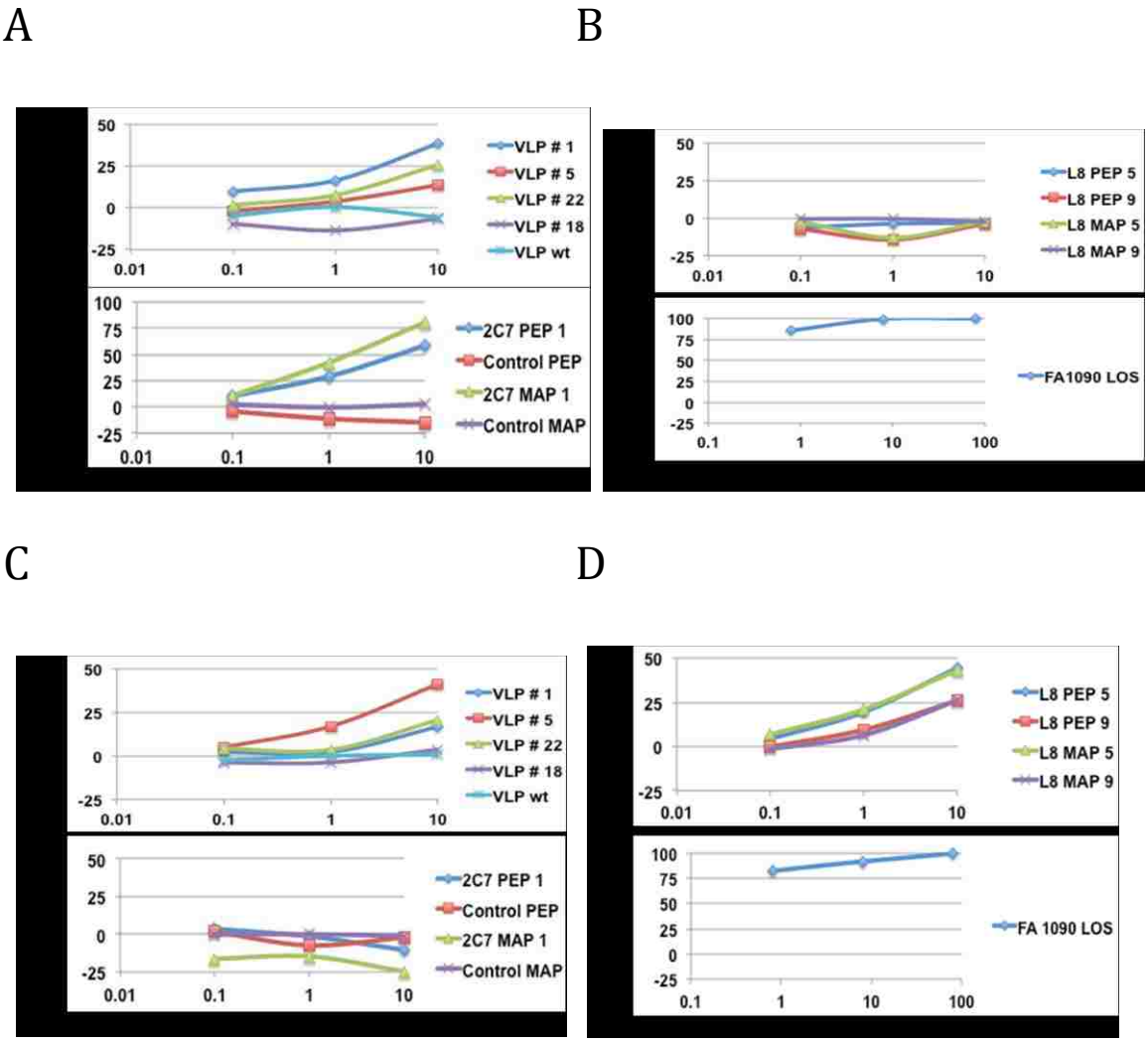

Figure 3.5 Inhibition of Binding of 2C7 or 2-1-L8 to FA1090 by VLPs or Specific Peptides. Inhibition assay was performed by incubating various amounts of potential inhibitor with either 2C7 (Panels A and B) or 2-1-L8 (Panels C and D) and then testing for binding inhibition to *N. gonorrhoeae* strain FA1090. (A) VLPs (top panel) demonstrate low-level inhibition of binding in samples #1, #5, and #22; specific 2C7peptides (bottom panel) are also capable of inhibiting binding. (B) Specific peptides to 2-1-L8 are incapable of inhibiting binding of 2C7 (top panel); control inhibitor shows complete inhibition of binding (bottom panel). (C) VLPs (top panel) demonstrate low-level inhibition of binding in samples #1, #5, and #22, while specific 2C7 peptides cannot inhibit binding of 2-1-L8 (bottom panel). (D) Specific 2-1-L8 peptides efficiently inhibit binding of 2-1-L8 (top panel); control inhibitor shows complete inhibition of binding (bottom panel). MAP = Multi-Antigen Protein, an octomer of the parent peptide.

there is still low-level inhibition of binding due to our VLPs. The upper panel of B shows inhibition of 2C7 binding by various peptides affinity-selected by Dr. Rice against 2-1-L8; it is clear that there is no inhibition of the antibody binding. This indicates that there is no cross-reactivity between the specific synthesized peptides to 2-1-L8 and 2C7. The experiment in Panel C is the same as in A except that neutralization of 2-1-L8 (rather than 2C7) binding to FA1090 is measured. Once again, we see VLPs #1 #5, and #22 providing 20-45% inhibition of binding and #18 not inhibiting binding above wild-type background. This indicates that our VLPs are in fact cross-reactive with both 2C7 and L8, and there is strong evidence for them binding to the same epitope. In the lower panel of C, we see that the specific 2C7-binding peptides do not react with 2-1-L8, the reverse of what we saw in Panel B. Panel D is a confirmation that 2-1-L8 can be inhibited by the peptides specific to it, and while that inhibition is higher than that seen with the VLPs, the VLPs still show low-level inhibition.

Taken together, these data show that VLPs #1, #5, and #22 are capable of binding to and neutralizing both 2C7 and 2-1-L8, providing more evidence that the two antibodies do in fact recognize the same epitope.

3.3.2 Affinity Selections - MDVP-55A and GTX29202

Dengue virus occurs as four distinct serotypes, named numerically. Although many individuals suffer temporarily debilitating and painful disease, a first (or primary) infection is often mild or even sub-clinical. However, a second infection with a different serotype increases the risk of severe disease, including hemorrhagic fever. [79] There is evidence suggesting that this is due to the presence of virus-

binding antibodies from the first infection which, rather than neutralizing the second infection, actually facilitate viral entry to a second serotype. This is so-called antibody-dependent enhancement of infection (or ADE). Therefore, any Dengue vaccine should elicit antibodies that neutralize all four serotypes to avoid rendering a person susceptible to a ADE as a result of vaccination. The antibodies that we chose to perform affinity selections against, MDVP-55A and GTX29202, react with the envelope protein, E, of all four Dengue serotypes. Importantly, the epitopes recognized by these mAbs are apparently conformational and discontinuous [81]. A prinicpal objective of these experiments was not to find a Dengue vaccine *per se*, but rather to the test the idea that affinity-selection on the MS2 VLP could find an immunological peptide mimic of a complex protein epitope.

3.3.2.1 Affinity Selections, VLP Selectants, and Sequencing

The affinity selection procedure, including the starting library mixture, was identical to the process used for 2C7 and 2-1-L8, except that a library consisting only of random sequence 10-mers was used. Once again, after the final round of selection, the final library population was plated (rather than grown in liquid media) and 12 individual colonies were selected for both MDVP-55A and GTX29202. These colonies were tested for their ability to form VLPs, and those that produced VLPs were sequenced to determine the composition of the peptide insertion in the AB-loop. In both cases, phosphate agarose gel stained with ethidium bromide determined proper VLP formation was occurring in all samples (data not shown).

Once we had determined which samples created functional VLPs, we sequenced those clones. Figure 3.6 shows the results of this sequencing. Because the original

A

55A1	CGG CAG GAG AAG ATC GAC GTG ACC TAC AGG	R Q E K I D V T Y R
55A2	CGG CAG GAG AAG ATC GAC GTG ACC TAC AGG	R Q E K I D V T Y R
55A3	CGG CAG GAG AAG ATC GAC GTG ACC TAC AGG	R Q E K I D V T Y R
55A4	CGG CAG GAG AAG ATC GAC GTG ACC TAC AGG	R Q E K I D V T Y R
55A5	CGG CAG GAG AAG ATC GAC GTG ACC TAC AGG	R Q E K I D V T Y R
55A6	CGG CAG GAG AAG ATC GAC GTG ACC TAC AGG	R Q E K I D V T Y R
55A7	TGG GAC CGC TTC GAC ACG AAG CGC CAG AAC	W D R F D T K R Q N
55A8	GGG GAG AGG GCC CGC AAG TCG TAC ATC TCG	G E R A R K S Y I S

B

GTX1	ACC GAC CAC TGG GAG AAG CAC GGC TCC CGC	T D H W E K H G S R
GTX2	ACC GAC CAC TGG GAG AAG CAC GGC TCC CGC	T D H W E K H G S R
GTX3	ACC GAC CAC TGG GAG AAG CAC GGC TCC CGC	T D H W E K H G S R
GTX4	ACC GAC CAC TGG GAG AAG CAC GGC TCC CGC	T D H W E K H G S R
GTX5	ACC GAC CAC TGG GAG AAG CAC GGC TCC CGC	T D H W E K H G S R
GTX6	ACC GAC CAC TGG GAG AAG CAC GGC TCC CGC	T D H W E K H G S R
GTX7	GTC AAG CGC CGG AAG GTG GGG GAC ATC ACG	V K R R K V G D I T
GTX8	GTC AAG CGC CGG AAG GTG GGG GAC ATC ACG	V K R R K V G D I T

Figure 3.6 Sequences from Final Round Selections against MDVP-55A and GTX29202. Here we see results of final-round sequencing for both MDVP-55A (A) and GTX29202 (B). Note that both selections yield a single predominant peptide, though only the peptide from MDVP-55A yields a peptide that produces anti-E protein antibodies upon immunization (highlighted here in red).

starting library was composed entirely of 10-mer amino acid peptides, it is unsurprising that this is the only sequence length we see in these selections. Both selections also yield a single peptide in a majority of the cases. For MDVP-55A, the peptide R Q E K I D V T Y R predominates; for GTX29202, the peptide that predominates is T D H W E K H G S R. In both cases, these two peptides represent six of the eight total selectants sequenced. Interestingly, these two peptides are fairly different. This is of note because of how similar the original E-protein epitopes are for both mAbs. Also, none of the peptides isolated (even the minority members from each selection) appear within the linear Dengue E protein sequence. This leads us to believe that these antibodies do in fact recognize a discontinuous epitope on the surface of the protein, and our small peptide is capable of mimicking that epitope.

3.3.2.2 Functional Testing of VLP Selectants

We now wanted to determine if, upon immunization, our VLPs stimulated an immune response that resulted in antibodies that recognize Dengue E protein. To this end, we took either wild-type VLPs or VLPs bearing the selected predominant sequences (MDVP-55A: R Q E K I D V T Y; GTX29202: T D H W E K H G S R) and administered 5 ug of them to Balb/c mice. Mice were subsequently boosted with the same 5 ug VLP dose before serum was harvested and purified. To perform the ELISA to detect anti-Dengue antibodies, 250 ng of recombinant Dengue E protein was used to coat plates. From there, serial dilutions of serum from each of the four mice (three mice were administered recombinant VLP, one mouse was administered wild-type VLPs) were incubated in the wells, and detection was with a standard goat anti-mouse IgG conjugated to HRP with ABTS as the detection reagent. The

GTX29202 selectant did not yield sera that bound to recombinant E protein in ELISA (data not shown); however, the MDVP-55A selectant did, and the results of this ELISA are seen in Figure 3.7. The sera from the three mice that were administered recombinant VLPs bearing our selected peptide show a clear ability to bind to Dengue E protein, indicating that antibodies to this protein were created during immunization. In contrast, there is no response from the serum of the mouse that was administered wild-type VLPs. Taken together, these data are strong evidence that our selections properly identified a small peptide immunological mimic of the epitope recognized by MDVP-55A, and that vaccination with VLPs bearing this peptide mimic are capable of raising antibodies that bind to the same antigen to which the selecting antibodies bind.

3.3.3 Affinity Selection - MCA5792

Staphylococcus aureus is a usually-harmless, common bacterium that can thrive in many different environments, including on human skin. Some strains of *S. aureus* are pathogenic, however, and can have developed resistance to antibiotics such as methicillin (MRSA) and vancomycin (VRSA). In a situation very similar to that of gonorrhea discussed earlier, there is now an impetus to develop vaccines to the bacterium. As noted in the introduction, the peptidoglycan (PG) found on the surface of *S. aureus* is an attractive vaccine target. To this end, we obtained MCA5792, an antibody that specifically targets the PG of *S. aureus*, for use with our affinity selection protocol.

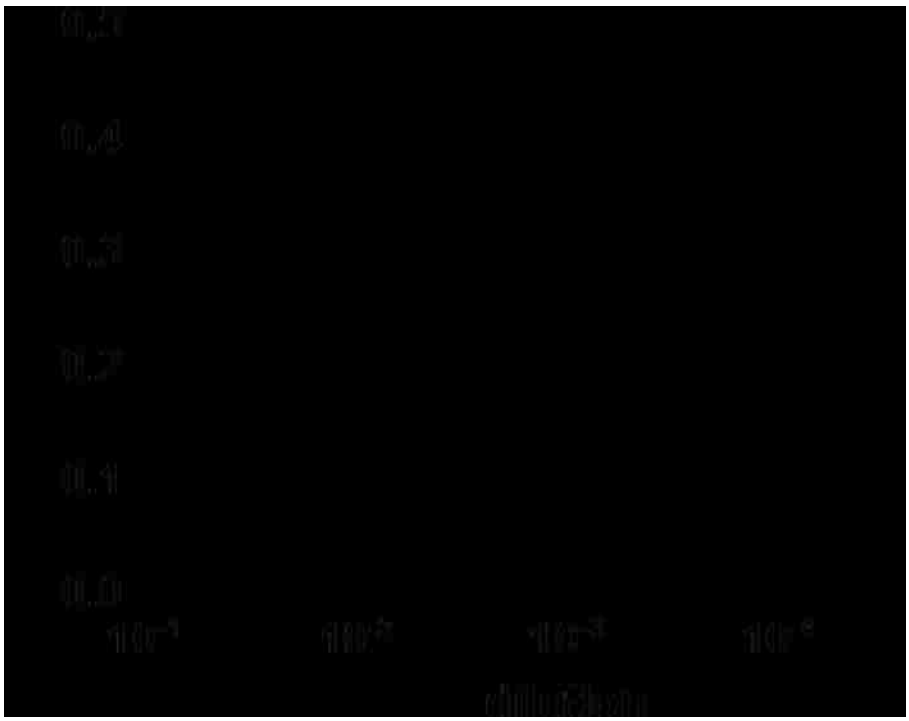

Figure 3.7 Results of ELISA Using Sera From Mice Immunized with Recombinant VLP selectants from MDVP-55A/GTX29202 Selections. 5 ug of either wild-type VLPs (diamonds) or VLPs bearing the selected sequence common to both MDVP-55A and GTX29202 selections (R Q E K I D V T Y R) (circles, triangles, squares) were administered to Balb/c mice. Mice were subsequently boosted with the same 5 ug VLP dose before serum was harvested and purified. To perform the ELISA to detect anti-Dengue antibodies, 250 ng of recombinant Dengue E protein was used to coat plates, and serial dilutions (x-axis) of harvested serum were used to test for reactivity. Each shape on the graph represents a different mouse.

3.3.3.1 Affinity Selection, VLP Selectants, and Sequencing

Selections for MCA5792 proceeded as in previous selection cases, except that selection was halted after three rounds instead of four. Because of this, we expect to see more diversity in peptide insertions after sequencing than the previous four selections discussed. After the third round of selection, the selected library was transformed into C41(DE3) cells, plated, and then 12 individual colonies were selected for further analysis. An agarose gel to assess proper VLP formation is shown in Figure 3.8 A. Here we see that all selectants have drastically different mobilities than the wild-type particles; we also note that some selectants appear to have similar mobilities with respect to one another. The radical upward shift in mobility would imply that the peptide inserts in these VLPs contain some positive charge character, retarding mobility toward the positive pole.

Figure 3.8 B shows the results of sequencing of some of the clones seen in A. Of the four sequences, three are 8-mers and one is a 10-mer. However, all sequences share a couple of common elements. The first is a run of at least four glycines in a row; in most cases, this is actually a run of five glycines. Flanking those glycines are the positively-charged residues that we predicted would be present from the mobility in the agarose gel – arginine and lysine. This is especially interesting because, as noted in the introduction to this chapter, this very closely mimics the structure of the *S. aureus* peptidoglycan, indicating that even at Round 3, our selections appear to be discovering logical binding partners for the selecting antibody.

A

B

```
St1    GGC GGG GGC GGG GGC CGG AAG GGG                  G G G G G R K G
St2    AAG GGG GGC GGG GGG GGC AGG AAG ACC GTC          K G G G G G R K T
V
St6    AAG CGG GGC GGC GGG GGC GGG GGG                  K R G G G G G G
St8    AAG CGC GGG GGG GGC GGC ACG CGG                  K R G G G G T R
```

Figure 3.8 Individual VLP clones and Final Round Sequencing for Selectants Against MCA5792. (A) shows an agarose gel stained with ethidium bromide to test for the formation of functional VLPs. Note the radical difference in mobility of the selectants when compared to the wild-type control. (B) shows the results of sequencing of a select few of these clones. Though this is only from Round 3, the selectants show common themes, including the presence of a run of four or five glycines and flanking arginine/lysine residues.

3.3.3.2 Functional Testing of VLP Selectants

To test the ability of our MCA5792 selectants to stimulate an immune response that included antibodies to *S. aureus* peptidoglycan, we followed the same immunization strategy of mice that was used in the case of MDVP-55A and GTA29202 with the exception that mice were immunized with four different VLPs bearing the sequences found in Figure 3.8 B (these are St1 - G G G G G R K G, St2 - K G G G G G R K T V, St6 - K R G G G G G G, and St8 - K R G G G G T R). Once serum was collected from mice, it was used in serial dilution in an ELISA against commercially-available *S. aureus* peptidoglycan to determine reactivity. The results of the assay are shown in Figure 3.9. In all four recombinant VLP immunizations, the resulting serum binds to the peptidoglycan as well as the MCA5792 (positive control) antibody does at various dilutions. Though the background on this assay appears to be high, the samples and positive control still have roughly four-fold higher signal at OD405 than the negative control does. These preliminary data indicate that our selectants against antibody MCA5792 do in fact stimulate an immune response in mice against *S. aureus* peptidoglycan.

3.3.4 Affinity Selections - 2H1 and SYA/J6

The final selections performed in this work are against 2H1, a monoclonal antibody that binds to the capsular glucuronoxylomannan (GXM) of the fungus *Cryptococcus neoformans*[86], and SYA/J6, a monoclonal antibody that binds to the trisaccharide epitope of the *O*-polysaccharide of the *Shigella flexneri* variant Y lipopolysaccharide. [87] These two antibodies again target carbohydrate epitopes,

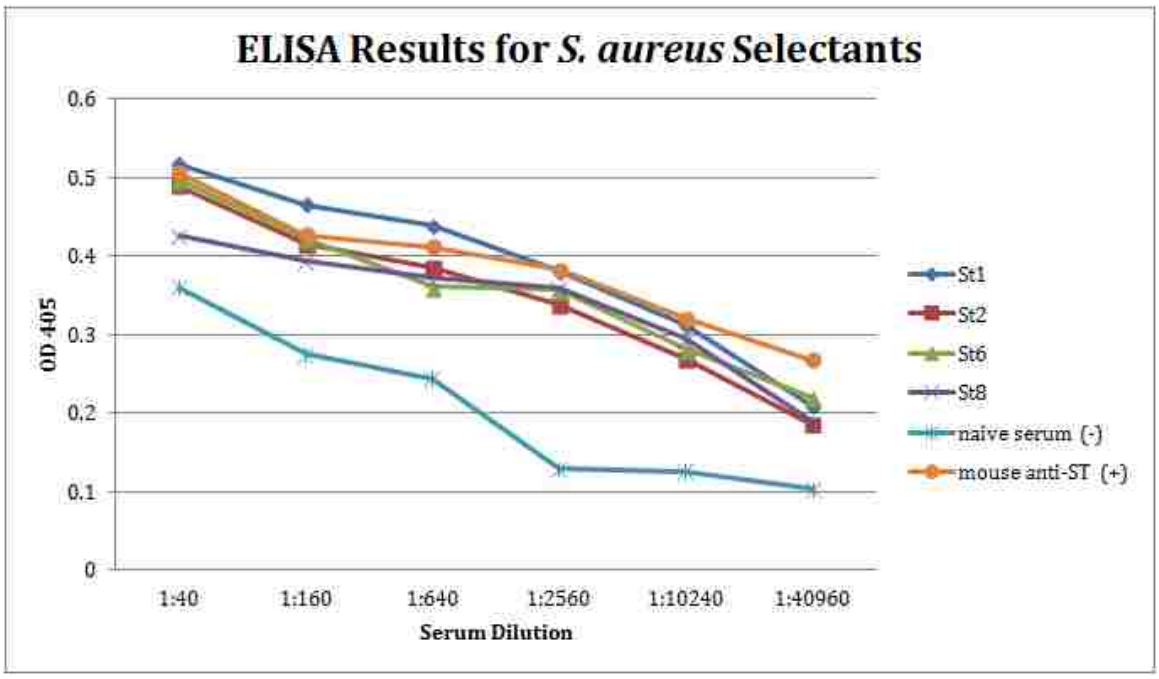

Figure 3.9 Results of ELISA Using Sera From Mice Immunized with Recombinant VLP selectants from MCA5792 Selections. 5 ug of VLPs bearing the selected sequences for 11-248.2-8A3 (see Figure 3.9; labels there are identical to samples here) were administered to Balb/c mice. Mice were subsequently boosted with the same 5 ug VLP dose before serum was harvested and purified. To perform the ELISA to detect anti-*S. aureus* peptidoglycan antibodies, 250 ng of peptidoglycan was used to coat plates, and serial dilutions (x-axis) of harvested serum were used to test for reactivity. Each color on the graph represents a different mouse with a different VLP vaccination.

much like 2C7, 2-1-L8, and MCA5792. Though we have not yet obtained functional testing results for selectants from either antibody, we have performed the same rounds of selection as in previous antibodies and have obtained and sequenced individual clones. This should facilitate additional work/testing of the selectants in the future.

3.3.4.1 Affinity Selections, VLP Selectants, and Sequencing

For 2H1, selections proceeded through four rounds (as with 2C7, 2-1-L8, MDVP-55A, and GTX29202); however, for SYA/J6, selection was halted after three rounds (as with MCA5792). This was to obtain a relative idea of how diverse a peptide population still is before the fourth and final round of selection. After the final round of selection in either case, the selected VLP library was re-transformed into C41(DE3) cells and plated. From these plates, either 24 (2H1) or 12 (SYA/J6) individual colonies were selected for confirmation of production of VLPs and sequencing.

The results of testing for VLP formation are seen in Figure 3.10. The selection against 2H1 yielded many individual VLPs that appear to have identical (or very similar) mobility on the agarose gel while still differing from the wild-type control mobility. This would suggest low variation in peptide composition within the AB-loop. The SYA/J6 selection shows a little more variation in mobility, so we expect that the peptides within the AB-loop are more diverse. This would be expected for the additional reason of the selection being stopped after three (rather than four) rounds; the added stringency from a fourth round of selection may wind up restricting the final population quite a bit.

A

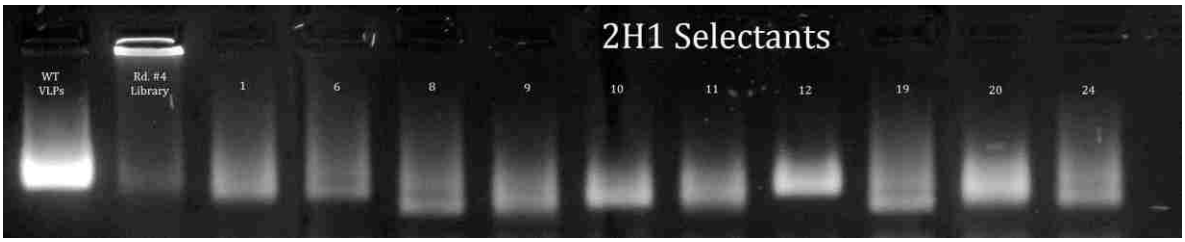

B

Figure 3.10 Individual VLP Clones for Final-Round Selectants from 2H1 and SYA/J6. Gels are phosphate agarose (1%) stained with ethidium bromide to visualize RNA within capsids. (A) shows VLP selectants from 2H1 (four rounds of selection) and (B) shows VLP selectants from SYA/J6 (three rounds of selection). Once again, some colonies did not yield functional VLPs and are thus not included in these gels. Also note the mobility differences in VLPs between selectants and when compared to the wild-type control. 2H1 selectants display the most uniformity in mobility of any selection performed yet.

Finally, we sequenced the selectants that yielded VLPs in our agarose gel. The result of this sequencing is found in Figure 3.11. Nearly every sequence found for 2H1 selectants is a 6-mer (D T Q C Q F); this corresponds to the lack of differing mobilities found in the agarose gel. Those sequences that are not 6-mers are 8-mers, most frequently of the sequence W D A T L Q P A. These are the two sequences that would be ideal to use in the event of further studies with selectants from this antibody. For SYA/J6, only four sequences were recovered, three 6-mers and a 10-mer. There does not appear to be much sequence homology in these sequences. The sample size is low, but it is also important to note that this is after only three rounds of selection. It is expected that there will be at least a little more sequence variation in the population without an additional round of selection to further narrow it.

3.4 Discussion

In this study we utilized our affinity selection on the MS2 VLP platform to find specific peptide binding partners for a variety of antibodies against different types of carbohydrate epitopes (and, in the case of MDVP-55A and GTX29202, a discontinuous protein epitope). In each case, we began with vast random peptide libraries of various lengths (6-, 8-, and 10-amino acids) displayed on the surface of MS2 and, through 3-4 rounds of affinity selection, discovered peptides that bind to the selecting antibodies. In most cases, we were able to demonstrate that the affinity-selected peptides are able to immunogenically mimic the epitopes recognized by the selecting antibodies.

For 2C7 and 2-1-L8, we note some very interesting features of the two selections. The first is that only one size of peptide insertion (a 6-amino acid

2H1

H1	GAC ACG CAG TGC CAG TTC	D T Q C Q F
H2	GAC ACG CAG TGC CAG TTC	D T Q C Q F
H3	GAC ACG CAG TGC CAG TTC	D T Q C Q F
H4	GAC ACG CAG TGC CAG TTC	D T Q C Q F
H5	TGG ACC GCC GAC TTG CAG CCG GAG	W T A D L Q P E
H6	GAC ACG CAG TGC CAG TTC	D T Q C Q F
H7	GAC ACG CAG TGC CAG TTC	D T Q C Q F
H9	GAC ACG CAG CGC CAG TTC	D T Q R Q F
H11	GAC ACG CAG TGC CAG TTC	D T Q C Q F
H12	GAC ACG CAG TGC CAG TTC	D T Q C Q F
H13	TGG GAC GCG ACC TTG CAG CCG GCC	W D A T L Q P A
H14	GAC ACG CAG TGC CAG TTC	D T Q C Q F
H15	GAC ACG CAG TGC CAG TTC	D T Q C Q F
H16	GAC ACG CAG TGC CAG TTC	D T Q C Q F
H19	TGG GAC GCG ACC TTG CAG CCG GCC	W D A T L Q P A
H20	GAC ACG CAG TGC CAG TTC	D T Q C Q F
H21	GAC ACG CAG TGC CAG TTC	D T Q C Q F
H22	GAC ACG CAG TGC CAG TTC	D T Q C Q F
H23	GAC ACG CAG TGC CAG TTC	D T Q C Q F
H24	GAC ACG CAG TGC CAG TTC	D T Q C Q F

SYA/J6

Sh1	GGG GCG TTC GGG GGG GAC	G A F G G D
Sh2	AAC GAC TAC AGG TCG GAC	N D Y R S D
Sh4	GGC TCG GGG TTC GGG GGG GAC CCC AAC GGG	G S G F G G D P N G
Sh12	CTG GGC TGG CAC CCG GAG	L G W H P E

Figure 3.11 Sequences from Final Round Selections against 2H1 and SYA/J6. Here we see results of final-round sequencing for both 2H1 and SYA/J6. Because the selecting antibodies are against two completely different targets, we do not expect or note any similarities between the two sets of sequences. The population of 2H1 selectants are mostly 6-mers, with a few 8-mers; of the four sequences for SYA/J6, three are 6-mers and one is a rare 10-mer.

peptide) is present in all sequenced clones. Because the starting library contained 6-, 8-, and 10-amino acid peptides, this result illustrates that any individual antibody may show a strong preference for peptides of a particular length. This is not surprising when we consider that peptides displayed in the AB-loop are conformationally constrained, and that loop size can dramatically influence loop conformation. Especially in the case of antibodies against carbohydrate epitopes, we are searching for a mimotope of a potentially complex structure; it is entirely possible that for reasons of spatial restriction, only peptides of a particular size show the best affinity for the antibody binding pocket.

It is also notable that the sequences of insertions selected by the two antibodies were either identical or very closely related. This was interesting because it is known that these two antibodies bind to the lipooligosaccharides found on the surface of *N. gonorrhoeae*, but the epitopes to which they bind are not exactly identical. Here, we have provided several different types of evidence to suggest that they bind to identical (or perhaps overlapping) epitopes within the structural context of our MS2 VLPs. Importantly, though Peter Rice and his group have characterized the two antibodies and even have isolated specific affinity-selected peptides for each, his peptides show no cross-reactivity between antibodies. The selections performed here were therefore vital in demonstrating evidence of a common epitope. In future experiments our VLPs will be used to immunize mice to see whether they will elicit anti-gonorrhea antibodies, the best way of determining whether we have in fact created a peptide mimic of this carbohydrate epitope.

As mentioned in the introduction, the LOS of *N gonorrhoeae* is both an attractive and frustrating target for vaccination. The LOS of the bacterium can be modified to help mask or change epitopes to assist in immune invasion. Also, traditional antibodies against *N. gonorrhoeae* are not long-lived; there is little memory response in most cases of infection. Utilizing peptide mimics of this carbohydrate should allow for a long-lived, T-dependent immune response to the bacterium. Structure context effects of affinity-selected peptides are clearly important in this case; though Peter Rice's affinity-selected peptides do not demonstrate any cross-reactivity between 2C7 and 2-1-L8, our peptides do cross-react when presented in the AB-loop of MS2 VLPs. Immunization with these VLPs will hopefully yield antibodies that are capable of binding to both 2C7 and 2-1-L8 epitopes, allowing for a broad range of protection against *N. gonorrhoeae* infection.

In the case of MDVP-55A and GTX29202, two antibodies that were selected as a way to determine whether we could find a mimic of a discontinuous epitope, we noted a predominant 10-mer amino acid peptide selectant for each antibody. Though neither population shared any selectants, the primary amino acid sequences are not found within the Dengue E-protein. As the two antibodies recognize discontinuous epitopes on the protein surface, this is unsurprising. As seen in Figure 3.7, immunization with VLPs displaying the peptide selectant from MDVP-55A (R Q E K I D V T Y) leads to a strong anti-E response in the serum of the mice that was not present in the negative control, wild-type VLP mouse. Future work will determine whether the antibodies elicited by this VLP are able to neutralize Dengue virus.

As previously stated, creating a vaccine to Dengue virus is not a straightforward procedure. This is due to antibody-dependent enhancement (ADE) of disease; if a vaccine to a single Dengue serotype is administered, an antibody response will be generated. This antibody response can facilitate infection by a second Dengue serotype, however, leading to increased chances of more severe disease. This means that rigorous testing of any potential Dengue vaccine is required to ensure that the generated antibody response provides cross-protection against all four serotypes while also minimizing ADE.

MCA5792, the antibody against *S. aureus* peptidoglycan (PG), generated striking affinity selection results, especially in the sequencing of the selected peptides. As discussed in the introduction, the structure of *S. aureus* PG is quite unique, including a glycine linker between lysine residues that forms when the amino sugars begin to form the lattice-like structure. All of our selectants (even though they are only from Round 3 and thus have not been subjected to all four rounds of affinity selection) display that glycine linker in their make-up, and most of them also show bulky, basic residues (lysine, arginine) flanking this linker. From these sequencing data, it becomes clear that the glycine bridge area is the epitope targeted by MCA5792.

Upon immunization of mice with all four clones sequenced in this work, there is a clear anti-PG response in the serum. In fact, this response is as great or greater than the positive control, which in this case is simply MCA5792 interacting with the PG bound to the plate. As was the case for MDVP-55A and GTX29202, we do not yet have data that indicate whether or not this response is actually protective against *S. aureus* infection. However, it is encouraging that we see serum responses that

indicate anti-PG antibodies are being raised, especially because our vaccine is entirely protein-based and is targeting an antigen with a carbohydrate component. As discussed in the introduction, by using a strictly protein-based vaccine, we have a better chance of raising high-affinity, long-lived antibodies that will actually prove protective against infection.

Interestingly, as *S. aureus* is a common bacterium, it is known that most individuals have antibodies to *S. aureus* PG even if they do not have a current systemic infection. [88], [89] These antibodies have been shown to have opsonizing activity, allowing for neutralization of the bacterium. This would provide another onus for development of an anti-PG vaccine; by raising serum anti-PG antibody levels, it should be possible to also provide the individual more protection against infection. However, it has also been shown that anti-PG antibodies can be cross-reactive, in some cases even binding to *E. coli* PG. [88] This could pose a concern because it is vital that commensal bacteria are not destroyed by a vaccine intended to protect against a different infection. This may actually increase the value of using MCA5792 as the selecting antibody in affinity selections, however. Our results indicate that MCA5792 targets the pentaglycine bridge of *S. aureus* PG; this is a unique bridging structure among various PGs. Thus, if we have discovered immunological mimotopes with our peptides, the antibodies generated should also be specific to that pentaglycine bridge. This would mitigate potential cross-reactivity while also increasing protection against *S. aureus* infection.

The final selections discussed in this work, against 2H1 and SYA/J6, are still considered works in progress. We have not yet performed any functional analyses

with the selectants for either of these antibodies. However, we can still speak on the results of the sequencing that we have performed so far. For 2H1, there are two clear sequences present – a 6-mer and an 8-mer – and of these two, the 6-mer is by far the more numerous. This should provide a solid foundation for functional testing in the future, as the two peptides most likely to have a chance at eliciting an antibody response similar to the selecting antibody have already been determined. For SYA/J6, the results are different. Like in the case of MCA5792, the SYA/J6 selectants sequenced and shown here are from Round 3 selectants. However, unlike MCA5792, the sequences that we find do not show very much homology to one another, either in actual sequence or in size. It is clear that more work must be done here, whether it is to perform another round of selection or to sequence more individual clones (or both). As of now, we do not have enough reliable data to even feel confident that we have discovered the highest-affinity or best binders; however, as this study demonstrates the power of the affinity selection process, we do feel confident that with additional work, we will be able to advance SYA/J6 selectants to the same stage as the others presented here.

Chapter 4: Conclusion

In this work, we have demonstrated the power of using bacteriophage MS2 VLPs as platforms for heterologous peptide display. We showed successful, functional display of single-chain antibodies (scFvs) on the surface of the VLPs via a genetic insertion strategy. We also demonstrated, both in ELISA and against live cells, the ability of scFv-bearing VLPs to bind to the target that is specified by the scFv. We demonstrated potential applications of scFv-bearing VLPs, including detection of cell surface markers and neutralization of pseudotyped virus.

The true power in the display of scFvs on the surface of MS2 VLPs comes from the display of random scFv libraries. This will allow for the selection of novel scFv binders to peptides and then the direct use of the scFvs in the selecting system by, for example, loading the VLPs with imaging agents or cytotoxic drugs. This is unique to our system compared to, say, filamentous or yeast display, where the scFv must be removed from its selecting environment before use. Also unique to our system is the ability to perform the entirety of the library construction, expression, and affinity-selection *in vitro*. This is due to the overall simplicity of the MS2 VLP. This will allow for automation of the process of library construction and affinity selection, making this an incredibly powerful platform for display of scFv libraries.

In addition, we showed the power of random peptide library display on the surface of MS2, allowing for affinity selection of highly specific peptides that tightly bind to a selecting antibody. We demonstrated that these selected sequences not only bind to their selecting antibody, but also that immunization with these peptides displayed on VLPs allows for the raising of a desired antibody response in mice.

Though more work needs to be done to determine the protective nature of these antibodies, it is clear that the technique of affinity selection of random peptide libraries on MS2 VLPs is a promising method of vaccine discovery.

Once again, there is addition power in this technique owing to the possibility of performing the entire procedure *in vitro*. This will allow for the rapid screening of complex libraries in an automated fashion. Also, especially critical for small peptides is structural context, as peptides tend to fold differently and adopt different conformations depending on the folding pressures exerted upon them. Because the MS2 VLP display and affinity selection system allows for the selected peptides to be immediately utilized in the same context under which they were selected, MS2 VLPs have clear advantages in random peptide library display and screening compared to other display systems.

References

[1] G. P. Smith, "Filamentous fusion phage: novel expression vectors that display cloned antigens on the virion surface.," *Science*, vol. 228, no. 4705, pp. 1315–1317, 1985.

[2] M. Russel and P. Model, "Filamentous Phage." [Online]. Available: http://www.thebacteriophages.org/frames_0120.htm.

[3] V. F. de la Cruz, a a Lal, and T. F. McCutchan, "Immunogenicity and epitope mapping of foreign sequences via genetically engineered filamentous phage.," *The Journal of Biological Chemistry*, vol. 263, no. 9, pp. 4318–22, Mar. 1988.

[4] N. Sternberg and R. Weisberg, "Packaging of coliphage lambda DNA: II. The role of the gene D protein," *Journal of Molecular Biology*, vol. 117, no. 3, pp. 733–759, Dec. 1977.

[5] N. Sternberg and R. H. Hoess, "Display of peptides and proteins on the surface of bacteriophage lambda.," *Proceedings of the National Academy of Sciences of the United States of America*, vol. 92, no. 5, pp. 1609–13, Feb. 1995.

[6] Y. Gi Mikawa, I. N. Maruyama, and S. Brenner, "Surface Display of Proteins on Bacteriophage λ Heads," *Journal of Molecular Biology*, vol. 262, no. 1, pp. 21–30, Sep. 1996.

[7] A. Gupta, M. Onda, I. Pastan, S. Adhya, and V. K. Chaudhary, "High-density Functional Display of Proteins on Bacteriophage Lambda," *Journal of Molecular Biology*, vol. 334, no. 2, pp. 241–254, Nov. 2003.

[8] I. Katsura, "Structure and function of the major tail protein of bacteriophage lambda: Mutants having small major tail protein molecules in their virion," *Journal of Molecular Biology*, vol. 146, no. 4, pp. 493–512, Mar. 1981.

[9] I. N. Maruyama, H. I. Maruyama, and S. Brenner, "Lambda foo: a lambda phage vector for the expression of foreign proteins.," *Proceedings of the National Academy of Sciences of the United States of America*, vol. 91, no. 17, pp. 8273–7, Aug. 1994.

[10] Z. J. Ren, G. K. Lewis, P. T. Wingfield, E. G. Locke, a C. Steven, and L. W. Black, "Phage display of intact domains at high copy number: a system based on SOC, the small outer capsid protein of bacteriophage T4.," *Protein Science*, vol. 5, no. 9, pp. 1833–43, Sep. 1996.

[11] J. Jiang, L. Abu-Shilbayeh, and V. B. Rao, "Display of a PorA peptide from Neisseria meningitidis on the bacteriophage T4 capsid surface.," *Infection and Immunity*, vol. 65, no. 11, pp. 4770–7, Nov. 1997.

[12] E. Boder and K. Wittrup, "Yeast surface display for screening combinatorial polypeptide libraries," *Nature Biotechnology*, vol. 15, no. 6, pp. 553–7, 1997.

[13] L. Pepper and Y. Cho, "A decade of yeast surface display technology: where are we now?," *Combinatorial Chemistry & High Throughput Screening*, vol. 11, no. 2, pp. 127–134, 2008.

[14] J. a Francisco, R. Campbell, B. L. Iverson, and G. Georgiou, "Production and fluorescence-activated cell sorting of Escherichia coli expressing a functional antibody fragment on the external surface.," *Proceedings of the National Academy of Sciences of the United States of America*, vol. 90, no. 22, pp. 10444–8, Nov. 1993.

[15] P. S. Daugherty, G. Chen, M. J. Olsen, B. L. Iverson, and G. Georgiou, "Antibody affinity maturation using bacterial surface display.," *Protein Engineering*, vol. 11, no. 9, pp. 825–32, Sep. 1998.

[16] J. Hanes and a Plückthun, "In vitro selection and evolution of functional proteins by using ribosome display.," *Proceedings of the National Academy of Sciences of the United States of America*, vol. 94, no. 10, pp. 4937–42, May 1997.

[17] I. Fukuda, K. Kojoh, N. Tabata, N. Doi, H. Takashima, E. Miyamoto-Sato, and H. Yanagawa, "In vitro evolution of single-chain antibodies using mRNA display.," *Nucleic Acids Research*, vol. 34, no. 19, p. e127, Jan. 2006.

[18] R. Golmohammadi, K. Valegård, K. Fridborg, and L. Liljas, "The refined structure of bacteriophage MS2 at 2.8 A resolution.," *Journal of Molecular Biology*, vol. 226, no. 3, pp. 620–639, 1993.

[19] S. Peabody, "Translational Repression by Bacteriophage Expressed from a Plasmid OF A PROTEIN-RNA MS2 Coat Protein," *Journal of Biological Chemistry*, vol. 265, no. 10, pp. 5684–9, 1990.

[20] R. a Mastico, S. J. Talbot, and P. G. Stockley, "Multiple presentation of foreign peptides on the surface of an RNA-free spherical bacteriophage capsid.," *The Journal of General Virology*, vol. 74 (Pt 4), pp. 541–8, Apr. 1993.

[21] D. S. Peabody, B. Manifold-Wheeler, A. Medford, S. K. Jordan, J. do Carmo Caldeira, and B. Chackerian, "Immunogenic display of diverse peptides on virus-like particles of RNA phage MS2.," *Journal of Molecular Biology*, vol. 380, no. 1, pp. 252–63, Jun. 2008.

[22] D. Peabody, "Subunit fusion confers tolerance to peptide insertions in a virus coat protein," *Archives of Biochemistry and Biophysics*, vol. 347, no. 1, pp. 85–92, 1997.

[23] S. K. Jordan, "Engineering RNA Phage MS2 Virus-Like Particles for Peptide Display," *Dissertation*, 2010.

[24] I. Vasiljeva, T. Kozlovska, I. Cielens, A. Strelnikova, A. Kazaks, V. Ose, and P. Pumpens, "Mosaic Qbeta coats as a new presentation model.," *FEBS Letters*, vol. 431, no. 1, pp. 7–11, Jul. 1998.

[25] R. Golmohammadi, K. Fridborg, M. Bundule, K. Valegård, and L. Liljas, "The crystal structure of bacteriophage Q beta at 3.5 A resolution.," *Structure (London, England : 1993)*, vol. 4, no. 5, pp. 543–54, May 1996.

[26] C. E. Ashley, E. C. Carnes, G. K. Phillips, P. N. Durfee, M. D. Buley, C. a Lino, D. P. Padilla, B. Phillips, M. B. Carter, C. L. Willman, C. J. Brinker, J. D. C. Caldeira, B. Chackerian, W. Wharton, and D. S. Peabody, "Cell-specific delivery of diverse cargos by bacteriophage MS2 virus-like particles.," *ACS Nano*, vol. 5, no. 7, pp. 5729–45, Jul. 2011.

[27] J. Caldeira, A. Medford, R. Kines, and C. Lino, "display of diverse peptides, including a broadly cross-type neutralizing human papillomavirus L2 epitope, on virus-like particles of the RNA bacteriophage PP7," *Vaccine*, vol. 28, no. 27, pp. 4384–4393, 2010.

[28] B. Chackerian, J. D. C. Caldeira, J. Peabody, and D. S. Peabody, "Peptide epitope identification by affinity selection on bacteriophage MS2 virus-like particles.," *Journal of Molecular Biology*, vol. 409, no. 2, pp. 225–237, 2011.

[29] C. E. Hagemeyer, C. von zur Muhlen, D. von Elverfeldt, and K. Peter, "Single-chain antibodies as diagnostic tools and therapeutic agents," *Thrombosis and Haemostasis*, pp. 1012–1019, 2009.

[30] J. Scott and G. Smith, "Searching for peptide ligands with an epitope library," *Science*, vol. 249, no. 4967, pp. 386–90, 1990.

[31] K. a Noren and C. J. Noren, "Construction of high-complexity combinatorial phage display peptide libraries.," *Methods (San Diego, Calif.)*, vol. 23, no. 2, pp. 169–78, Mar. 2001.

[32] R. Tungtrakanpoung, P. Pitaksajjakul, N. Na-Ngarm, W. Chaicumpa, P. Ekpo, P. Saengjaruk, G. Froman, and P. Ramasoota, "Mimotope of Leptospira from phage-displayed random peptide library is reactive with both monoclonal antibodies and patients' sera.," *Veterinary Microbiology*, vol. 115, no. 1–3, pp. 54–63, Jun. 2006.

[33] N. Na-ngam, T. Kalambaheti, P. Ekpo, P. Pitaksajjakul, N. Jamornthanyawat, N. Chantratita, S. Sirisinha, M. Yamabhai, V. Thamlikitkul, and P. Ramasoota, "Mimotope identification from monoclonal antibodies of Burkholderia pseudomallei using random peptide phage libraries," *Transactions of the Royal Society of Tropical Medicine and Hygiene*, vol. 102, Suppl, no. 0, pp. S47–S54, Dec. 2008.

[34] N. Tewawong, P. Pitaksajjkul, P. Dekumyoy, P. Ekpo, and P. Ramasoota, "Mimotope identification using phage displayed random peptide libraries against monoclonal antibodies specific to house dust mite.," *The Southeast Asian Journal of Tropical Medicine and Public Health*, vol. 43, no. 3, pp. 614–23, May 2012.

[35] A. Shanmugam, R. Suriano, D. Chaudhuri, S. Rajoria, A. George, A. Mittelman, and R. K. Tiwari, "Identification of PSA peptide mimotopes using phage display peptide library.," *Peptides*, vol. 32, no. 6, pp. 1097–102, Jun. 2011.

[36] Merck, "PneumoVax." [Online]. Available: http://www.merck.com/product/usa/pi_circulars/p/pneumovax_23/pneumovax_pi.pdf.

[37] Wyeth, "Prevnar 13." [Online]. Available: http://www.prevnar13.com/.

[38] R. D. Astronomo and D. R. Burton, "Carbohydrate vaccines: developing sweet solutions to sticky situations?," *Nature reviews. Drug discovery*, vol. 9, no. 4, pp. 308–24, Apr. 2010.

[39] A. H. Lucas, M. a Apicella, and C. E. Taylor, "Carbohydrate moieties as vaccine candidates.," *Clinical Infectious Diseases*, vol. 41, no. 5, pp. 705–12, Sep. 2005.

[40] S. Alam, M. McAdams, and D. Boren, "The role of antibody polyspecificity and lipid reactivity in binding of broadly neutralizing anti-HIV-1 envelope human monoclonal antibodies 2F5 and 4E10 to glycoprotein 41 membrane proximal envelope epitopes.," *The Journal of Immunology*, vol. 178, no. 7, pp. 4424–4435, 2007.

[41] M. Monette, S. Opella, and J. Greenwood, "Structure of a malaria parasite antigenic determinant displayed on filamentous bacteriophage determined by NMR spectroscopy: implications for the structure of continuous peptide," *Protein Science*, vol. 10, no. 6, pp. 1150–1159, 2001.

[42] R. Acharya, E. Fry, D. Stuart, and G. Fox, "The three-dimensional structure of foot-and-mouth disease virus at 2.9 Å resolution," *Nature*, vol. 337, no. 23, pp. 709–716, 1989.

[43] D. E. Spratt and N. Lee, “Current and emerging treatment options for nasopharyngeal carcinoma.,” *OncoTargets and Therapy*, vol. 5, pp. 297–308, Jan. 2012.

[44] J. Tol and C. J. a Punt, “Monoclonal antibodies in the treatment of metastatic colorectal cancer: a review.,” *Clinical Therapeutics*, vol. 32, no. 3, pp. 437–53, Mar. 2010.

[45] H. Modjtahedi, S. Ali, and S. Essapen, “Therapeutic application of monoclonal antibodies in cancer: advances and challenges.,” *British Medical Bulletin*, vol. 104, pp. 41–59, Jan. 2012.

[46] P. Pansri, N. Jaruseranee, K. Rangnoi, P. Kristensen, and M. Yamabhai, “A compact phage display human scFv library for selection of antibodies to a wide variety of antigens.,” *BMC Biotechnology*, vol. 9, p. 6, Jan. 2009.

[47] X. Ge, Y. Mazor, S. P. Hunicke-Smith, A. D. Ellington, and G. Georgiou, “Rapid construction and characterization of synthetic antibody libraries without DNA amplification.,” *Biotechnology and Bioengineering*, vol. 106, no. 3, pp. 347–57, Jun. 2010.

[48] J. Glanville, W. Zhai, J. Berka, D. Telman, G. Huerta, G. R. Mehta, I. Ni, L. Mei, P. D. Sundar, G. M. R. Day, D. Cox, A. Rajpal, and J. Pons, “Precise determination of the diversity of a combinatorial antibody library gives insight into the human immunoglobulin repertoire.,” *Proceedings of the National Academy of Sciences of the United States of America*, vol. 106, no. 48, pp. 20216–21, Dec. 2009.

[49] J. W. Froude, P. Thullier, and T. Pelat, “Antibodies against anthrax: mechanisms of action and clinical applications.,” *Toxins*, vol. 3, no. 11, pp. 1433–52, Nov. 2011.

[50] J. a T. Young and R. J. Collier, “Anthrax toxin: receptor binding, internalization, pore formation, and translocation.,” *Annual Review of Biochemistry*, vol. 76, pp. 243–65, Jan. 2007.

[51] C. Leysath and A. Monzingo, “Crystal structure of the engineered neutralizing antibody M18 complexed to domain 4 of the anthrax protective antigen,” *Journal of Molecular Biology*, vol. 387, no. 3, pp. 680–693, 2009.

[52] N. N. C. Institutes, “Liver Cancer.” [Online]. Available: http://cancer.gov/cancertopics/types/liver.

[53] D. Moradpour, B. Compagnon, B. E. Wilson, C. Nicolau, and J. R. Wands, “Specific targeting of human hepatocellular carcinoma cells by immunoliposomes in vitro.,” *Hepatology*, vol. 22, no. 5, pp. 1527–1537, 1995.

[54] Y. A. Yeung, "Antibody Engineering for Cancer Therapy By Antibody Engineering for Cancer Therapy," *Dissertation*, 2005.

[55] K. B. Chua, "Nipah Virus: A Recently Emergent Deadly Paramyxovirus," *Science*, vol. 288, no. 5470, pp. 1432–1435, May 2000.

[56] B. Lamp, E. Dietzel, L. Kolesnikova, L. Sauerhering, S. Erbar, H. Weingartl, and A. Maisner, "Nipah virus entry and egress from polarized epithelial cells.," *Journal of Virology*, no. January, Jan. 2013.

[57] V. Guillaume, H. Contamin, P. Loth, A. Lefeuvre, P. Marianneau, K. B. Chua, S. K. Lam, V. Deubel, T. F. Wild, and R. Buckland, "Nipah Virus : Vaccination and Passive Protection Studies in a Hamster Model Nipah Virus : Vaccination and Passive Protection Studies in a Hamster Model," *Journal of Virology*, vol. 78, no. 2, pp. 834–40, 2004.

[58] H. C. Aguilar, K. a Matreyek, D. Y. Choi, C. M. Filone, S. Young, and B. Lee, "Polybasic KKR motif in the cytoplasmic tail of Nipah virus fusion protein modulates membrane fusion by inside-out signaling.," *Journal of Virology*, vol. 81, no. 9, pp. 4520–32, May 2007.

[59] H. C. Aguilar, Z. A. Ataman, V. Aspericueta, A. Q. Fang, M. Stroud, O. a Negrete, R. a Kammerer, and B. Lee, "A novel receptor-induced activation site in the Nipah virus attachment glycoprotein (G) involved in triggering the fusion glycoprotein (F).," *The Journal of Biological Chemistry*, vol. 284, no. 3, pp. 1628–35, Jan. 2009.

[60] G. Notani and D. Engelhardt, "Suppression of a coat protein mutant of the bacteriophage f2," *Journal of Molecular Biology*, vol. 12, no. 2, pp. 439–447, 1965.

[61] D. G. Gibson, L. Young, R.-Y. Chuang, J. C. Venter, C. A. Hutchison, and H. O. Smith, "Enzymatic assembly of DNA molecules up to several hundred kilobases," *Nature Methods*, vol. 6, no. 5, pp. 343–345, May 2009.

[62] IDT, "Integrated DNA Technologies." [Online]. Available: http://www.idtdna.com/site. [Accessed: 02-Dec-2013].

[63] A. Tamin, B. Harcourt, M. Lo, and J. Roth, "Development of a neutralization assay for Nipah virus using pseudotype particles," *Journal of Virological Methods*, vol. 160, pp. 1–6, 2009.

[64] J. Jiao, A. Hindoyan, S. Wang, L. M. Tran, A. S. Goldstein, D. Lawson, D. Chen, Y. Li, C. Guo, B. Zhang, L. Fazli, M. Gleave, O. N. Witte, I. P. Garraway, and H. Wu, "Identification of CD166 as a surface marker for enriching prostate

stem/progenitor and cancer initiating cells.," *PloS One*, vol. 7, no. 8, p. e42564, Jan. 2012.

[65] S. M. Smith and L. Cai, "Cell specific CD44 expression in breast cancer requires the interaction of AP-1 and NFκB with a novel cis-element.," *PloS One*, vol. 7, no. 11, p. e50867, Jan. 2012.

[66] M. Yarus, "Translational efficiency of transfer RNA's: uses of an extended anticodon.," *Science (New York, NY)*, vol. 218, no. 12, pp. 646–652, 1982.

[67] D. Tawfik and A. Griffiths, "Man-made cell-like compartments for molecular evolution," *Nature Biotechnology*, vol. 16, pp. 652–56, 1998.

[68] J. McCafferty, A. Griffiths, G. Winter, and D. Chiswell, "Phage antibodies: filamentous phage displaying antibody variable domains," *Nature*, vol. 6, no. 348, pp. 552–4, 1990.

[69] S. Gulati, D. P. McQuillen, R. E. Mandrell, D. B. Jani, and P. a Rice, "Immunogenicity of Neisseria gonorrhoeae lipooligosaccharide epitope 2C7, widely expressed in vivo with no immunochemical similarity to human glycosphingolipids.," *The Journal of Infectious Diseases*, vol. 174, no. 6, pp. 1223–37, Dec. 1996.

[70] D. C. Stein, E. F. Petricoin, J. M. Griffiss, and H. Schneider, "Use of transformation to construct Neisseria gonorrhoeae strains with altered lipooligosaccharides.," *Infection and Immunity*, vol. 56, no. 4, pp. 762–5, Apr. 1988.

[71] CDC, "Centers for Disease Control and Prevention." [Online]. Available: http://www.cdc.gov/.

[72] W. Zhu, C.-J. Chen, C. E. Thomas, J. E. Anderson, A. E. Jerse, and P. F. Sparling, "Vaccines for gonorrhea: can we rise to the challenge?," *Frontiers in Microbiology*, vol. 2, no. June, p. 124, Jan. 2011.

[73] S. R. Hedges, D. a Sibley, M. S. Mayo, E. W. Hook, and M. W. Russell, "Cytokine and antibody responses in women infected with Neisseria gonorrhoeae: effects of concomitant infections.," *The Journal of Infectious Diseases*, vol. 178, no. 3, pp. 742–51, Sep. 1998.

[74] S. R. Hedges, M. S. Mayo, J. Mestecky, E. W. H. Iii, and M. W. Russell, "Limited Local and Systemic Antibody Responses to Neisseria gonorrhoeae during Uncomplicated Genital Infections Limited Local and Systemic Antibody Responses to Neisseria gonorrhoeae during Uncomplicated Genital Infections," *Infection and Immunity*, vol. 67, no. 8, pp. 3937–46, 1999.

[75] C. Elkins, N. H. Carbonetti, V. a Varela, D. Stirewalt, D. G. Klapper, and P. F. Sparling, "Antibodies to N-terminal peptides of gonococcal porin are bactericidal when gonococcal lipopolysaccharide is not sialylated.," *Molecular Microbiology*, vol. 6, no. 18, pp. 2617–28, Sep. 1992.

[76] S. D. O'Connor ET, Swanson KV, Cheng H, Fluss K, Griffiss JM, "Structural requirements for monoclonal antibody 2-1-L8 recognition of neisserial lipooligosaccharides.," *Hybridoma (Larchmt)*, vol. 27, no. 2, pp. 71–9, 2008.

[77] P. Rice, "Molecular basis for serum resistance in Neisseria gonorrhoeae.," *Clinical Microbiology Reviews*, vol. 2, pp. S112–S117, 1989.

[78] D. Gubler, "Dengue and dengue hemorrhagic fever," *Clinical Microbiology Reviews*, vol. 11, no. 3, pp. 480–96, 1998.

[79] I. Kurane, A. L. Rothman, P. G. Livingston, S. Green, S. J. Gagnon, J. Janus, B. L. Innis, S. Nimmannitya, A. Nisalak, and F. A. Ennis, "Immunopathologic mechanisms of dengue hemorrhagic fever and dengue shock syndrome.," *Archives of Virology. Supplementum*, vol. 9, pp. 59–64, 1994.

[80] K. Matsui, G. D. Gromowski, L. Li, A. J. Schuh, J. C. Lee, and A. D. T. Barrett, "Characterization of dengue complex-reactive epitopes on dengue 3 virus envelope protein domain III.," *Virology*, vol. 384, no. 1, pp. 16–20, Feb. 2009.

[81] G. D. Gromowski, N. D. Barrett, and A. D. T. Barrett, "Characterization of dengue virus complex-specific neutralizing epitopes on envelope protein domain III of dengue 2 virus.," *Journal of Virology*, vol. 82, no. 17, pp. 8828–37, Sep. 2008.

[82] S. Sharif, M. Singh, S. Kim, and J. Schaefer, "Staphylococcus aureus peptidoglycan tertiary structure from carbon-13 spin diffusion," *Journal of the American Chemical Society*, vol. 131, no. 20, pp. 7023–7030, 2009.

[83] A. C. Schaffer and J. C. Lee, "Vaccination and passive immunisation against Staphylococcus aureus.," *International Journal of Antimicrobial Agents*, vol. 32 Suppl 1, pp. S71–8, Nov. 2008.

[84] R. Capparelli, N. Nocerino, C. Medaglia, G. Blaiotta, P. Bonelli, and D. Iannelli, "The Staphylococcus aureus peptidoglycan protects mice against the pathogen and eradicates experimentally induced infection.," *PloS One*, vol. 6, no. 12, p. e28377, Jan. 2011.

[85] Y. Chen, B. Liu, D. Yang, X. Li, L. Wen, P. Zhu, and N. Fu, "Peptide mimics of peptidoglycan are vaccine candidates and protect mice from infection with Staphylococcus aureus.," *Journal of Medical Microbiology*, vol. 60, no. Pt 7, pp. 995–1002, Jul. 2011.

[86] J. Mukherjee, M. Feldmesser, M. D. Scharff, and A. Casadevall, "Monoclonal antibodies to Cryptococcus neoformans glucuronoxylomannan enhance fluconazole efficacy.," *Antimicrobial Agents and Chemotherapy*, vol. 39, no. 7, pp. 1398–405, Jul. 1995.

[87] R. S. McGavin, R. a Gagne, M. C. Chervenak, and D. R. Bundle, "The design, synthesis and evaluation of high affinity macrocyclic carbohydrate inhibitors.," *Organic & Biomolecular Chemistry*, vol. 3, no. 15, pp. 2723–32, Aug. 2005.

[88] H. Wergeland and C. Endresen, "Antibodies to various bacterial cell wall peptidoglycans in human and rabbit sera.," *Journal of Clinical Microbiology*, vol. 25, no. 3, pp. 540–545, 1987.

[89] H. Wergeland and L. Haaheim, "Antibodies to staphylococcal peptidoglycan and its peptide epitopes, teichoic acid, and lipoteichoic acid in sera from blood donors and patients with staphylococcal," *Journal of Clinical Microbiology*, vol. 27, no. 6, pp. 1286–1291, 1989.